DEVELOPMENT AND OPTIMISATION OF THREE DIMENSIONAL FREEZE-DRIED COLLAGEN-BASED SCAFFOLDS

Bin Xue (Andy)
Kellogg College

Michaelmas 2014

Thesis submitted for the Degree of Master of Science by Research

UNIVERSITY OF OXFORD
DEPARTMENT OF ENGINEERING SCIENCE

Abstract

Development and optimisation of three-dimensional freeze-dried collagen-based scaffolds

A thesis submitted for the Degree of Master of Science by Research

Bin Xue (Andy)

Three-dimensional collagen/chitosan scaffolds fabricated by freeze-drying technique in 96-well polystyrene and PDMS plates were optimized during this study. Surface tension is, by and large, one of the most limiting factors in fabricating freeze-dried scaffolds in small format well plates. Traditionally, bowl-shaped top surfaces of collagen/chitosan scaffolds were common in polystyrene 96-well plate; whereas for PDMS 96-well plate, dome-shaped surfaces were formed. These surface tension phenomena are not desirable in cell studies especially during initial cell seeding. A combination of surface treatment and change of freeze-drying regime were developed to mitigate the surface tension problem in PS and PDMS 96-well plates respectively. Collagen/chitosan scaffolds of varying concentration and composition were experimented in both polystyrene and PDMS 96-well plates. Thin water film treatment with UV cross-linking was successfully used to eliminate meniscus in PS well plates; pre-cooling, on the other hand, was utilised to treat scaffold solutions in PDMS well plates. The resultant matrices all had flat top surfaces and average thickness of 1 mm. As expected, scaffolds with lower overall polymer concentration or, from a compositional perspective, scaffolds with high chitosan content generally had larger pores. Microscopic observation by multi-photon microscope was performed and chemical analyses were conducted to characterize the surface-treated scaffolds. In addition, scaffolds were tested *in vitro* using DLD-1 cells, hMSCs and fibroblasts for their biological performance. The purpose of this study was to address the problem of using small format culture wells for the fabrication of freeze-dried collagen-based scaffolds for studies of cell growth in 3D culture and in microfluidic perfusion bioreactors.

Acknowledgements

My single most debt remains to Prof. Zhanfeng Cui for his encouragements and invaluable advices. The author would also like to extend his appreciation to the following people who have made the completion of this study possible: Dr. Heiko Schiffter, Dr. Cathy Ye, Dr. Renchen Liu, Dr. Julian George, Dr. Yasser El-sherbini, Jangho Lee, Shaoyang Yeh, Pirada Trongwongsa and Muhammad Yusof Omar.

Table of Contents

List of Figures

List of Tables

List of Equations

List of Abbreviations

(In order of appearance)

Three-dimensional	3D
Polystyrene	PS
Polydimethylsiloxane	PDMS
Extra-cellular matrix	ECM
Ultra-violet	UV
Differential scanning calorimeter	DSC
Fourier transform infra-red	FTIR
Multi-photon fluorescence microscope	MPM
Human mesenchymal stem cells	hMSCs
Two-dimensional	2D
Dulbecco's modified Eagle medium	DMEM
Foetal bovine serum	FBS
Penicillin Streptomycin	PenStrep
Phosphate buffered saline	PBS
Ethylenediaminetetraacetic acid	EDTA
Mesenchymal cell growth supplements	MCGS
alamarBlue®	AB
Standard deviation	SD

1. Introduction

1.1 Background

The emergent field of tissue engineering provides viable solutions for replacement of damaged tissue [1]. To restore the very functionalities of the original tissue, three-dimensional (3D) scaffolds are employed to act as templates for cell adhesion, proliferation and differentiation; with the ultimate goal of promoting tissue re-growth in the body. The scaffolds should have a porous yet adequately strong structure to promote cell in-growth and facilitate mass transport of nutrients and waste. The nature of the scaffolding material should be biocompatible and degrade into immunologically inert by-products over a timeframe comparable to new tissue formation [2, 3]. In the meantime, 3D scaffold has been shown to influence cellular activities to a great extent. A controlled fabrication process has to be carefully designed in order to obtain a construct with desirable microstructure [4, 5]. In addition, the substrate used in scaffold fabrication is also an important factor prior to scale-up and potential clinical applications. Small-format well plate has seen its popularity and usage increased during recent years due to its convenience for basic research and the potential to save materials and costs. Two widely adopted small-format substrates in tissue engineering are polystyrene (PS) and polydimethylsoloxane (PDMS).

This chapter will lay the foundations of 3D culture used in this study, namely, materials, processes used to generate the 3D constructs, and substrates that host the 3D constructs; followed by aims and objectives; and the scope of this thesis.

1.1.1 Materials

To promote favourable cell-scaffold interactions, scaffolding materials must satisfy a number of constraints including biocompatibility, biodegradability as well as non-toxicity.

Natural polymers such as agarose, alginate, fibronectin, hyaluronic acid, Matrigel, gelatin, fibrin, collagen and chitosan have shown promising properties as scaffolding materials. The biological nature of these materials has demonstrated distinctive advantages of biocompatibility and favourable overall interactions with native tissue [3].

Collagen plays a significant role in forming and functioning of the extra-cellular matrix (ECM). A number of tissue engineering applications have adopted collagen as the scaffolding material as it has been observed to promote cell attachment and in-growth [3].

On the other hand, chitosan, a linear polysaccharide and a structural element in the exo-skeleton of crustaceans, has been commonly adopted in tissue engineering applications because of its capability to be modified chemically and physically to tailor to the requirement of a specific application. It is also biocompatible and non-toxic.

1.1.2 Fabrication

Porous 3D scaffolds have been widely adopted in tissue engineering applications for *in vitro* study of cellular interaction, and *in vivo* study of tissue regeneration. Methods commonly used to fabricate the 3D constructs include salt leaching, gas forming, electro-spinning, 3D printing and lyophilisation [6-8]. Fabrication technique used in this study was lyophilisation, or freeze-drying.

Freeze-drying, or lyophilisation is essentially a process to separate the solute and solvent into two phases, solute-rich and solvent-rich. During lyophilisation, the solvent-rich phase is solidified and removed, and the solute-rich phase is left with a porous structure stimulating that of the solvent-rich phase [8-13].

There are a number of parameters during lyophilisation that could affect the final outcome. The freezing temperature, primary drying and secondary drying setups, the chamber pressure, and the time it takes to complete each stage are factors that to be considered.

1.1.3 Substrates

The most widely adopted substrate in tissue engineering is PS. It is non-toxic and chemically inert in most cases and appropriate for general purposes. In addition, multi-well plates made of PS used in biological laboratories offer excellent optical and thermal properties.

Over the past few years, silicon-based elastomer PDMS has been widely used as an alternative for casting 3D geometries in which tissue engineered scaffolds were produced. Its simple and fast fabrication process and flexibility in design

have earned the material a reputation in casting complex geometries and surface features. In addition, the material is gas permeasible, optically transparent, and compatible with the prevailing cell culture infrastructure.

Small format well plate made of PS or PDMS has been widely adopted in laboratories as it is important to understand cell interactions with scaffold materials on a small scale prior to scale-up and potential clinical applications, hence there is a strong need to develop 3D scaffolds for cell culture on a small scale for basic research. However, substrate associated problems in small-format well plate have hardly been acknowledged, and remain poorly understood. In fact, over the past decade, little attempt has been made to rectify drawbacks caused by the hydrophilic surface of the widely-adopted small-format PS system. As with small-format PS well-plates, the surface phenomenon is only significantly pronounced in small-format PDMS well plates. In this case, the hydrophobic surface causes the polymer solution to be repelled.

1.2 Aims and objectives

The purpose of this study was to address the problem of using small-format culture wells for the fabrication of freeze-dried collagen-based scaffolds for studies of cell growth in 3D culture in static and microfluidic perfusion bioreactors.

The aims of the study were, therefore, to develop methods for fabricating freeze-dried collagen-based scaffolds in 96-well plates made of PS and PDMS. The objectives are as follows:

1. To prepare collagen/chitosan 3D porous scaffolds by freeze-drying blended collagen/chitosan solutions in PS and PDMS 96-well plates;
2. To enhance the durability of the scaffolds by ultra-violet (UV) cross-linking;
3. To investigate methods of overcoming the problems of surface tension to produce scaffolds with a flat surface in PS and PDMS 96-well plates;
4. To investigate the morphology of the scaffolds by multi-photon fluorescence microscopy;
5. To investigate the chemical properties of the scaffolds by differential scanning calorimeter (DSC) and Fourier transform infra-red (FTIR);
6. To investigate the growth of three cell types (DLD-1, hMSCs, and fibroblasts) in collagen/chitosan scaffolds.

1.3 Scope of thesis

This research begins with a comprehensive literature review discussing the current state of tissue engineering, requirements, materials used, fabrication processes, substrates, and cell studies.

Chapter 3 introduces materials and methodologies applied during the course of this study, which include scaffolding materials and scaffold preparation, PDMS well plate fabrication, characterisation techniques employed, and lastly, *in vitro* cell studies used to assess the freeze-dried scaffolds. In particular, characterisation techniques include multi-photon microscope (MPM), FTIR, and DSC. Cell types used during *in vitro* studies were cancer cells DLD-1, human

mesenchymal stem cells (hMSCs) and fibroblasts. The method used to assess *in vitro* performance of cell proliferation is alamarBlue assay.

In chapter 4, development of scaffolds and implications of surface phenomena are discussed in detail in both PS and PDMS well plates. Optimisation of the scaffolds is then discussed. Results from MPM, FTIR, DSC and *in vitro* cell studies are presented followed by discussions.

In conclusion and future works, all results and analyses are consolidated to present a whole picture of this project, followed by future works where the author outlines the roadmap for future studies.

2. Literature Review

2.1 Needs for tissue engineering scaffolds

In the past decade, tissue engineering has emerged as a potentially viable solution to repair damaged tissue and restore its original functions. It has attracted the knowledge of biochemistry, cell biology, molecular biology and materials engineering to elucidate the right direction to address some current issues [14-15].

Tissue engineered scaffolds play an important role by mimicking the ECM to promote cell adhesion, proliferation and differentiation; and thus they serve as the site for cell regeneration [4]. Engineered 3D scaffolds function to support cell growth by providing a large surface area and porous structure within the 3D construct. The structure aims to provide support to cell adhesion, facilitate nutrients and waste transport, and possibly elicit cell-scaffold interactions [16]. Past research has demonstrated that a porosity of higher than 50 percent would be favourable for cell growth [17]. Greater interconnectedness is imperative for cell in-growth as it promotes transportation of nutrients and removal of waste; in addition, cell morphology may be affected by the shape and size of pores [18].

2.2 Three-dimensional scaffolds

In vitro cell studies are commonly conducted in two-dimensional (2D) monolayer culture. However, there has been an increasing emphasis on growing cells in a 3D environment to better understand the cellular responses in

conditions that mimic those *in vivo* [19-28]. Cellular activities are known to be related to communication, local chemical environment and geometry [29]. Cells need to be embedded in a structure that mimics the ECM and other biological cues in order to guide cell development [30]. In 3D culture, cells are able to adopt their native morphology, facilitate cell-cell contact as well as make interactions with the ECM [21]. The ECM is a support structure containing biological cues such as collagen, elastin, laminin and glycosylated proteins. Additionally, the receptors on the cell membrane, or cell-binding motifs, anchor to the ECM and determine how cells interpret the biochemical cues from their milieu [31-33]. An example in mind is RGD, or Arg-Gly-Asp tripeptide, which was identified as the sequence within fibronectin that mediates binding to integrin (e.g. β3 integrin) and cell attachment. This enables signalling between cells as well as cell patterning and differentiating [34].

3D scaffolds are developed to mimic these characteristics of the native ECM and promote cell proliferation until they produce their own ECM [16]. Living cells are harvested from donors' site and seeded into the constructs to proliferate and differentiate either *in vitro* or *in vivo*. Either way, cell growth is guided by the structure and properties of this man-made structure. However, culturing cells in 3D has introduced a large number of additional considerations not normally required in 2D monolayer culture. Scientific challenges remain both in the choice of materials for specific tissue engineering application and the method to fabricate those scaffolds in a controllable and reproducible manner.

To start with, there is a plethora of scaffolding materials for different tissue engineering applications. While metal and ceramics possess high tolerance and mechanical strength in load-bearing applications, they lack biocompatibility and biodegradability. Biocompatible polymers are commonly used in tissue engineering today, and most of them are adapted from other surgical applications such as suture, fixture, and controlled drug delivery system. In general, the polymeric materials can divided into synthetic polymers and natural polymers. Synthetic polymers such as polyglycolide are commonly used to make scaffolds; however, they are known to contravene biological interactions such as cell signalling [35]. Natural, or biologically-derived polymers, include ECM derivatives such as collagen, are superior in terms of biocompatibility and overall interaction with cells [36]. It has been suggested that the favourable interactions stem from the fact that natural polymers are found in animal body or plant, and hence there is high probability to promote cell growth [37]. However, variation of properties across different batches and contamination issues are inevitable drawbacks [38].

Another challenge in tissue engineering is to fabricate the materials into scaffolds with specific structural, morphological, chemical and physical requirements. Generally, fabrication process would contribute to the overall profile (i.e. thickness, shape, and surface) of the scaffolds on a macro-level; microscopically, pore size and distribution matter a great deal to mass transfer of nutrients and waste, and is often controllable by adjusting the fabrication parameters.

2.3 Requirements for 3D scaffolds

2.3.1 Porosity

Porosity is defined as the ratio of the volume of void space to the volume of the whole in a solid [42]. Porous structure is essential in 3D scaffolds as it allows proliferation and migration of cells to take place [43], and in the same time, enhances mechanical interlocking between the implanted scaffolds and the surrounding surfaces. Commonly used techniques employed to create pores in solid biomaterials are: salt leaching, gas forming, electrospinning, 3D printing and phase separation (e.g. freeze-drying). The optimal pore size is considered to be about 75-150 μm in diameter, depending on the specific application. Larger pores (150-200 μm) would likely result in substantial deterioration of the structure at early stage, while smaller pores (10-75 μm) would hinder cell migration [44].

2.3.2 Biodegradability

Biopolymers usually can be decomposed but their degraded by-products will remain inside the human body for a considerable amount of time. Two different modes of degradation are defined as follows:

1) hydrolysis which is mediated by water;

2) enzymatic degradation mediated by enzymes.

The advantages of biodegradable materials over their non-degradable counterparts include the reduction of stress shielding during the course of

application, and, in some specific applications, the alleviation of pain, due to lessened likelihood of adverse immunological responses [45].

2.3.3 Mechanical properties

For most native tissues, the metabolism of the cells, the organisation and synthesis of ECM, as well as degradation of the cells are all subject to mechanical loading and stresses from the surrounding environment. Tissue engineered scaffolds should be able to withstand applied stress from both internal sources and external sources before and during tissue re-growth to mimic the physiological loading environment. Furthermore, the impact experienced during implantation could have a significant effect on the scaffold. During scaffold degradation, the remaining structure must be able to offer the corresponding strength that is able to withstand stress loading in line with new tissue re-growth. If the structure of the scaffold is too weak, it would fail before neo-tissue re-growth is completed. If the structure of the scaffold is too strong, it would inhibit proper tissue functioning by providing stress-shielding [45].

2.3.4 Biocompatibility

Biocompatible generally means that the material in question is safe to use inside the human body and in the endogenous fluids without inducing inflammatory or immunogenicity reactions. The term refers to the behaviour of a biomaterial in a specific context, such as the ability to elicit appropriate certain host response. The material itself should not be toxic to native cells. In addition,

the by-products from the gradual degradation of the tissue engineering material should not cause any adverse effect [45].

2.3.5 Scaffold surface and morphology

An important parameter in terms of surface morphology is the pore size and distribution of the 3D scaffold in tissue engineering application. Optimisation of pore size and distribution has a big impact on cellular activities [46]. In the context of this study, this could be achieved by tailoring collagen and chitosan content in the polymer and altering the key parameters in the freeze-drying regime.

In addition, topological surface shape plays a vital role in cell/scaffold attachment. Past research has shown that initial cell-scaffold interactions may be categorized into four stages [47]:

1) Protein adsorption;
2) Initial contact made by rounded cells;
3) Cell attachments;
4) Flattening of cells.

Generally speaking, stage 1-3 reflects the first 90 or so minutes of interactions after cell seeding. In stage 4, a full flattening could be observed with the spreading of cells. After 24 h the cells are expected to be flat and to have started proliferating [48-52].

On a macro-level, flat surface is preferred in tissue engineering applications especially in thin constructs. Several studies in the past compared cell proliferation in bulk and cell-scaffold interaction during the initial cell seeding and concluded that there was a strong correlation [53-55]. In other words, while it was important to improve cell differentiation and proliferation in bulk, it was equally important to ensure favourable initial cell attachment during seeding. Therefore, top surface features of the scaffolds are bound to play a potentially much more significant role than previously thought. The same studies confirmed that cells generally favoured flat surface during cell seeding [53-55]. Scaffold with sharp features would cause seeded cells to distribute unevenly on the surface, which ultimately, leads to different speed in in-growth. In addition, surface feature produced without any control would not be suitable for scale-up applications. Difference in growth of cells and in transport of nutrients and waste caused by either a bowl-shaped or dome-shaped surface would add another layer of uncertainty into the experiments. In contrast, thick scaffolds would normally have no such issue as surface features would be insignificant comparing to the overall dimension.

2.4 Biomaterials for scaffolds

A number of biomaterials have been shown to produce 3D porous scaffolds for tissue engineering applications through a compatible fabrication technology. Biomaterials used in tissue engineering can be classified into two categories, namely, natural and synthetic biomaterials.

Natural material can be obtained from their natural sources. Natural material is a superior candidate for scaffolding materials because of its better biocompatibility and better overall interaction with cells. It has been suggested that the favourable interactions stem from the fact that natural polymers are found in human or animal body, and therefore an enhanced likelihood to promote cell re-growth. However, one common drawback with natural materials is their limited mechanical properties and thus some are unsuitable for load-bearing applications [56-60].

Synthetic material can be categorised into inorganic biomaterial such as ceramics, and organic biomaterial such as silicone rubber. Most synthetic scaffolds are inexpensive and superior in mechanical properties. However, biocompatibility could potentially become an issue for synthetic materials [61-64].

An ideal system is one which can be synthetically produced with chemical and physical properties that replicate all components of the natural system. Not all factors required to mimic the natural ECM are known and thus natural sources are more likely to provide the appropriate environment. For these reasons, natural materials were selected for experimental studies in the present work.

Some commonly used naturally derived polymers include agarose, alginate, fibronectin, hyaluronic acid, Matrigel, gelatin, fibrin, collagen and chitosan.

2.4.1 Agarose

Agarose is a polysaccharide usually extracted from seaweed. Many studies have demonstrated that agarose promotes the maintenance of the chondrocyte phenotype *in vitro*, therefore rendering it preferable for some tissue engineering applications [65-74]. It is non-toxic and inexpensive; however the material itself is mechanically weak. Another disadvantage of this material is that there is little evidence showing the ability to support adult hMSC proliferation and differentiation. Researchers suggested that agarose gels needed to be combined with other biomaterials, i.e. collagen, to support cell growth [72].

2.4.2 Alginate

Alginate, derived from brown seaweed, is inexpensive and biodegradable [75-83]. It has controllable porosity, and may be coupled to other biologically active molecules [84, 85]. The processing conditions of alginate gels are mild which also makes them attractive for tissue engineering applications. Alginate has been used successfully for the growth of rat MSCs, however, it has been shown that hMSCs do not proliferate in alginate gels [23, 86, 87]. Lawson et al. attempted to improve the functionality by combining alginate with various other materials including collagen, fibronectin, fibrin and chitosan [85]. The gel with the addition of collagen type I was the only one which resulted in cell attachment. However, there were observations that cells experienced unexpected prolongation in alginate beads, leading to possible explanation of immune

rejection. In addition, the purity of alginate cannot be confirmed, even in commercially available products [88].

2.4.3 Fibronectin

Fibronectin is a major ECM protein [86-89]. Ogura et al. [89] demonstrated the ability of hMSCs to adhere and proliferate in fibronectin on 2D surfaces, but when grown in 3D the cells did not attach [86]. Martino et al. [90] however, was able to alter cell interaction and stem cell differentiation on fibronectin by controlling the protein length. The primary usage for this biomaterial is for cell adhesion and signaling.

2.4.4 Hyaluronic acid

Hyaluronic acid is a chief component of the ECM of many connective tissues except bones [90]. This material plays a crucial role in some biological processes such as cell differentiation, proliferation and tissue hydration [91]. Hyaluronic acid has been successfully used for the adherence and proliferation of hMSCs [92, 93]. Using this material as a scaffold for hMSCs has been shown to promote differentiation by detection of collagen type II and other major molecules of the ECM [94-96].

2.4.5 Matrigel

Matrigel is a commercially available protein mixture secreted by a type of mouse tumour cells [97, 98]. Although successful in promoting cell adherence

and proliferation [97], Matrigel is expensive and the composition is not entirely known [99].

2.4.6 Gelatin

Gelatin is a protein produced by the denaturation of collagen, which can be obtained from various tissues including skin, bones, cartilage, and ligaments. It has many biological functional groups within its polypeptide backbone, thus making it beneficial for tissue engineering applications [100]. Gelatin is biodegradable, biocompatible, and has a high level of plasticity [100, 101]. Gelatin encourages hMSC adhesion, proliferation and differentiation [102], however, it has weak mechanical properties and dissolves in culture medium at 37 °C. To use gelatin, it must be bind to another material, such as chitosan, to improve the mechanical properties [103-104].

2.4.7 Fibrin

Fibrin is a protein involved in blood clotting mechanism. It is most often used as a biological adhesive to close small wound. hMSCs have been successfully cultured in fibrin gels [105-110], over time these cells are known to break down the fibrin into its degraded products, fibrinopeptides [110]. To create fibrin gel, fibrinogen monomers are cleaved with a catalyst, thrombin, and form fibrin monomers [110]. These are then assembled into fibrils, which eventually form fibres and a 3D network. In terms of application, fibrin is known to be effective for the short-term culturing of hMSCs [106-110].

2.4.8 Collagen

Collagen-based 3D porous scaffolds have been used in a number of tissue engineering applications due to its many favourable properties [111-124] and capability to promote cell attachment and proliferation [123]. Collagen is the major constituent of ECM, tendons and ligaments; and it is found in cartilage, skin, arteries [118-121].

There are circa 20 different types of collagen. Collagens commonly found in mammals are of type I, II and III [116]. Collagen type I discussed in the following paragraph is the one of the most abundant and extensively used types in tissue engineering applications due to its abundance [116].

Glycine, proline and hydroxyproline usually appear in the polypeptide chain of type I collagen. These three amino acids make up the repeating unit of Glycine-X-Y, where X and Y can be any amino acid [112].

The basic structural unit of collagen is a 300-nm-long, 1.5-nm-wide (in diameter) rod-like structure that consists of three polypeptide chains (Figure 1). Each chain consists of 1050 amino acids wound around one another in a right-handed triple-helical manner [112-116]. Many rod-like macromolecules pack side-by-side to form fibrils, stabilised by covalent bonding [112, 116-120]. The fibrils then bundle together and form fibres which are normally a few micrometre-long and 50 nm-wide (diameter).

In addition to its remarkable tensile strength, collagen type I has many other attractive characteristics, including: thermal stability, and the ability to engage in specific interactions with other biomolecules [118-123].

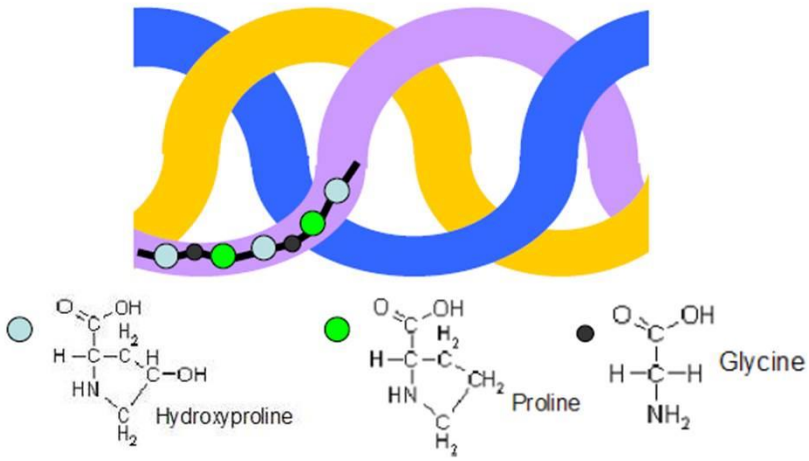

Figure 1: Common repeating motifs in type I collagen polypeptide chain, and three chains winding around one another to form the triple-helical structure in a rod-like fashion [112]

However, collagen is known to degrade rapidly and for this reason the addition of other biomaterials has been employed to produce collagen-based scaffolds with desirable features [125-128].

2.4.9 Chitosan

Chitosan is an amino polysaccharide (polu-1,4-D-glucosamine) made by treating crustacean shells with alkali sodium hydroxide through a process called deacetylation (figure 2). Since chitosan contains both hydroxyl and amino groups that can be easily modified or associated with other polymers, it is widely adopted as an addition to other natural polymers. Current applications involving chitosan include wound dressings and some drug-delivery systems [125].

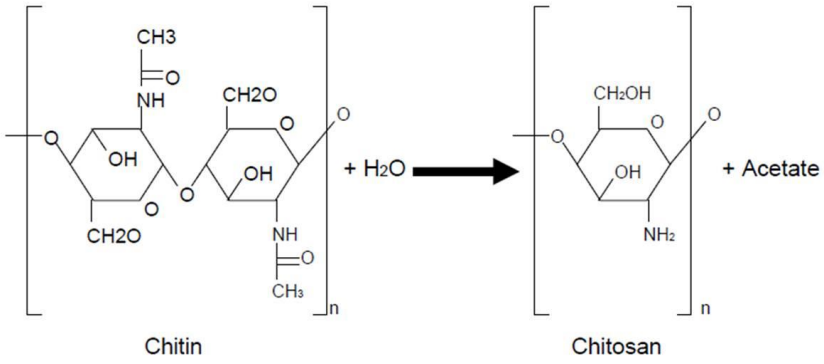

Figure 2: Deacetylation of chitin to chitosan; chitin and water react to yield chitosan and acetate [8]

2.4.10 Collagen and chitosan scaffolds

According to Domard and Taravel, two kinds of interactions can give rise to the interactions between collagen and chitosan when they are dissolved in solution [6]:

- Electrostatic force leading to the formation of polycation and polyanion complex.
- Hydrogen bonding would be formed between the two polymer molecules.

Tangsadthakun et al., investigated different compositions of collagen/chitosan mixture for 3D scaffolds and they concluded that the addition of chitosan could prolong the time to degrade the scaffolds [8]. During their FTIR analyses, they found that the intensity of the characteristic peak of chitosan increased when the concentration of chitosan was increased in the collagen/chitosan scaffold. They

further concluded that the compressive moduli of those 3D scaffolds gradually decreased with increased chitosan concentration [9].

Past studies have revealed that collagen/chitosan scaffolds have a wide range of applications in tissue engineering due to their interactions in polymer solution, and favourable combined properties [5, 7, 127, 128].

2.5 Scaffolds fabrication

Fabrication methods are crucial for scaffolds to support cell growth. Common methods to create 3D porous constructs have been developed in the past years which include salt-leaching, gas-foaming, electrospinning, 3D-printing, and freeze-drying [129-130]. The following section briefly introduces each technique and discusses pros and cons.

2.5.1 Salt leaching

In salt leaching, macromolecules are dissolved in an organic solvent. Salt particles of specific size are added to the mixture. The mixture is then either casted onto a platform to form a membrane or into a mould to produce a scaffold. Upon solvent evaporation, the mixture is left with macromolecules and salt particles. The salt particles are then leached away, leaving a porous membrane or a 3D porous construct [131]. The process is illustrated in figure 3. The resulting membrane or scaffold has equiaxed pores, uniformly distributed [132].

Advantages of salt leaching include controlled porosity and control of pore size as the size of the particulates could be tailored to meet the specification. Disadvantages are:

1) Lack of required strength for load-bearing application;

2) Salt residue may be harmful to the cells.

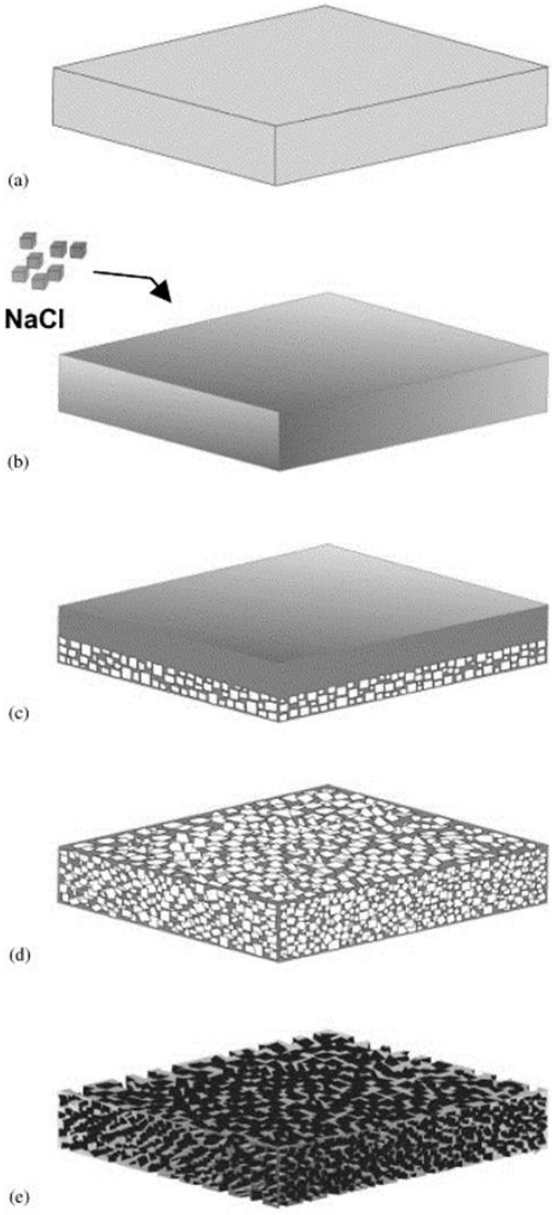

Figure 3: Illustration of the salt leaching technique; a) polymer dissolved in an organic solvent; b) salt, in this case NaCl, is added into the mixture; c) and d) Solvent evaporation; and e) salt particles dissolved to form a porous structure [132]

2.5.2 Gas foaming

Some of the fabrication processes in tissue engineering require use of various chemicals. The chemical residual after completion of the process could be detrimental to cells. Gas foaming (Figure 4) does not require the use of solvent and high temperature. In particular, the technique employs high pressure carbon dioxide gas at high pressure to saturate the polymer with gas [133, 134]. Carbon dioxide gas molecules cluster inside the scaffold until they reach equilibrium. Nucleation is initiated upon reducing the high pressure and 3D porous structure is formed upon completion of de-pressurisation [134, 135].

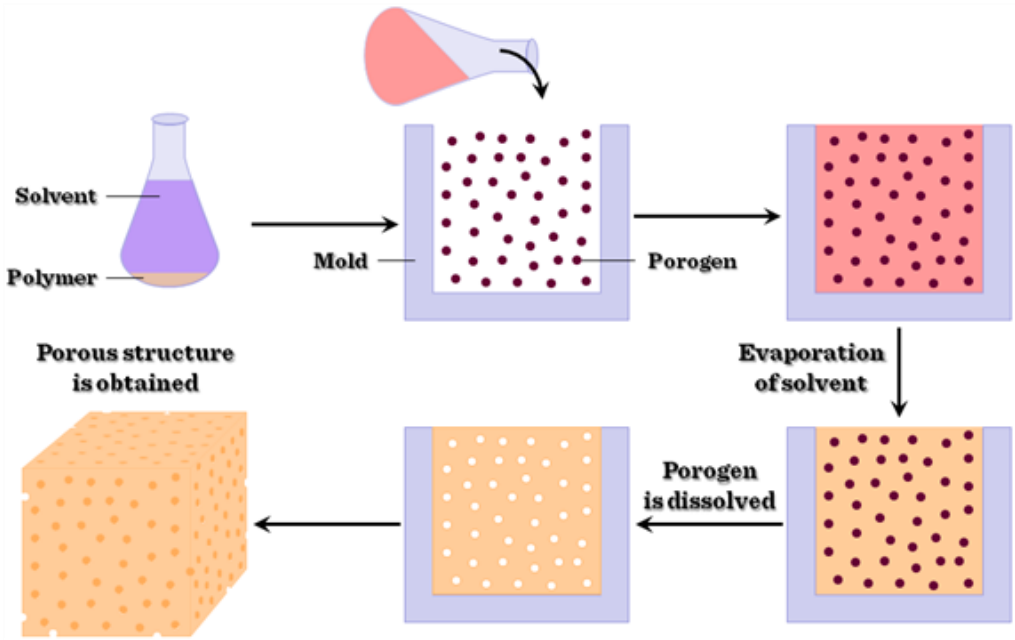

Figure 4: Schematic illustration of the gas forming technique [135]

The main issue associated with gas forming is that pores do not form inter-connected structures.

2.5.3 Electrospinning

Electrospinning has been widely adopted to fabricate polymers into orderly structures. Materials used include natural polymers, synthetic polymers, and co-polymers made up of natural and synthetic polymers. [136-138].

Electrospinning uses an accelerating voltage to draw fibres from a liquid (Figure 5). This process is particularly suited to the production of fibres with strict geometry and structure requirement. Limitations of this technique include limited application on material type and controlling difficulties during the manufacturing process. Variables during the process such as fibre diameter, degree of anisotropy can be controlled by regulating the composition and viscosity of the solution, the air-gap distance, voltage and mandrel properties [136, 139-143]. Polymers and their additives could be electrospun into fibres similar but not quite the same to that of the native ECM [144].

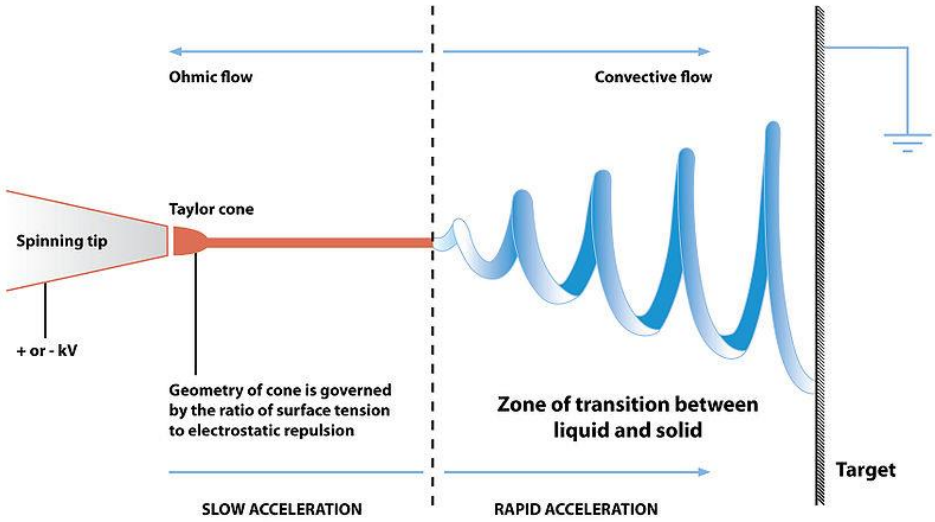

Figure 5: Illustration of electrospinning principles; high voltage is applied at the spinning tip which stretches the polymer liquid droplet and ultimately a stream erupts at Taylor cone; the jet is elongated by electrostatic repulsion until it finally hits the target collector [136]

2.5.4 3D printing

3D printing was derived from ink-jet printing technology. It functions by writing a binder solution onto composite materials with regard to precise CAD data [145, 146]. The process is repeated layer by layer until the 3D structure is completed and a final sintering step is usually followed [147-148].

This technology is still in its nascent development and applications are limited.

2.5.5 Freeze-drying

Freeze-drying, or lyophilisation, is a method of drying the scaffolds by freezing the water components and then directly subliming the water to vapour phase by exposure to low pressure [123]. The scaffold is frozen in a controlled

manner before undergoing drying to control the size of the ice crystals. While fast freezing there is less damage to the scaffold during the sublimation process, but consequently results in smaller pores. Slower freezing allows time for the ice crystals to grow and results in larger pores. The polymer solution solidifies during pre-defined cooling stage and forms solute-rich and solvent-rich phases. After solidification, ice crystals are sublimed under high vacuum [149-156]. Temperature higher than the freezing temperature of the solution needs to be maintained in the freeze-dryer chamber as to provide energy for ice sublimation. A secondary drying step is usually needed to evaporate residual moisture in the matrices. It is already known that. freezing temperature, cooling rate, chamber pressure, primary and secondary drying rate, as well as the composition of the polymer have influence on pore size and distribution of the porous scaffold, as well as interconnectedness [156-158]. In addition, cross-linking mechanism needs to be fine-tuned to produce a gel with suitable mechanical properties, and in the meantime, without risking its biocompability [155]. Generally, the whole cycle consisted of three stages that may partially overlap:

1) The collagen/chitosan solution, was frozen on refrigerated shelf inside the lyophiliser (freezing);
2) The shelf temperature was maintained at a predetermined value and the ice was sublimed upon lowered chamber pressure (primary drying);
3) Residual water remained in the scaffold was dried by an increase shelf temperature (secondary drying).

Only shelf temperature, chamber pressure and time could be directly controlled. Other variables, such as cooling time, annealing, and primary drying were controlled indirectly by these three primary variables.

The setting of the three primary variables required knowledge of:

1) The freezing temperature;
2) The chamber pressure;
3) The time required for primary drying to complete.

The following paragraphs will discuss the process in more detail.

Cooling

During cooling, the temperature of the collagen/chitosan solution continues to drop once the solution underwent a critical point, T_g', the glass transition temperature of collagen/chitosan polymer mixture in solution. The product now constituted of interconnected ice crystals distributed in the frozen mixture.

Primary drying

During primary drying, heat is supplied from the shelf to the polymer. If the shelf temperature is too high, ice would melt, causing structural collapse. If the temperature is not high enough, the heat transfer rate would not be sufficient to initiate ice sublimation.

During primary drying, chamber pressure mainly contributed to the removal of sublimed water molecules in air.

Secondary drying

During this last stage of the lyophilisation cycle, any dissolved or remaining water in the mixture is removed. This process is not easily quantifiable and thus it is customary to set the shelf temperature to room temperature.

2.6 Substrate

A micro-well plate, or just microplate, is used as a standardised testing tool in laboratories [159, 160]. A microplate typically has 6, 24, 96, 384, or 1536 wells arranged in a 2:3 rectangular matrix [159].

The most commonly used material in microplate is polystyrene. It can be coloured by different additives during manufacturing process [159-161]. Polypropylene is best suited for experiments subject to wide changes in temperature, such as thermal cycling [160]. Polycarbonate is cheap and easy to mould and has been used for DNA amplification reactions [160].

Injection moulding is normally used for polystyrene and polypropylene. Polycarbonate is manufactured by vacuum forming [160, 162-165]. PDMS microplates are usually made on site involving a curing process in a master mould, which will be discussed in detail in chapter 3.1.3.

2.6.1 Polystyrene

Polystyrene is a synthetic polymer made from the monomer styrene. It is naturally transparent, hard, brittle and inexpensive. Polystyrene displays typical thermoplastic polymeric behaviour, i.e. it is solid at room temperature, and liquid when heated above 100 °C and becomes solid again when cooled. This

temperature behaviour is exploited for injection moulding during manufacturing [162, 163]. Polystyrene multi-well plates used in biological laboratories offer excellent optical and thermal properties. They are non-toxic and chemically inert in most cases and appropriate for general purposes [164, 165].

2.6.2 PDMS

PDMS is a member of the siloxane family that is transparent, chemically inert, biocompatible, thermally stable, non-toxic, permeable to gases, simple to handle [166-171]. In addition, it has been traditionally used in a number of biomedical applications such as catheters, drainage tubing, and ear and nose implants [166, 172, 173, 174-180].

Its compatibility with current system of glass and polystyrene culture wares renders it an ideal substitute for the current system and yet maintains its flexibility while in use. Its optical property makes it able to be used with optical and fluorescence microscopy without much hassle to adjust the system [174-177, 181-182]. PDMS is essentially a network of hydrophobic dimenthysiloxane oligomers. $SiO(CH_3)_2$ is the key functional group in the synthesis of PDMS (Figure 6). The polymer has recently been the focus of microfluidic perfusion bioreactors.

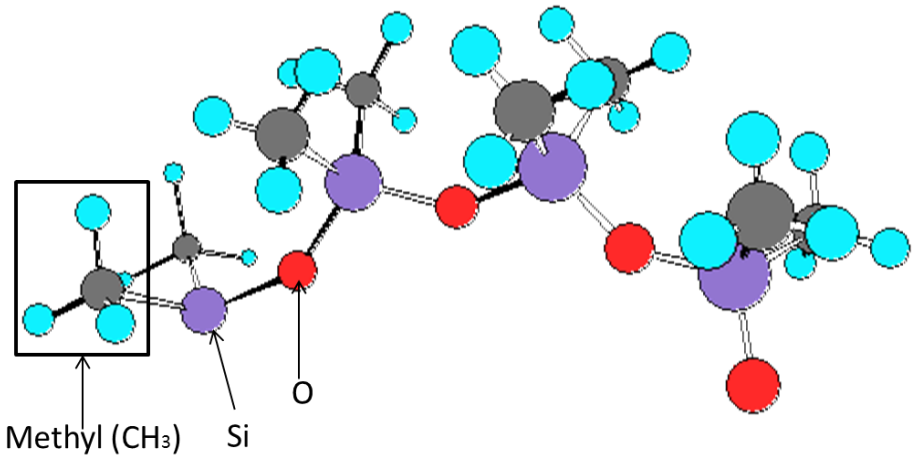

Figure 6: Illustration of PDMS polymer chain, showing methyl (grey and blue block), silicon (purple), and oxygen (red) [182]

2.6.2.1 Application of PDMS --- bioreactors

In static culture, poor diffusion is probably the single most limiting factor for transport of nutrients and wastes. This would in turn, limit the size of the scaffold under static culture, as previous studies have shown, cells were only able to reach a depth of 250 mm [178-181]. Therefore, different dynamic culture techniques have been attempted: orbital shaker [179, 182]; rotating wall vessel bioreactor [179, 183, 184]; spinner flask [179, 184, 185]; perfusion bioreactor [179, 185, 186]. The most prominent advantage posed by dynamic culture is that the shear stress resulting from flows acts as mechanical stimulus to the cells and studies have shown that it has a positive effect on cellular activities [187-190].

The interest in perfusion bioreactors has been rapidly developing as it enables the study of cell-cell and cell-matrix interaction on a small scale at relatively low cost. The bioreactor is essentially a vessel in which biochemical process is

carried out either aerobically or anaerobically with organisms and biochemical [191-193]. Channels and culture wells can be designed for specific needs depending on the particular area of research. Microfluidic pumping systems may be incorporated into the design of the bioreactor [194-196].

2.7 *In vitro* 3D cell culture

2.7.1 3D culture of cancer cells

Traditionally, the culture of cancer cells in 2D environment was known to mask several biological activity signals [197-199], which means that cancer cells growing on a 2D substrate would exhibit altered behaviour. 3D culture, on the other hand, more close replicates the intra-tumoral environment *in vivo* [198, 200]. Prior to the adoption of 3D culture, the study of tumourigenesis has been impaired significantly by limitations inherent to existing 2D system. In addition, 3D system is able to maintain co-culture involving other cells such as endothelial cells, fibroblasts and immune-competent cells [201-205].

Collagen-based 3D scaffold could offer satisfactory environment for the study of cancer cell proliferation *in vitro*. Due to the varied behaviour of cancer cells, i.e. some can metastasize rather rapidly while others may take many years to become invasive, 3D culture system should accommodate the dynamic nature of cancer cells [206-209].

2.7.2 3D culture of human mesenchymal stem cells

hMSCs are multi-potential cells that can differentiate into a number of tissue types such as bone, cartilage, fat and muscle when induced by appropriate biological cues [210-218]. hMSCs are regarded as excellent source of cells due to their osteogenic potential [212, 219, 220].

However, culturing hMSCs in 3D scaffolds is not as straight-forward as it seems. Collagen has proven to be a preferred candidate among many scaffolding materials for this purpose. Type I collagen is the single most abundant ECM protein [221-227]. On the other hand, excessive contraction of collagen scaffolds observed during culture greatly limits the size of the construct after prolonged period of culture [218, 226-230].

2.7.3 3D culture of fibroblasts

The major functions of fibroblast cells are to maintain, organise and synthesise into connective tissue during development and response to injury and disease [231]. The ability to carry out these functions depends on the capability of the cellular response to external stress [213-233]. If cultured inside a 3D scaffold, fibroblasts experience an environment closer to that of the native physiological environment and exhibit completely different geometry than those on 2D culture.

In addition, the final presentation of fibroblasts in 3D culture depends not only on the extent of cell migration but also on the capability of ECM re-modeling by fibroblasts [231-234]. Tissue formation depends not only on the functioning of a

collection of fibroblasts but also on the reciprocity of the interactions that happen between cells and ECM [235].

2.7.4 alamarBlue assay

alamarBlue assay is a water-soluble, commercially available organic dye that has been widely used to quantify viability of cells *in vitro* [236, 237]. It is non-toxic and stable at culturing conditions (i.e. at 37 ℃, 5% v/v CO_2 in air). Thus it makes continuous monitoring of cell growth over time possible.

It is essentially a fluorometric/colorimetric indicator based on the state of oxidation-reduction. In particular, it indicates metabolic activity based on cellular growth [236-240]. As cells grow, it results in a reduction reaction of alamarBlue, and hence causes the fluorescence to change from oxidised blue to reduced red [237, 241, 242].

2.8 Summary

The emergence of 3D culture, presented both opportunities and challenges in tissue engineering. The ultimate goal of scaffold design is to produce a temporary support to act as ECM until native cells re-occupy the vacant sites and replace the structure with newly-synthesized ECM [235]. But a major challenge with growing cells in 3D culture *in vitro* is to ensure that all cells receive an adequate supply of nutrients. For this reason, scaffolds are designed to be porous, and thin to reduce the mass transport requirement. Various biomaterials and fabrication techniques have been presented above, and their pros and cons

discussed. In addition, substrate used in 3D culture in small-sized well plate, namely, PS and PDMS, were discussed above. Furthermore, the usage of PDMS as bioreactors was also presented above to shed light on the application of this polymer in tissue engineering. The purpose of this study was therefore to make and optimise 3D scaffolds in PS and PDMS 96-well plates for basic research. In this study, the scaffolds were to be fabricated by freeze-drying technique. Collagen was chosen as the major component to make scaffolds in this study as it is the main constituent of ECM and has huge potential in terms of biocompatibility and biodegradability. In addition, chitosan was used to add strength to the structure of the constructs. Cross-linking by ultra-violet radiation was employed to further strengthen the construct. Moreover, three cell lines, all discussed above in this chapter, were to be used to assess the performance of the scaffolds *in vitro*.

3. Materials and Methods

3.1 Materials

3.1.1 Collagen

Type I collagen solution from rat-tail was purchased from Sigma-Aldrich with a concentration of 5 mg/ml (equivalent to 0.5 wt.%). The product was supplied as an aqueous solution in 20 mM acetic acid at 4 ^{0}C. The collagen solution was stored in a refrigerator.

3.1.2 Chitosan

Chitosan from crab shells was purchased from Sigma-Aldrich in powder form and was kept at room temperature.

3.1.3 PDMS 96-well plates

A master mould was built by the workshop in Department of Engineering as shown in figure 7.

Figure 7: PDMS 96-well master mold [163]

Silicone elastomer and silicon elastomer curing agent (both from Dow Corning) was mixed at 10:1 weight ratio and mixed thoroughly. Degassing was performed in a vacuum chamber and the content was poured into the master mold. The content was heated at 60 ^{0}C inside an oven for 24 hours. Previous studies carried out by Japanese researchers [243, 244] have suggested an elevated oven temperature of over 80 ^{0}C and much shorter curing time. However, during this research, the author noticed that the PDMS well-plate, due to its intricate structures, was extremely fragile when separating from the master mold. In fact, when cured for 12 hours and at 80 ^{0}C, the PDMS well plate usually broke off upon separation from the master mould. It was therefore decided that the oven temperature was best to be kept at 60 ^{0}C and cured for 24 hours. PDMS 96-well plates (dimensions shown in figure 8) were kept at room temperature.

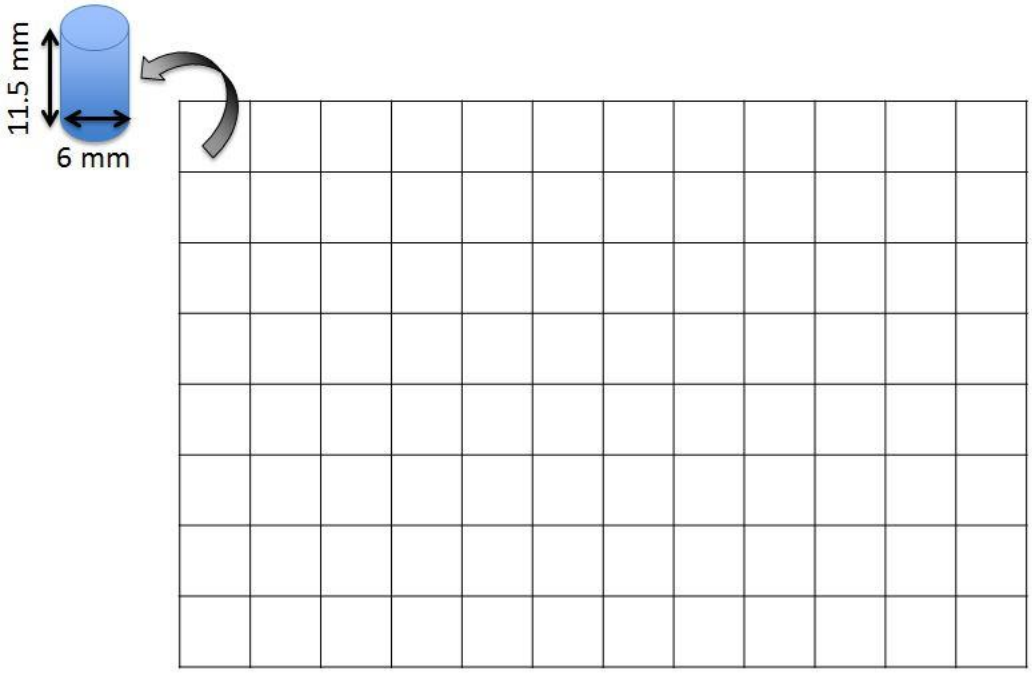

Figure 8: Dimensions of 96-well plate [178]

3.2 Scaffold preparation

Chitosan solution was prepared by dissolving 5 mg chitosan powder into 1 ml of 20 mM acetic acid and stirring for 4 hr until complete dissolution was achieved. The solution was then mixed with collagen solution and/or acetic acid to achieve the desired concentration and composition (chitosan content). 0.5 wt.% pure chitosan and 0.5 wt.% pure collagen solutions were prepared as references in the experiments.

The mixing ratios of collagen/chitosan solution and their absolute concentrations are listed in table 1.

Table 1: Experimental matrix

	% of chitosan	0%	10%	30%	50%	70%	100%
Overall conc.	**Collagen:chitosan**	Collagen	9:1	7:3	5:5	3:7	Chitosan
0.5 wt%	Absolute conc. of collagen	0.5 wt%	0.45 wt%	0.35 wt%	0.25 wt%	0.15 wt%	0
	Absolute conc. of chitosan	0	0.05 wt%	0.15 wt%	0.25 wt%	0.35 wt%	0.5 wt%
0.4 wt%	Absolute conc. of collagen	0.4 wt%	0.36 wt%	0.28 wt%	0.2 wt%	0.12 wt%	0
	Absolute conc. of chitosan	0	0.04 wt%	0.12 wt%	0.2 wt%	0.28 wt%	0.4 wt%
0.3 wt%	Absolute conc. of collagen	0.3 wt%	0.27 wt%	0.21 wt%	0.15 wt%	0.09 wt%	0
	Absolute conc. of chitosan	0	0.03 wt%	0.09 wt%	0.15 wt%	0.21 wt%	0.3 wt%
0.2 wt%	Absolute conc. of collagen	0.2 wt%	0.18 wt%	0.14 wt%	0.1 wt%	0.06 wt%	0
	Absolute conc. of chitosan	0	0.02 wt%	0.06 wt%	0.1 wt%	0.14 wt%	0.2 wt%
0.1 wt%	Absolute conc. of collagen	0.1 wt%	0.09 wt%	0.07 wt%	0.05 wt%	0.03 wt%	0
	Absolute conc. of chitosan	0	0.01 wt%	0.03 wt%	0.05 wt%	0.07 wt%	0.1 wt%

The polymer solutions were mixed thoroughly using a Vortex shaker to form homogeneous disperse solutions and then degassed under vacuum for 30 min.

Each of the 96-well plates (see figure 8 for dimension) was to receive collagen/chitosan solution with a particular mixing ratio, e.g. 30% chitosan. Moreover, five different concentrations were present in the same well plate in five blocks as shown in figure 9 below.

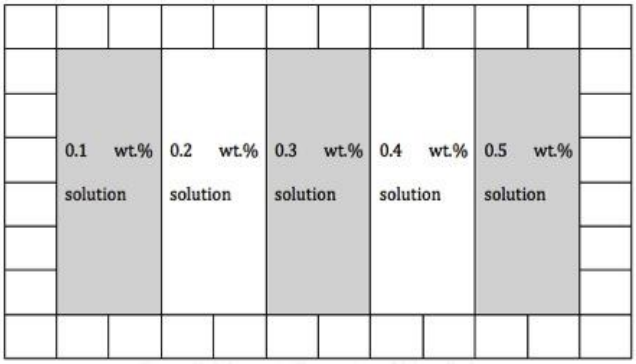

Figure 9: Schematic illustration of partition of the 96-well plate for five groups of polymer solutions during the experiment

An average of 40 µl of collagen/chitosan solution was pipetted into each well, which translated into scaffolds with the thickness of approximately 1 mm.

3.2.1 Cross-linking of scaffolds.

Polymer solutions were subject to 254 nm UV light for 30 minutes for cross-linking to take place before freeze-drying.

3.2.2 Freeze-drying of scaffolds

The freeze-drying technique was selected as the only fabrication technique for this study as it is simple, widely adopted and easy to control [123, 124]. The protocol used for freeze-drying of collagen-based scaffolds in PS and PDMS are the same in principle, with some tweaks in PDMS (which will be discussed later in chapter 4.5.5). Freeze-drying protocols used in PS and PDMS 96-well plate are presented in table 2 and table 3 respectively.

Table 2: Freeze-drying protocol used in PS 96-well plate

Stage	Step	Temperature (°C)	Time (min)	Status (R or H)
Cooling	1	20	5	H
	2	5	15	R
	3	5	15	H
	4	-5	10	R
	5	-5	15	H
	6	-40	70	R
	7	-40	60	H
Primary drying	8	-40	5	H
	9	-5	70	R
	10	-5	1020	H
Secondary drying	11	20	100	R
	12	20	360	H

*R: Ramp; H: Hold

Table 3: Freeze-drying protocol used in PDMS 96-well plate

Stage	Step	Temperature (°C)	Time (min)	Status (R or H)
Cooling	1	20	1	H
	2	-5	5	R
	3	-5	20	H
	5	-40	70	R
	6	-40	60	H
Primary drying	7	-40	5	H
	8	-5	70	R
	9	-5	1020	H
Secondary drying	10	20	100	R
	11	20	360	H
		*R: Ramp; H: Hold		

In PS wells, the polymer solutions were on hold at 20°C during cooling to stabilize the environment before the cycle kicked off. The chamber temperature was then gradually lowered to -40°C with two holding intervals at 5°C and -5°C to again stabilize the environment in the chamber. -40°C was chosen to ensure that the water would sublime later from solid to vapour and would not melt. The collagen/chitosan solutions were solidified at this stage and formed polymer-rich phase and ice crystal phase.

When the scaffold was completely frozen at -40°C, the primary drying phase began. At this stage the pressure was reduced to 0.1 mBar and the temperature raised to -5°C. The increase in temperature supplied energy in the form of heat to cause the frozen water to sublime under reduced chamber pressure.

In secondary drying stage, the temperature was raised further to break any connection that the water molecules may have made with the scaffolds.

For scaffolds in PDMS wells, some tweaks were made (detailed explanation in chapter 4.5.5) to take into account the nature of PDMS material with the aim to optimise and streamline the freeze-drying process (Table 3).

The only difference between freeze-drying protocol in PS wells and PDMS wells was the rapid cooling stage at the beginning in PDMS wells. During cooling, the temperature was lowered from room temperature to -5 °C in 5 min, and then stabilized for another 20 min. The rest of the protocol was the same for both substrates.

3.3 Morphology

Morphology, both on the surface and in the bulk, of collagen/chitosan scaffolds was analysed using a Bio-Rad Radiance 2011MP multi-photon fluorescence microscope (MPM) at 20X magnification. The main advantage of MPM is its ability to image turbid tissues or constructs.

In brief, the MPM used in this study was an upright Nikon E600FN microscope coupled to a multi-photon dedicated Bio-Rad Radiance 2100MP laser scanning imaging system. The schematic of the MPM system is shown in figure 10 below.

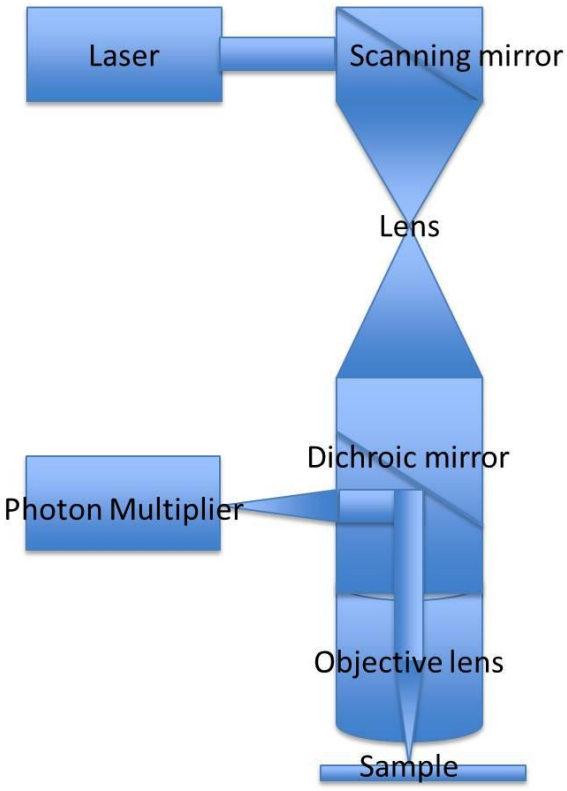

Figure 10: Schematic illustration of MPM

The upright configuration allowed the use of high numerical aperture and long working distance lens to ensure a highly efficient transmission path from the laser to the sample. Collagen/chitosan scaffolds were carefully removed from the wells without incurring too much damage to the overall structure. To avoid additional damage to the scaffolds during laser scanning, a low power laser beam with fast scanning speed was preferred. The 3D images generated then went through deconvolution using AutoQuant X3 imaging software. Components of the MPM used in this study are shown in figure 11, which include Nikon microscope and BioRad Radiance 2100 for scanning; MIRA laser, Verdi laser power supply for laser generation; the beam conditioning unit, spectrum analyser and oscilloscope for regulating the laser beam; and a chiller to cool down the system.

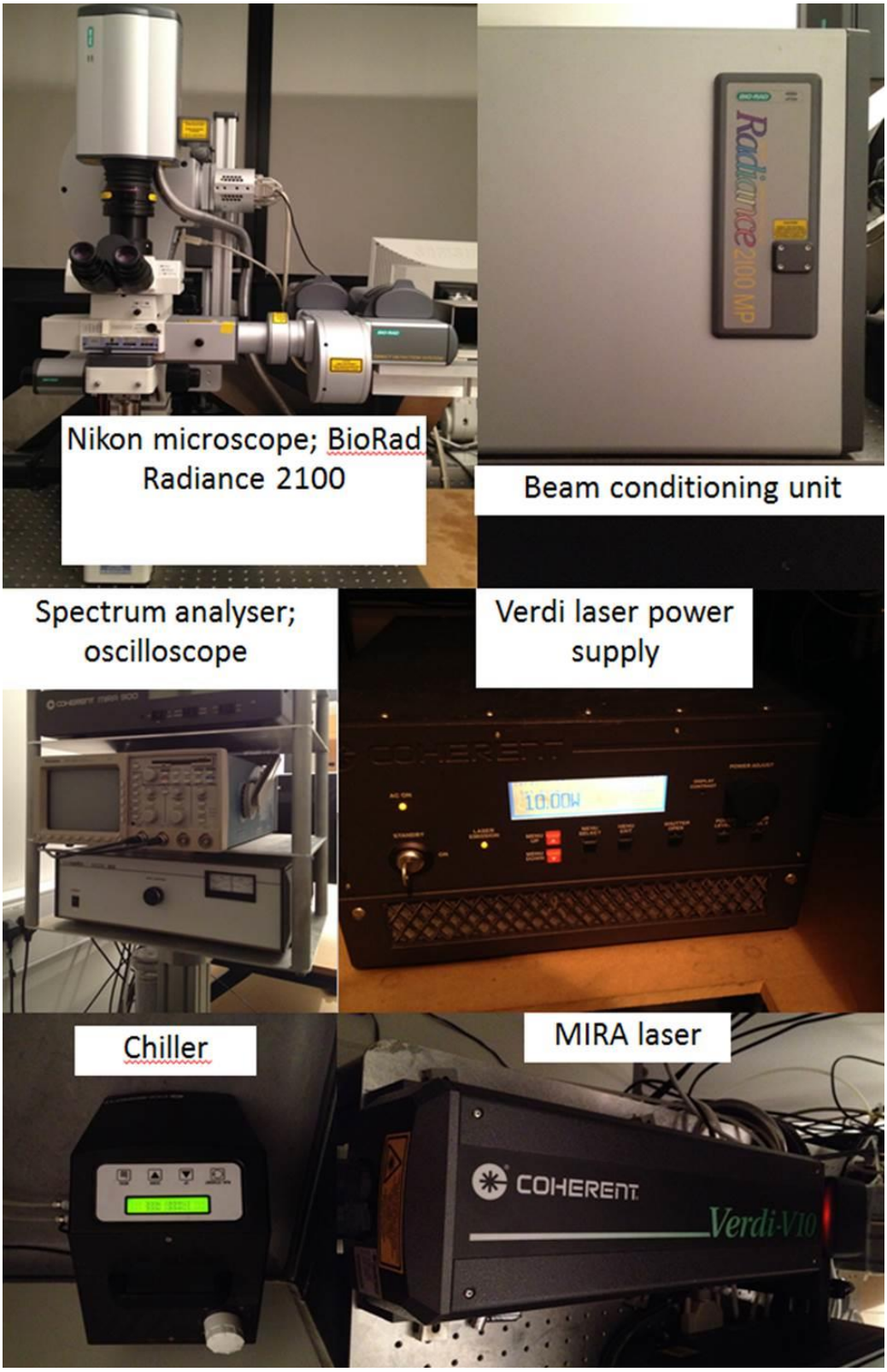

Figure 11: Components of MPM used in this research

3.4 Pore size

MPM was used to study the pore distribution of the collagen/chitosan scaffolds. The images generated by this technique were probably a better presentation of the true structure of the constructs, as it could take 3D snapshots of structures within the scaffolds without cutting through the constructs.

To determine the average pore size and distribution of the scaffolds, MPM 3D images were taken for three scaffolds from each sample group (same composition and concentration). For each of the 3D images, 200 random locations (pores) were selected. Each pore diameter were measured using a diameter measurement tool in NIS-Elements Suite.

3.5 Fourier transform infra-red spectroscopy

A Bruker Tensor 37 FTIR was used in this study to obtain the transmission and absorption wave spectra by emitting infra-red beam onto the sample and calculating its respective interactions with the beam.

The FTIR machine was pre-cooled using liquid nitrogen prior to use. A scaffold was taken out from the well and grinded in a mortar until it reached its powdery form. The powder was then transferred into the sample pan and pressed gently and evenly. A reference scan was performed prior to the sample pan being loaded into the FTIR machine. The samples were then loaded onto the sample platform for characterization. Information on the absorption band of collagen/chitosan scaffolds was collected and analysed by OPUS software.

3.6 Differential scanning calorimeter analysis

A TA Instruments® Q2000 differential scanning calorimeter (DSC) was used to determine the amount of heat required to increase the temperature of the sample. Heat flow from both the reference and the sample were measured against temperature rise, and a plot of heat versus temperature was produced using TA Universal Analysis software.

Scaffolds were taken out of the wells and placed into T-Zero aluminum pans. Empty pans and pans with sample scaffolds were weighted prior to differential scanning calorimeter (DSC) experiments. An empty sealed aluminum pan served as reference sample during the analysis.

3.7 Cell culturing

All cell lines were obtained from the cell bank in the laboratory. Culture PS 96-well plates, flasks, pipettes and other consumables were purchased from Falcon Fahrenheit (Milton Keynes, UK) unless otherwise stated. Cells were maintained under standard culture conditions of 5% v/v CO_2 in air and at 37 ℃ with medium renewed every second day. Culturing medium used was Dulbecco's modified Eagle medium (DMEM) high glucose (4500 mg/l glucose and 580 mg/l L-Glutamine), with 10% v/v foetal bovine serum (FBS) (≤250 mg/l hemoglobin) from Sigma-Aldrich (Dorset, UK), and 1% v/v penicillin streptomycin (PenStrep) (5000 units/ml of penicillin and 5000 µg/ml of streptomycin) (the combination will be referred to as "*culture medium*").

To wrap up, initial concentration of chemicals and their final concentration after mixing are listed in table 4.

Table 4: Initial and final concentration of chemicals used in cell studies

	Initial concentration	Final concentration
Glucose (in DMEM)	4.5 mg/ml	4.5 mg/ml
L-Glutamine (in DMEM)	0.58 mg/ml	0.58 mg/ml
FBS	≤ 0.25 mg/ml	≤ 0.025 mg/ml
Penicillin (in PenStrep)	5000 units/ml	50 units/ml
Streptomycin (in PenStrep)	5 mg/ml	0.05 mg/ml

3.8 Disintegration

Samples were immersed in *culture medium* in PS or PDMS 96-well plates in standard culture environment (37° C, 5% v/v CO_2 in air). No enzyme was presence as the aim of this study was to establish the hydrolytic degradation characteristics. Each scaffold was dried and weighted every four days, and put back into a fresh *culture medium*. The weight was compared with initial weight to determine the hydrolytic degradation profile.

3.9 3D culture of cancer cells DLD-1

External surfaces were decontaminated using 70% v/v ethanol. 25 ml of *culture medium* were added to a 75 cm^2 flask and the flask was allowed to equilibrate at 37 ℃, in 5% v/v CO_2 in air, incubator for at least 30 minutes. Cryo-

preserved vials containing DLD-1 cells with passage number 20 from the cell bank were removed from the nitrogen tank and wiped with 70% v/v ethanol before opening. In the sterilised, laminar flow hood, the caps of the vials were briefly twisted a quarter turn to relieve pressure, then retightened again. The vials were then thawed in 37 ℃ water bath for 2 min. The vials were then wiped with 70% v/v ethanol again and transferred into the laminar hood. The thawed cell suspension were pipetted into 5 ml of temperature-equilibrated *culture medium* in a test tube and centrifuged at 800 rpm for 5 min at room temperature. Cell pellet was obtained after centrifuge and gently re-suspended in a minimum volume of temperature equilibrated *culture medium* by pipetting up and down gently several times. Total number of viable cells was counted using a hemocytometer. According to the recommended cell seeding density of 5,000 - 6,000 cells/cm^2, 400,000 cells were added to each temperature-equilibrated 75 cm^2flask and gently rocked to disperse the cell suspension over the surface. The flasks were incubated at 37 ℃, in 5% v/v CO_2 in air. At day-1, aseptically all non-adherent cells and spent medium were removed from the flasks and fresh *culture medium* was added. The medium was then changed every second day.

Maintenance

Spent medium was removed gently and completely from the flask and replaced with an equal volume of temperature-equilibrated fresh *culture medium* and the flask was returned to the incubator after spraying with 70% v/v ethanol.

Sub-culturing

When the culturing flask reached 80% confluency, spent medium from the flask was removed. The attached cell layer in the flask was washed with Dulbecco's phosphate buffered solution (PBS). In particular, PBS was added to the side of the flask opposite the attached cell layer, and rinsed by rocking the flask back and forth several times. Washed solution was aseptically discarded. 5 ml of Gibco trypsin/ ethylenediaminetetraacetic acid (EDTA) (0.025% v/v trypsin and 0.01% v/v EDTA in PBS) solution was added to cover the cell layer followed by gently rocking to ensure that the cells were completely covered by the trypsin solution. The flask was then incubated at 37 ℃, in 5% v/v CO_2 in air for 5 minutes, and observed under a light microscope. If the cells were less than 90% detached, continue incubating and observing every 3 min; and gently tapping the flasks to expedite cell detachment.

Once ≥ 90% of the cells were round and detached, 5 ml of temperature-equilibrated fresh *culture medium* was added to each flask and pipetted over the cell layer surface several times to neutralise the trypsin solution.

Cells were centrifuged at approximately 800 rpm for 5 min at room temperature and re-suspended in a minimal volume of temperature-equilibrated *culture medium*. Cells were counted using a hemacytometer and if necessary, the suspension was diluted with *culture medium* and added to temperature-equilibrated 175 cm^2 flask to accommodate for the expansion of cells.

3.10 3D culture of hMSCs

50 ml SingleQuots of mesenchymal cell growth supplements (MCGS) were added into 500 mL *culture medium* prepared prior to the experiment. The mixture would be referred to as *hMSC growth medium*. hMSCs from the cell bank with passage number 8 were used in this experiment. The rest of the procedure was exactly the same as that used for DLD-1 cells in Chapter 3.8, with two exceptions. The first one being the use of *hMSC growth medium* for culturing of cells; and the second one being the use of 75 cm^2 culturing flasks throughout, even after subculturing. As hMSCs grew relatively slow and a larger flask would make the cell density too low to sustain.

3.11 3D culture of fibroblasts

Fibroblasts obtained from the cell bank in liquid nitrogen tank with passage number 9 were used in this study. Cell culture procedure for fibroblasts was the same as that for DLD-1 cells in Chapter 3.8.

3.12 Sterilisation

Scaffolds and well-plates used in cell studies must be either manufactured aseptically or sterilised prior to use. For practical reasons, the freeze-dried scaffolds were fabricated in a non-sterilised environment, thus a non-destructive and efficient sterilisation method was needed.

PS or PDMS 96-well plates as well as their encased scaffolds were subject to sterilization under 254 nm UV light for 30 minutes prior to *in vitro* cell studies.

All other tools, consumables, solutions and chemicals entering the laminar hood were separately sterilised either by autoclave or by spraying 70% v/v ethanol.

3.13 Seeding into 3D culture

Before seeding, the scaffolds were pre-wetted overnight with 50 µl *culture medium* (or in the case of hMSCs, *hMSC growth medium*) in each well.

Spent medium from the confluent flask was removed. The attached cell layer in the flask was rinsed with PBS. Washed solution was aseptically discarded. 5 ml of Gibco trypsin/EDTA (0.025% v/v trypsin and 0.01% v/v EDTA in PBS) solution was added to cover the cell layer followed by gently rocking. Cells were observed under a microscope until cell layer was dispersed. Occasionally, the flask may be put inside the incubator for a brief period of time to facilitate dispersal.

The trypsin reaction was stopped by adding 5 ml of *culture medium/hMSC growth medium* and aspirated by gentle pipetting. The cell suspension was then centrifuged at 800 rpm for 5 min at room temperature. The cell pellet was suspended in minimal *culture medium/hMSC growth medium* and thoroughly mixed by repeated pipetting. Seeding volume for each 96-well was 100 µl of cell suspension and then another 100 µl of fresh *culture medium/hMSC growth medium* was added into each seeded well after 5 hrs.

Cells with the concentration of 1×10^4 cells/ml, or 2500 cells in one 96-well, were seeding into collagen-based scaffolds in PS and PDMS well plates and were were incubated at 37°C humidified incubator in 5% v/v CO_2 in air. Cells of

different concentration were seeded into 96-wells for calibration in alamarBlue assay and will be discussed in the next chapter.

3.14 alamarBlue assay

The protocol for alamarBlue assay was modified from O'Brien el al. [240]. alamarBlue, purchased from Life Technologies, was aliquoted and stored at -80°C. Prior to experiment, the solution was placed in 37°C water bath to thaw.

During calibration, cells with different cell concentration were seeded into the wells (Table 5).

Table 5: Number of cells used to calibration alamarBlue (AB) reduction

Cell Concentration (cells/ml)	Cell Number
1×10^3	250
5×10^3	1250
1×10^4	2500
2.5×10^4	6250
5×10^4	12500
7.5×10^4	18750
1×10^5	25000
2.5×10^5	62500
5×10^5	125000
7.5×10^5	187500
1×10^6	250000

25 µl alamarBlue solution was added into a PS or PDMS 96-well containing the collagen/chitosan scaffold in 250 µl *culture medium* in a dark environment. The well plate was then left in a 37°C humidified incubator in 5% v/v CO_2 in air for 5 hours. 100 µl mixed solution was pipetted from the well and placed into the well of a new PS 96-well plate. The absorbance of the solution was measured at 570 nm and 600 nm wavelength inside a Wallac Victor 2 multilabel counter and the data was analysed using the Wallac 1420 Workstation.

Fluorometric readings were recorded and calculated using Equation 1. Logarithmic cell densities were then plotted against percentage of alamarBlue reduction in figure 12.

Equation 1: Percentage of alamarBlue reduction

$$\%\text{AB reduction} = \frac{\varepsilon_{\text{ox},\lambda 2} \cdot \text{A}_{\lambda 1} - \varepsilon_{\text{ox},\lambda 1} \cdot \text{A}_{\lambda 2}}{\varepsilon_{\text{red},\lambda 1} \cdot \text{A}'_{\lambda 2} - \varepsilon_{\text{red},\lambda 2} \cdot \text{A}'_{\lambda 1}} \times 100\%$$

where,

$\varepsilon_{ox,\lambda 2}$ is the molar extinction coefficient of alamarBlue® oxidised form (blue)

$\varepsilon_{red,\lambda 1}$ is the molar extinction coefficient of alamarBlue® reduced form (red)

A is the absorbance of test wells

A’ is the absorbance of negative control wells

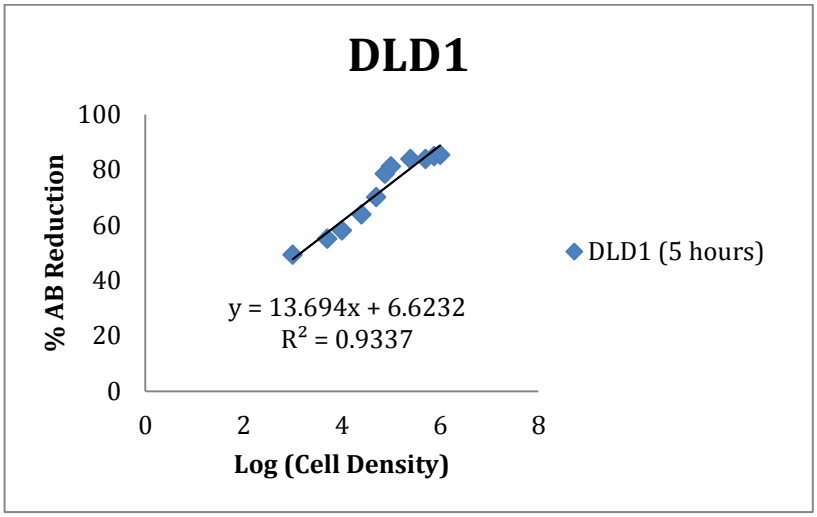

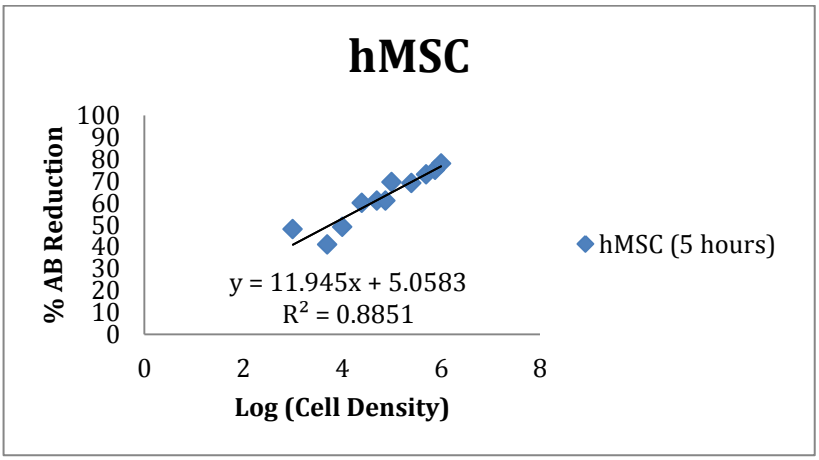

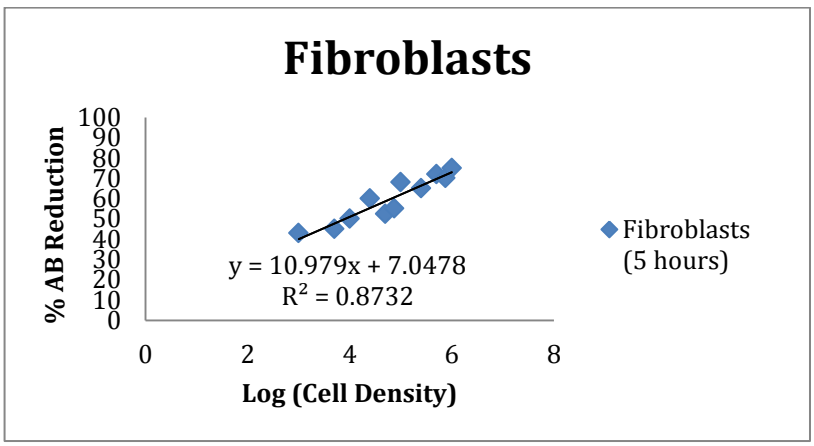

Figure 12: Calibration curve for percentage alamarBlue reduction against logarithmic cell density using a) DLD-1 cancer cells; b) hMSCs; and c) Fibroblasts

The linear relationships between cell density in log scale and their respective alamarBlue reduction for each cell type were generated from figure 12:

Equation 2: %AB Reduction versus DLD-1 cell density in logarithmic scale

$$\%AB\ Reduction = 13.694 \times Log\ (DLD\text{-}1\ cell\ density) + 6.6232$$

Equation 3: %AB Reduction versus hMSC cell density in logarithmic scale

$$\%AB\ Reduction = 11.945 \times Log\ (hMSC\ cell\ density) + 5.0583$$

Equation 4: %AB Reduction versus fibroblast density in logarithmic scale

$$\%AB\ Reduction = 10.979 \times Log\ (fibroblast\ density) + 7.0478$$

As alamarBlue is non-cytotoxic, the same well could be used for theoretically unlimited amount of times when measuring the percentage of alamarBlue reduction during the course of experiment. The *culture medium* was replenished each time after alamarBlue assay was performed and the well plate was returned to the incubator as fast as possible to ensure healthy growth of the cells.

During the actual experiments after calibration was done, 25 µl alamarBlue solution was directly added to the well containing the scaffold seeded with cells.

4. Results and Discussions

4.1 Scaffold fabrication

Scaffolds were fabricated in PS and PDMS 96-well plates following protocols as set out in table 2 and table 3. PS 96-well plates were purchased from commercial source and PDMS 96-well plates were made prior to the experiments in the laboratory.

Each well was filled with 40 µl of the polymer solution. Composition and concentration of the polymer solution were major factors in determining the resulting freeze-dried product, and the fill volume determined the thickness of the final scaffold. Effects of concentration and composition of the polymer solution during freeze-drying were investigated using the matrix set out in table 1 in chapter 3.2.

During the fabrication process, scaffolds made of 0.1 wt.% and 0.2 wt.% overall polymer concentration lost their structural integrity after freeze-drying. It was therefore not feasible to carry on experiments on these two groups of scaffolds.

Severe shrinkage occurred in most scaffolds made of 0.3 wt.% overall polymer concentration and some lost their structural integrity after freeze-drying. There was a great possibility that the ice crystal growth could have interacted with the more diluted solution (0.3 wt.%) and thus making it prone to collapse after ice sublimation. More concentrated solutions, such as 0.4 wt.% and 0.5 wt.%, retained their structural stability. The experiment proceeded and data analyses

were carried out on scaffolds with 0.4 wt.% and 0.5 wt.% overall polymer concentration.

4.2 Freeze drying process

The following section discusses the different stages in the freeze-drying process. Protocols (Table 2 and 3) were made after considering all the factors and variables presented below.

Freezing temperature

First of all, with regard to freezing temperature, previous work has investigated the effect of freezing temperature during lyophilisation [157] and it was found to influence the pore size. In particular, pore size decreased with freezing temperature down to -40 °C. Below this temperature, pore size was no longer correlated to further decrease in temperature.

-40 °C was used as the end point of freezing cycle for this experiment to generate smaller pores.

Cooling rate

Cooling rate determines the homogeneity of the pore structure during lyophilisation. For example, a lower cooling rate usually generates larger ice crystals, which correspond to larger pores upon sublimation.

Upon reaching the freezing temperature of -5 °C, the chamber was maintained at that temperature for 15 min to stabilise and promote ice growth. Constant cooling rate with a freezing time of 70 minutes (i.e. 0.5 °C/min) was experimented and the final pore structure compared with quenching (freezing

time of 10 min, or cooling rate of 3.5 °C/min). Structure appeared more homogeneous in scaffolds produced with constant cooling technique as comparing to those of quenching. When comparing to constant cooling with more freezing time (i.e. slower freezing rate of 0.4 and 0.3 °C /min), scaffolds fabricated with slower cooling rate showed no observable increase in pore homogeneity. MPM image (not shown) confirmed that scaffolds fabricated from constant cooling yield pores that are more equiaxed and distributed evenly throughout; while scaffolds made from quenching technique were more longitudinal in nature.

Chamber pressure

Chamber pressure was lowered to 0.1 mBar to facilitate the mass transfer during ice sublimation at solid-vapour interface.

Primary drying

Of the three main stages in lyophilisation, primary drying takes the longest time. Hence it is important to optimise this process to improve efficiency.

The end point of primary drying can be determined by placing thermocouples in the sample wells. Empirical evidence suggests that when the temperature of the wells containing the thermocouples approaches the pre-set shelf temperature, it indicates the end of primary drying. In addition, wells containing the thermocouples reach their end of primary drying faster [123]. Hence a 10-20 % more soak period was added onto the time frame of primary drying based on the time determined by the wells containing the thermocouples.

Temperatures in all the samples in the experiments reached the shelf temperature of -5 °C after 15 hours, or 900 minutes. Taking into consideration of the soak period and hence a total of 1020 minutes were set for primary drying.

Secondary drying

Secondary drying was designed to remove any residual water from the final constructs. Plateau-effect kinetics suggests that it is necessary to dry the product at a higher temperature in order to achieve lower water content [124]. Therefore shelf temperature was set at room temperature of 20 °C to dry the scaffolds for six hours. An extended drying time beyond six hours did not lead to any observable difference in the final product.

4.3 Pore size and distribution

For a biomaterial scaffold to promote favourable cell-scaffold interactions, the average pore size needs to be appropriate in a way that it can promote cell attachment and proliferation while still able to retain a critical surface area for structural stability. Moreover, the pores need to be interconnected to facilitate mass transport of nutrients and wastes, and to facilitate cell in-growth.

Pore size distribution charts were produced (Figure 13), after measuring the diameter of 200 pores on each sample scaffold. In addition, average pore size in different concentration and substrate groups were also charted (Figure 14) from the same data. Average pore size was approximately 150 μm overall, and pores range from 20–175 μm in diameter. Pore size is defined as the diameter of a pore, assuming a circular profile.

4.3.1 Effect of composition

Four pore size distribution charts were produced in figure 13. Pore size was measured under an inverted light microscope and 200 entries were recorded. Three different batches of the same concentration and composition were experimented. The distribution charts were produced to show the relative relationship between scaffolds with different composition.

Pore size was not normally-distributed, as this was likely due to randomness in ice crystal formation and sublimation during the freeze-drying process. The peak of the distribution curve shifts toward larger pore size with the increase of chitosan content. This trend could be observed in both 0.4 wt.% and 0.5 wt.% (overall polymer concentration) collagen/chitosan scaffolds in both PS and PDMS substrate.

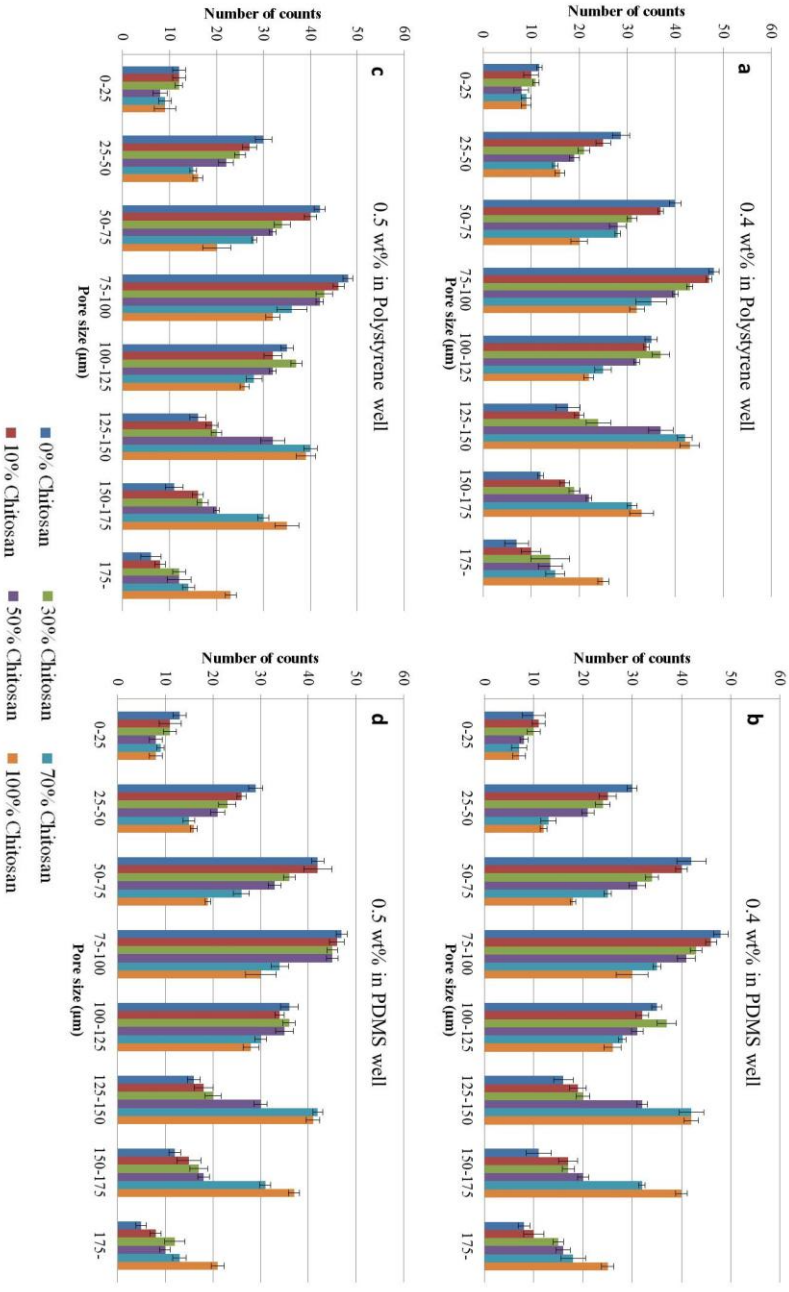

Figure 13: Distribution frequency of pore size in freeze-dried collagen/chitosan scaffolds with overall polymer concentration of a) 0.4 wt.% in polystyrene well; b) 0.4 wt.% in PDMS well; c) 0.5 wt.% in polystyrene well; and d) 0.5 wt.% in PDMS well. The data is plotted as the mean [n= 3] ± standard deviation (SD)

4.3.2 Effect of overall polymer concentration

A more concise figure was extracted to reveal the relationship between pore size and polymer concentration on pore size in figure 14.

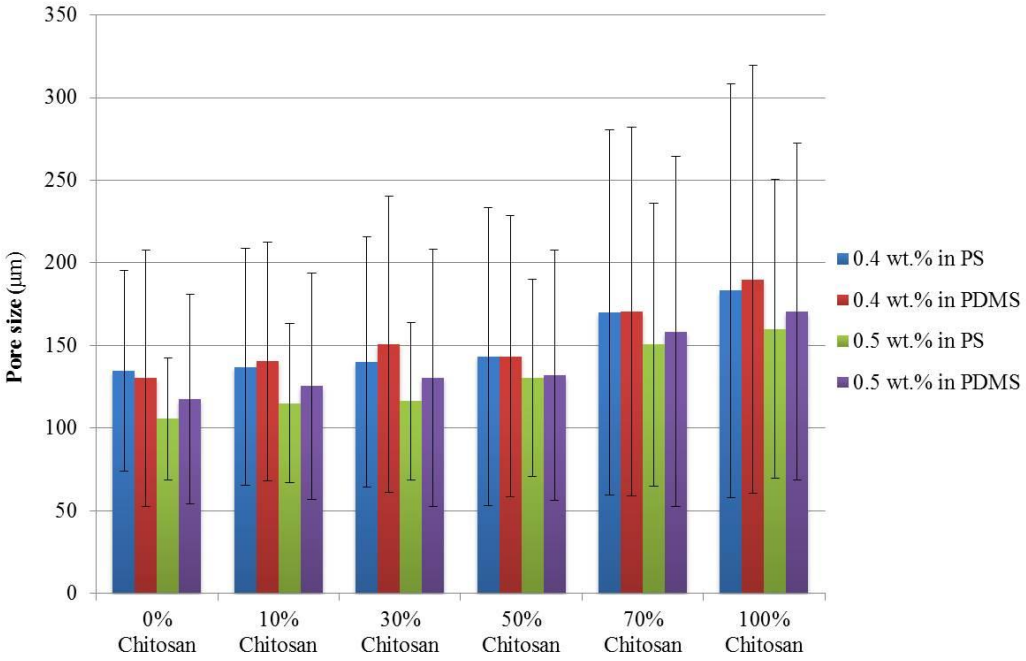

Figure 14: Average pore size of collagen/chitosan scaffolds made from 0.4 wt.% and 0.5 wt.% solutions in PS and PDMS wells. The data is plotted as the mean [n= 200] ± SD

No conclusive trend could be observed SD were generally very large for all the sample groups. Average pore size was observably larger in scaffolds with overall polymer concentration of 0.4 wt.% and this was pronounced in all compositional and substrate groups. This was most likely due to less polymer volume which translated into more void space in the construct. Scaffold composition and

concentration could be manipulated in future to tailor to the requirement of a specific tissue engineering application.

4.3.3 Effect of substrate

According to figure 13 and figure 14, there is no apparent difference in pore size and distribution between scaffolds in PS wells and those in PDMS wells.

4.4 Thickness and surface profile

The thickness of freeze-dried collagen/chitosan scaffolds in PS or PDMS 96-well was 1mm on average, as shown in figure 15. For cells, thicker matrices are hard to penetrate and nutrient transport is also an issue for cell to proliferate in bulk. Sponges less than 1 mm in thickness are technically feasible. However, thinner scaffolds have less room to accommodate cell proliferation and in-growth. Thus, 1 mm thickness is a compromise between the fabrication process and application. Previous researches had difficulties in fabricating 1 mm-thick scaffolds with flat surface as the problem of surface tension problem became significant in small wells with thinner scaffolds.

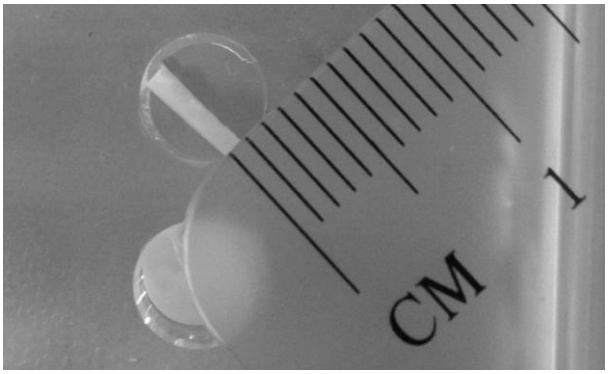

Figure 15: Thickness of freeze-dried collagen/chitosan scaffolds in PDMS wells

However, due to surface tension in the small format well plates, meniscus remained (not shown in figure 15). Therefore, the following optimisation aimed to fabricate and optimise scaffolds of 1 mm in thickness and without meniscus.

4.5 Scaffold optimization

The requirements for freeze-dried scaffolds are listed below:

- No defects;
- Flat surface profile
- Thickness preferably 1 mm or even less

4.5.1 Scaffold in polystyrene 96-well plate

Concentrations of 0.4 wt.% and 0.5 wt.% (overall polymer concentration) collagen/chitosan scaffold solutions prepared in PS 96-well were prone to form a curved or bowl-shaped surface instead of a flat surface as illustrated in the schematic drawing in figure 16. The schematic on the right illustrates the current

collagen/chitosan profile in a 96-well and the schematic on the left illustrates the surface profile this study wished to achieve after certain treatment.

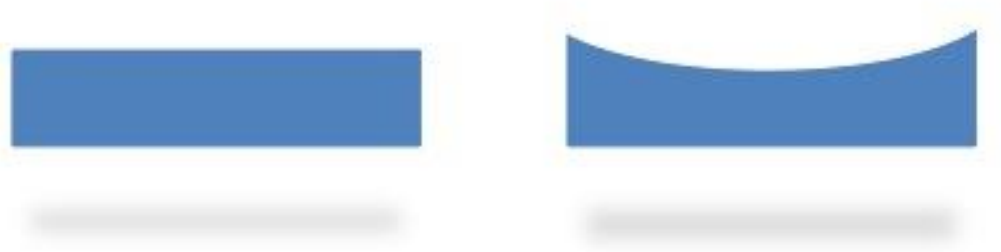

Figure 16: Schematic illustration of the surface feature of collagen/chitosan scaffold in PS 96-well. (Left) An ideal scaffold with flat top surface after treatment and (right) scaffold without any surface treatment. The two schematics are for illustration purpose only

Any attempt to mitigate the surface tension problem needed to address either one of the two correlated issues:

- The hydrophilicity of the surface of the well needed to be decreased just enough for the solution to be hydrophobically repelled such that it would form a flat top surface due to two counter-acting forces cancelling each other. The repelling force must not be strong; otherwise it would instead form a dome-shaped surface. The bottom of the well must also not be treated.
- Hydrophilicity property of the solution needed to be altered just enough such that it matched the hydrophilicity profile of the well surface.

The following section describes various attempts made by the author to address the surface tension problem.

4.5.2 Surface treatment in PS wells

4.5.2.1 Silicone oil

Silicone oil was purchased from Sigma-Aldrich and was applied onto the vertical well surface prior to pipetting in the polymer solution.

Pre-treatment of the well surface was concluded with no success. The oil introduced by a small swab easily contaminated the bottom surface and thus produced dome-shaped scaffolds after freeze-drying. Moreover, treatment of the surfaces was too time-consuming, thus was clearly not an ideal solution for engineering applications.

4.5.2.2 Pre-washed well

The well was pre-washed with 0.05 wt.% collagen solution prior to pipetting in the collagen/chitosan solution. This process aimed to match the hydrophilicity of the well surfaces with that of the collagen/chitosan solution. However, this treatment did not result in observable change in the shape of the top surface in the final freeze-dried product.

4.5.2.3 Water-film

In this treatment process, the author attempted to match the hydrophilicity properties of the solution with that of the well surface. After UV cross-linking

was completed, 10 µl de-ionised water was pipetted onto each cross-linked scaffold in the well as illustrated in figure 17. The 96-well plate was then placed into the lyophiliser for freeze-drying.

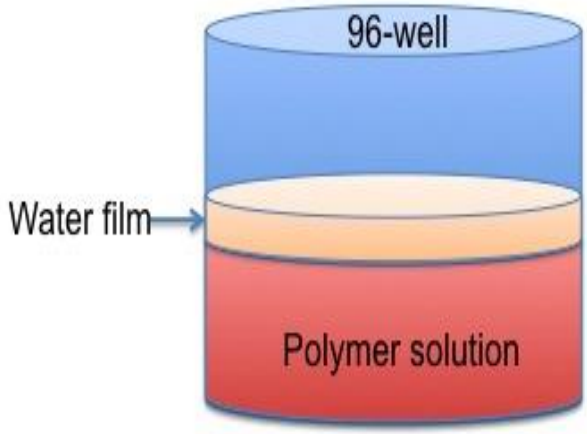

Figure 17: Schematic illustration of thin water film surface treatment

The freeze-dried scaffolds subject to this treatment displayed a flat top surface in all scaffolds made of 0.4 wt.%, 0.5 wt.% collagen/chitosan solutions.

The results showed that this water film treatment could be the solution to mitigate the surface tension in 96-well. The following section is a detailed explanation of the water film treatment and its effect on 0.4 wt.% and 0.5 wt.% collagen/chitosan solutions.

The water film itself was in its liquid form for a rather brief period before cool down into ice during the cooling stage in the freeze-drying cycle as the temperature dropped below the melting point of water. The water film therefore, could not react with more concentrated and cross-linked polymer solution due to the short time of contact before it turned into ice. Moreover, the cross-linked

construct was locked in a network of polymer meshes and thus had little room to accommodate additional water in such short time-frame. The ice was then sublimed during the primary drying cycle.

Without the water film, the scaffold was prone to form a bowl-shaped surface due to greater affinity to the surface of the well. The water film before freeze-drying and its solid ice form during the early stage of freeze-drying exerted pressure against the collagen/chitosan construct and flattened the bowl-shaped top surface in the process.

Pressure exerted by the water film also ensured that the scaffold stuck firmly onto the well surface. Immobilised scaffolds are generally preferable during *in vitro* cell studies.

In addition, the ice layer on top of the scaffold formed large ice crystals protruding into the collagen/chitosan construct and created larger pores. At the end of the freeze-drying cycle, the collagen/chitosan scaffold was formed with larger pores near the top surface and regular pores in the bulk. This heterogeneity in pore size is beneficial to cell in-growth as larger pores could accommodate cell penetration to a greater extent, while regular pores in the bulk ensured structural integrity and sufficient surface area for cell proliferation.

To conclude this section, the water film treatment was beneficial for the freeze-dried collagen/chitosan scaffold in three ways:

- The resulting top surface was flattened
- The scaffold attached firmly onto the well surface

- Heterogeneity in pore size provided greater cell penetration capability while retaining structural integrity

4.5.3 Scaffold in PDMS 96-well plate

On the other hand, scaffolds in PDMS well plate had dome-shaped top surface (Figure 18, right) as the hydrophobic surface of PDMS repel collagen/chitosan solution during fabrication.

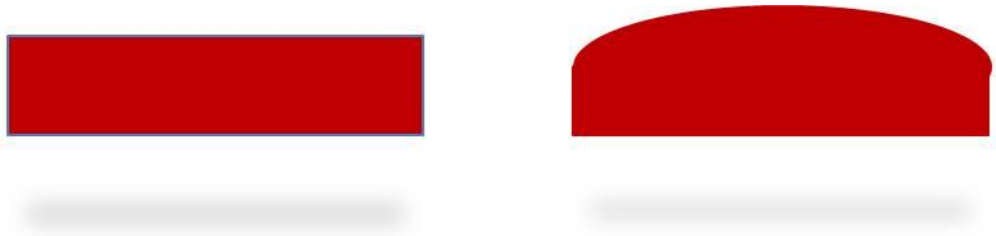

Figure 18: Schematic illustration of the surface feature of the collagen/chitosan scaffold in PDMS 96-well. (Left) An ideal scaffold with flat top surface after treatment and (right) scaffold without any surface treatment. The two schematics are for illustration purpose only

Due to hydrophobicity of PDMS itself, water-based solution, such as collagen solution would form a dome-shaped construct almost immediately. The resulting shape of the construct would resemble a dome rather than a thin, cylindrical shape with flattened top and bottom surfaces. This undesirable phenomenon occurred much due to the same principal as its bowl-shaped counterpart in previous section; i.e. the surface of the well plate and the polymer solution had different affinity towards water.

In the previous case in PS well, the surface of the well had greater affinity to water, and thus, rendered it hydrophilic. In this case, PDMS had less affinity to water, or in scientific terms, the material is hydrophobic; hence it repelled water-based solution to reduce contact as thermodynamically stable as possible. Thus collagen solution, once pipetted into PDMS wells, would spontaneously form a dome shape, which after freeze-drying cycle, would translate into a dome.

As explained in the previous section, any uneven surface would make cell culture highly unpredictable.

To reiterate: firstly, follow-up assays to be taken in different time-points would require uniformly distributed cells in order to have generalised outcomes. Cell growth would be roughly the same from a flat top surface. However, a dome-shaped top surface would complicate matters, as cells would grow slower into the centre as in the case of a dome and faster in the case of a bowl. This matters because during subsequent assay, a point could be taken with a huge cluster of cells or with no cells at all due to different ingrowth speed.

Secondly, in tissue engineering terms, different rates of cell ingrowth would translate into side effects such as randomised degradation and cell segregation, which at the end of the day would make it highly unpredictable and impossible to perform scientifically-sound replicates.

To make matters worse, freeze-dried collagen/chitosan scaffolds in PDMS wells were found to have larger-than-normal pores, or rather, defects, throughout the scaffold (Figure 19).

Figure 19: Defects in collagen/chitosan scaffold in PDMS 96-well plate after freeze-drying without prior treatment

These could be detrimental to cell culture as defects would contribute to faster degradation rate and cells would form clusters rather than attaching and interacting with the scaffold.

To understand the reasons behind the forming of those defects, intrinsic properties of PDMS material need to be discussed. PDMS has two notable characteristics:

- PDMS has unusually high gas permeability;
- Low surface energy.

One explanation of the defects could be that due to its unusually high gas permeability, air flows created during lyophilisation produced bubbles inside the polymer solution in the wells and some were inevitably trapped when frozen. The trapped air bubbles created voids that were later dried and became defects in the scaffolds.

Another explanation is that air molecules trapped in the voids of PDMS networks was unravelled during lyophilisation and thus the defects were

generated. But it overlooked the fact that PDMS had low excess volume upon mixing, which prevented molecules other than gas molecules from passing through. This selectivity makes the material rather popular among medical applications as it excluded bacteria and in the meantime allowed gas exchange to take place.

Therefore, the defects in the final freeze-dried collagen/chitosan scaffolds inside PDMS well plate were due to high gas permeability of PDMS itself.

Two things happened during the initial stage of freeze-drying cycle.

1) The door sealed, a small negative atmosphere is created inside the chamber to check if the seal was tight;
2) Cooling coils kicked in to cool down the chamber, which created convective air flow in the chamber.

Both mechanisms created airflow, which possibly contributed to gas molecules passing through PDMS well plates. During the experiment, as gas passed through the well plates, some was inevitably trapped inside the collagen/chitosan solutions. In order to prevent this to happen, a few treatments were attempted.

4.5.4 Pre-treatment in PDMS wells

Several treatments were attempted to tackle the hydrophobicity and high gas permeability of PDMS well.

4.5.4.1 Pre-washed wells

Wells pre-washed with 0.01 N sodium chloride in water before freeze-drying achieved limited success. The top surface was flattened to a satisfactory extent. However, this technique did not effectively resolve the high gas permeability issue and defects were still found both inside and on the surface of the scaffolds after freeze-drying.

4.5.4.2 Pre-cooling

The PDMS well plate was stored in a -80℃ freezer before the experiment. Collagen/chitosan solutions were filled into the wells on ice. These setups allowed the well plates and contents to stay at sub-zero temperature.

During the experiments, however, it became obvious that if no step was taken to address the freeze-drying regime, it would fail to keep the whole setup below zero.

The freeze-drying protocol therefore, was optimised for this purpose by shortening the time it took to cool down (Table 3).

Collagen/chitosan scaffolds were filled into the wells of pre-cooled PDMS 96-well plates on ice, and they instantly froze. Upon entering the freeze-drying chamber, the temperature was again lowered from room temperature to -5 °C in only 5 min. And it took another 20 min to stabilize at -5 °C, followed by normal freeze-drying cycle.

Following this change in freeze-drying regime, the defects were removed. Average thickness of the scaffold was 1 mm, and the scaffold had a flat top profile.

4.6 Characterisation

4.6.1 FTIR

FTIR spectra obtained from scaffolds made of different composition are shown in figure 20. Specifically, the figure represents spectra obtained from absorption in scaffolds made of 0.4 wt.% overall polymer concentration with 10%, 30%, 50% and 70% chitosan respectively.

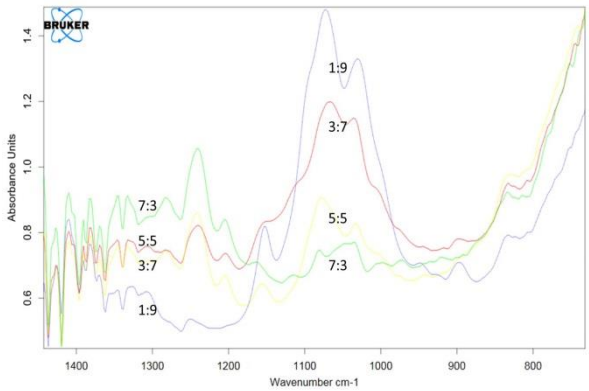

Figure 20: FTIR spectra of scaffolds made from 0.4 wt.% polymer solution in PS wells. The specific composition is stated in the figure above each spectrum as 1:9 (10% chitosan), 3:7(30% chitosan), 5:5(50% chitosan) and 7:3(70% chitosan); for absolute concentration of the polymer refer to table 1 in chapter 3.2

The spectrum of chitosan consists of six distinctive absorption bands. Vibration of hydroxyl groups appeared at 3439; vibration of free amine groups

appeared at 3300 cm^{-1}. The peaks at 1655, 1560 and 1381 cm^{-1} corresponded to C=O stretching, -NH_2 bending and C-O stretching. The absorption band at 1052 cm^{-1} indicated –C-O-C- glycosidic linkage [9, 19, 84, 85]. On the other hand, pure collagen had five characteristic peaks in the FTIR spectrum. A combination of N-H deformation and C-N stretching corresponded to peak at 1274 cm^{-1}. C=O stretching could be observed at 1659 cm^{-1}, and N-H bending at 1550 cm^{-1}. Vibration of hydroxyl groups happened at 3440 cm^{-1} and free N-H stretching occurred at 3324 cm^{-1} [84].

Spectra in figure 21 indicated that absorption of functional groups vary significantly, depending on the underlying characteristic peaks of the polymer. Specifically, the intensity of the characteristic chitosan peak of glycosidic linkage at 1052 cm^{-1} became clearer when chitosan content was increased. On the other hand, the trend reversed itself at 1274 cm^{-1}, at which the peak indicated the characteristic collagen absorption band. For instance, the highest peak at 1052 cm^{-1} corresponded to spectrum for scaffold with 10% chitosan. This particular spectrum registered the lowest value at the characteristic collagen absorption peak of 1274 cm^{-1}.

According to Taravel and Domard two kinds of interactions can give rise between collagen and chitosan when they are dissolved in solution [6].

1) Electrostatic force leading to the formation of polycation and polyanion complex; this usually occurs at low pH environment;

2) Hydrogen bonding would be formed between two polymers when they are mixed in their respective salt form.

From a solution preparation point of view, collagen/chitosan blends were mixed in the presence of 20mM acetic acid. This led to electrostatic interactions between collagen polyanions and chitosan polycations.

4.6.2 Differential scanning calorimetry analysis

The thermodynamics properties of collagen/chitosan scaffolds from various proportions of mixtures were studied using DSC. The polymer matrices were slowly heated in a nitrogen environment from room temperature until 150 ℃. DSC plots of 0.4 wt.% collagen/chitosan scaffolds with 10%, 30%, 50% and 70% chitosan are shown in figure 21. Overall speaking, plots reveal a transition band of 70 - 120 ℃ across all samples. The transition occurred mainly due to loss of bound water molecules at boiling temperature (100℃). The curves indicated general shifts

1) towards a lower temperature range with lower chitosan content. This may happen due to the fact that water molecules in chitosan were more strongly bounded than those in collagen.

2) towards lower heat capacity with lower chitosan content, which could be explained by the underlying difference in chemical nature between the two polymers.

Therefore, by increasing chitosan content in the scaffolds, the heat capacity of the polymer blends would be enhanced.

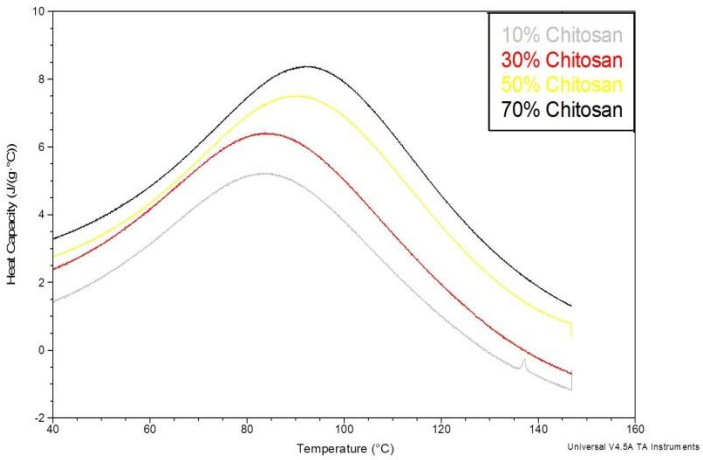

Figure 21: DSC plots of scaffolds with 10%, 30%, 50% and 70% chitosan content. All made of 0.4 wt.% overall polymer concentration in PS wells.

4.6.3 Microscopic observation

It is understood that the microstructure such as pore size and distribution, porosity as well as pore shape has profound influence over cellular activity. The morphology of the freeze-dried collagen-chitosan scaffolds made from 0.4 wt.% and 0.5 wt.% solutions were subjected to observation under MPM. Due to much smaller working distance and limitation of the sample platform of the MPM, the constructs had to be carefully taken out and placed onto glass slides, before loading onto the sample platform for observation under MPM. The following section is dedicated to discuss the results from MPM observations.

Treatment to mitigate the surface tension problem in PS 96-well plate did not have significant influence over pore distribution and size. But pore size was significantly large near the top surface in treated collagen/chitosan scaffolds in PS wells comparing to their untreated counterparts. During freeze-drying, the water film was cooled down to form an ice layer on top of the scaffold. This

process inevitably led to large ice crystals protruding into the collagen/chitosan construct and created larger pores near the top surface. During the drying stage, all the ice crystals were sublimed, leaving behind a porous 3D collagen/chitosan matrix with pores near the top surface significantly larger than those in the bulk. Heterogeneity of pore sizes was indeed beneficial to cell in-growth as larger pores could accommodate cell penetration to a greater extent, while regular pores in the bulk ensured structural integrity and sufficient surface area for cell proliferation. Pores were uniform, however, for scaffolds in PDMS wells.

The morphologies of collagen/chitosan scaffolds were revealed by MPM images in 5D-viewer mode (Figure 22a, b). A trend of increased pore size with increased chitosan content was conspicuous in the figure by comparing the left image (30% chitosan) with the right one (70% chitosan). The average pore sizes of the scaffolds in both images fall in the range of 100-200 μm. Smaller pores in larger pores as well as some indistinguishable pores were both present in the two images and were indicative of high interconnectedness. In Figure 22(b) the interconnection of pores can still be observed despite increased chitosan content, although the scaffold was predominantly made of larger pores.

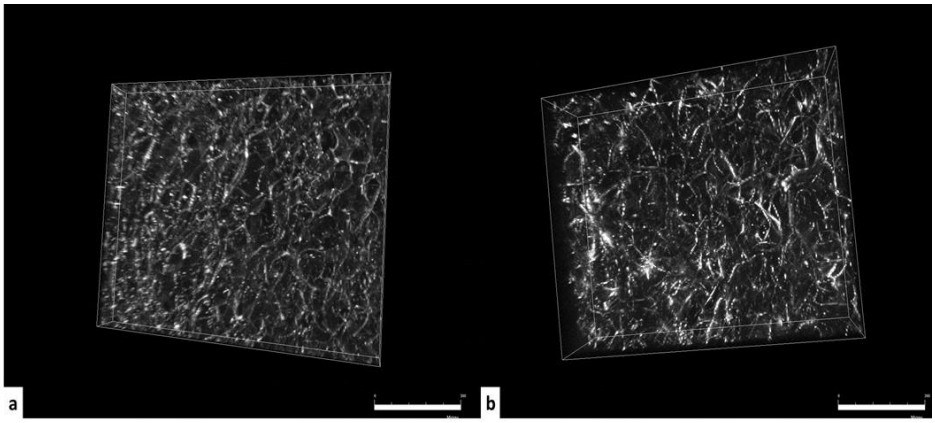

Figure 22: Collagen/chitosan scaffolds made from 0.4 wt.% overall polymer concentration in PS wells under MPM using 20X magnification with collagen/chitosan mixing ratio of (a) 30% chitosan (abs. conc. of collegen=0.28 wt.%; chitosan=0.12 wt.%) (b) 70% chitosan (abs. conc. of collegen=0.12 wt.%; chitosan=0.28 wt.%)

4.6.4 Disintegration

Disintegration of scaffold depends on many parameters, such as intrinsic chemical structure of the material, scaffold morphology as well as external factors such as pH and temperature [1-3]. A four-week study of hydrolytic degradability of freeze-dried scaffolds aimed to establish the disintegration profile of collagen/chitosan scaffolds in the absence of enzymes. The profiles were plotted in figure 23.

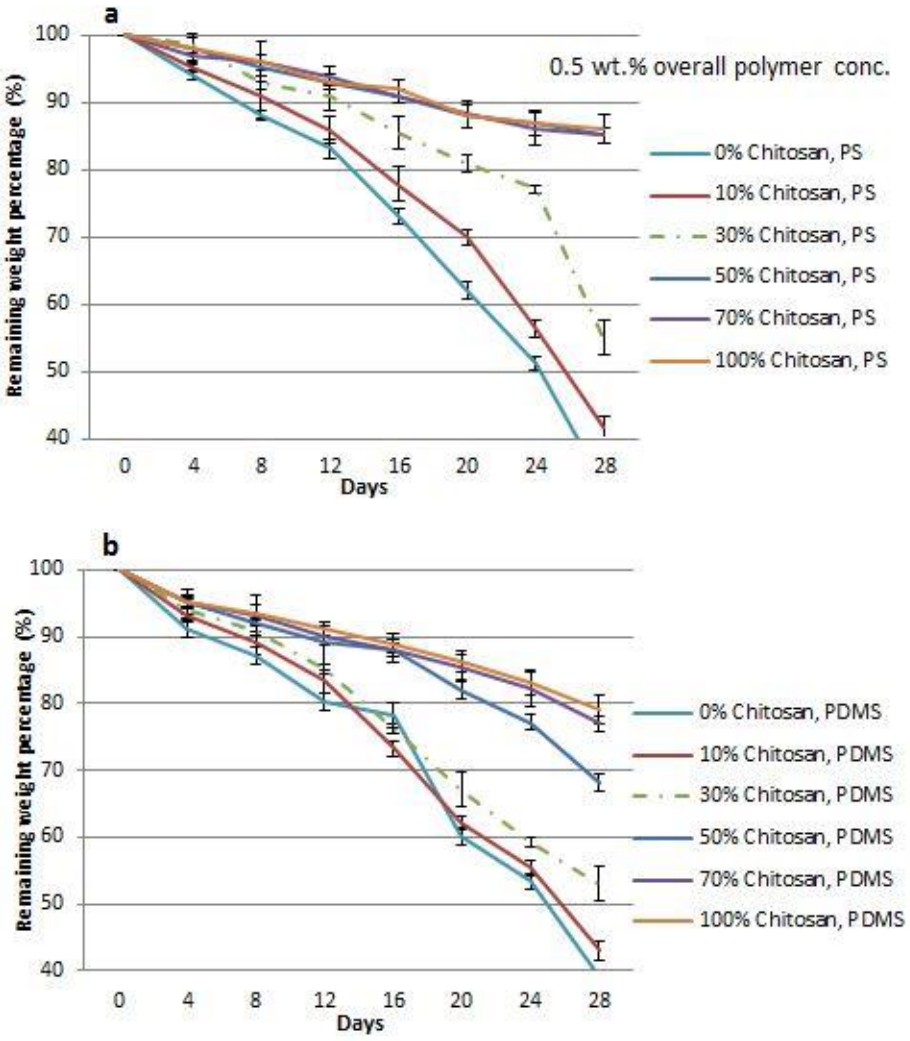

Figure 23: 4-week hydrolytic degradability profile of collagen/chitosan freeze-dried scaffolds in 0.5 wt.% overall polymer concentration in a) PS wells; and b) PDMS wells. The data is plotted as the mean [n=3] ± SD

In most cases, scaffolds disintegrated to a greater extent in scaffolds with less chitosan content, though a generalised trend could not be established from the data presented.

The graph suggested that the scaffolds with 0%, 10% and 30% chitosan experienced bulk disintegration in both PS and PDMS wells, which means the diffusion process was faster than the disintegration process. Although longer-

term disintegration profile was unknown, the linear and slow loss of mass were evidences that water uptake rate was much higher than the rate of hydrolysis.

On the other hand, collagen/chitosan scaffolds with 50%, 70% and 100% chitosan in PS and PDMS wells showed profiles very similar to that of the so-called surface erosion, where the structure remained throughout the study and scaffolds disintegrated by erosion of the surface layer by layer.

Therefore, scaffolds with less than 50% chitosan content would experience bulk disintegration whereas scaffolds with more than, or equal to 50% chitosan content would undergo surface erosion, which correpsonded to a much slower rate of disintegration.

In terms of the effect of concentration on scaffold degradation, the compositon was fixed at 50% chitosan and figure 24 was charted.

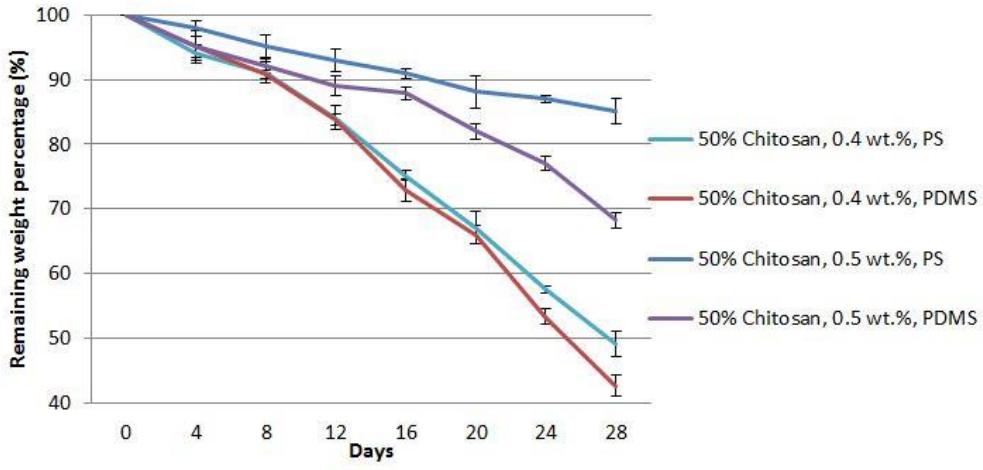

Figure 24: 4-week hydrolytic degradability profile of collagen/chitosan freeze-dried scaffolds in varying concentration and substrate. The data is plotted as the mean [n=3] ± SD

The profile showed firstly, that scaffolds with lower overall polymer concentration disintegraded faster than those of higher overall polymer concentration; and secondly, scaffolds in PDMS wells disintegraded faster than those in PS wells.

The first observation was most likely due to that more void volume in the constructs contributed to faster disintegration. And the second observation was probably because of the gas-permeable nature of PDMS material that facilitated nutrient and waste transport, which in turn, contributed to disintegration.

4.7 Cell proliferation

Studies of cell proliferation in the scaffolds in figure 25, 26 and 27 all revealed that cells proliferated in collagen/chitosan scaffolds across different cell types. DLD-1 cells started proliferating from day-1 whilst hMSCs and fibroblasts took a few days to settle and their numbers only started to increase from day-3 onward. Final DLD-1 cell yields were generally higher than those of hMSCs and fibroblasts both in PS and PDMS 96-well plates, this was however, only indicative of the characteristics of DLD-1 cells.

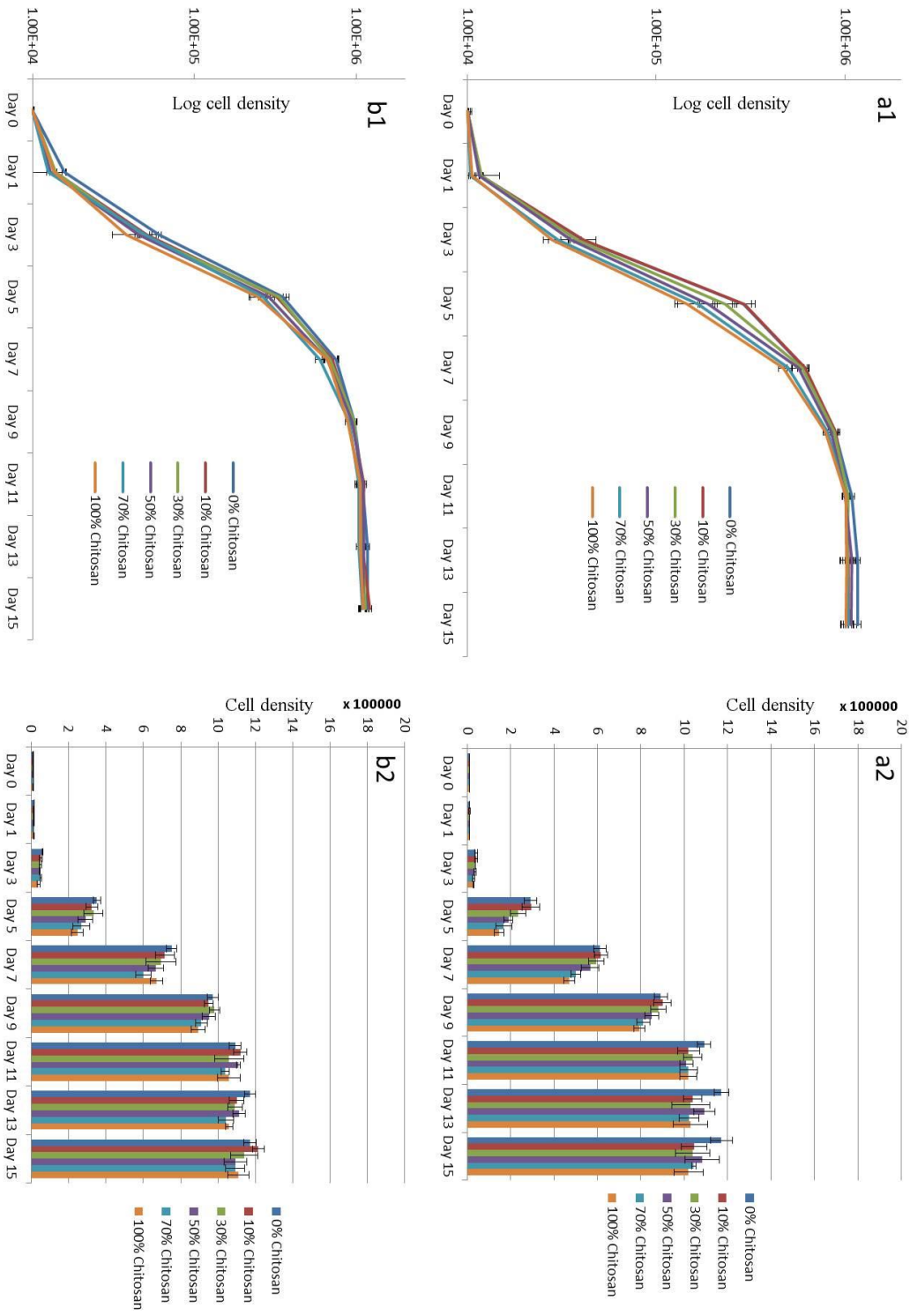

(Continued on next page)

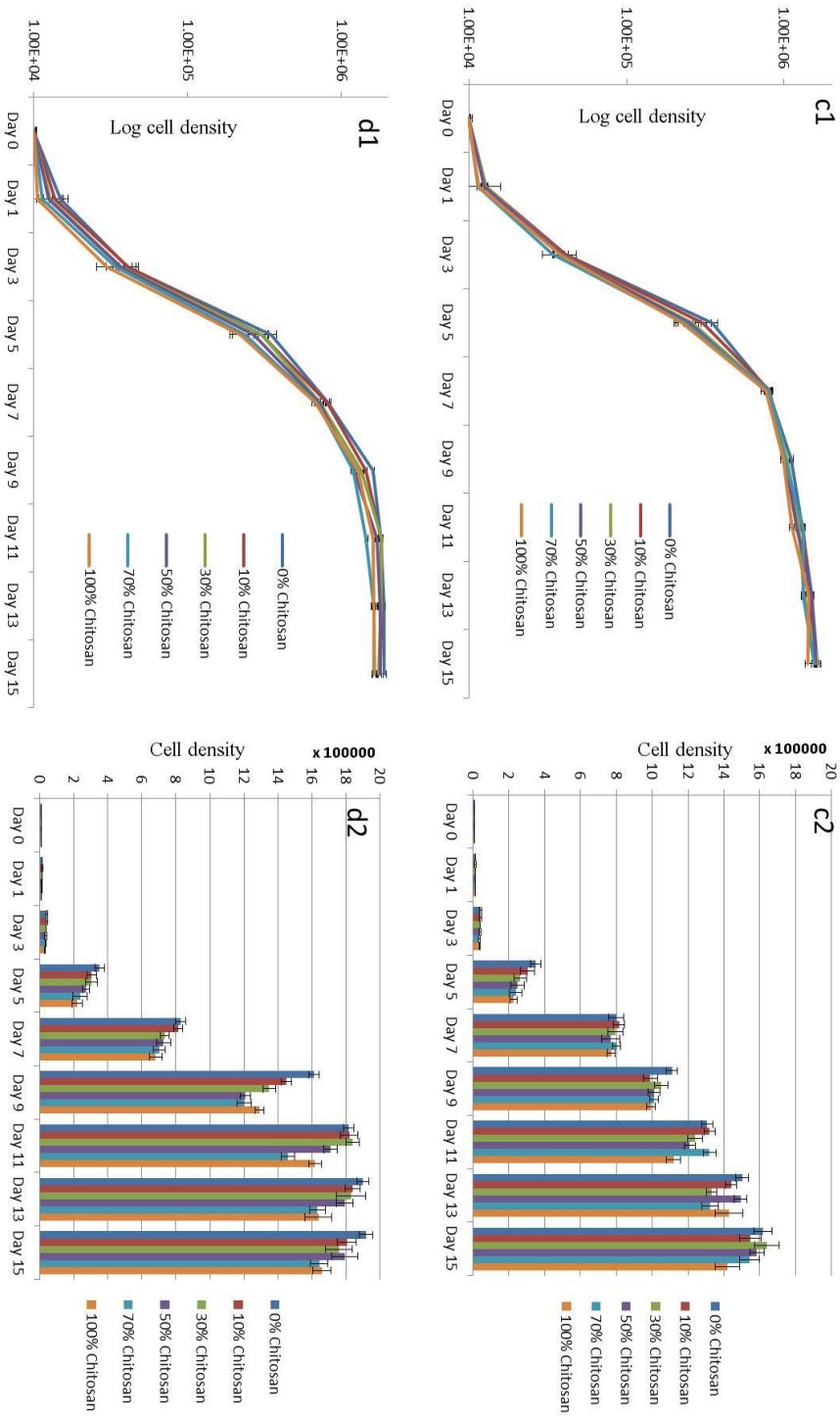

Figure 25: Logarithm of the number of DLD-1 cells as correlated to alamarBlue reduction in scaffolds with (a) 0.4 wt.% polymer conc., PS; (b) 0.4 wt.% polymer conc., PDMS; (c) 0.5 wt.% polymer conc., PS; and (d) 0.5 wt.% polymer conc., PDMS. The data is plotted as the mean [n=3] ± SD

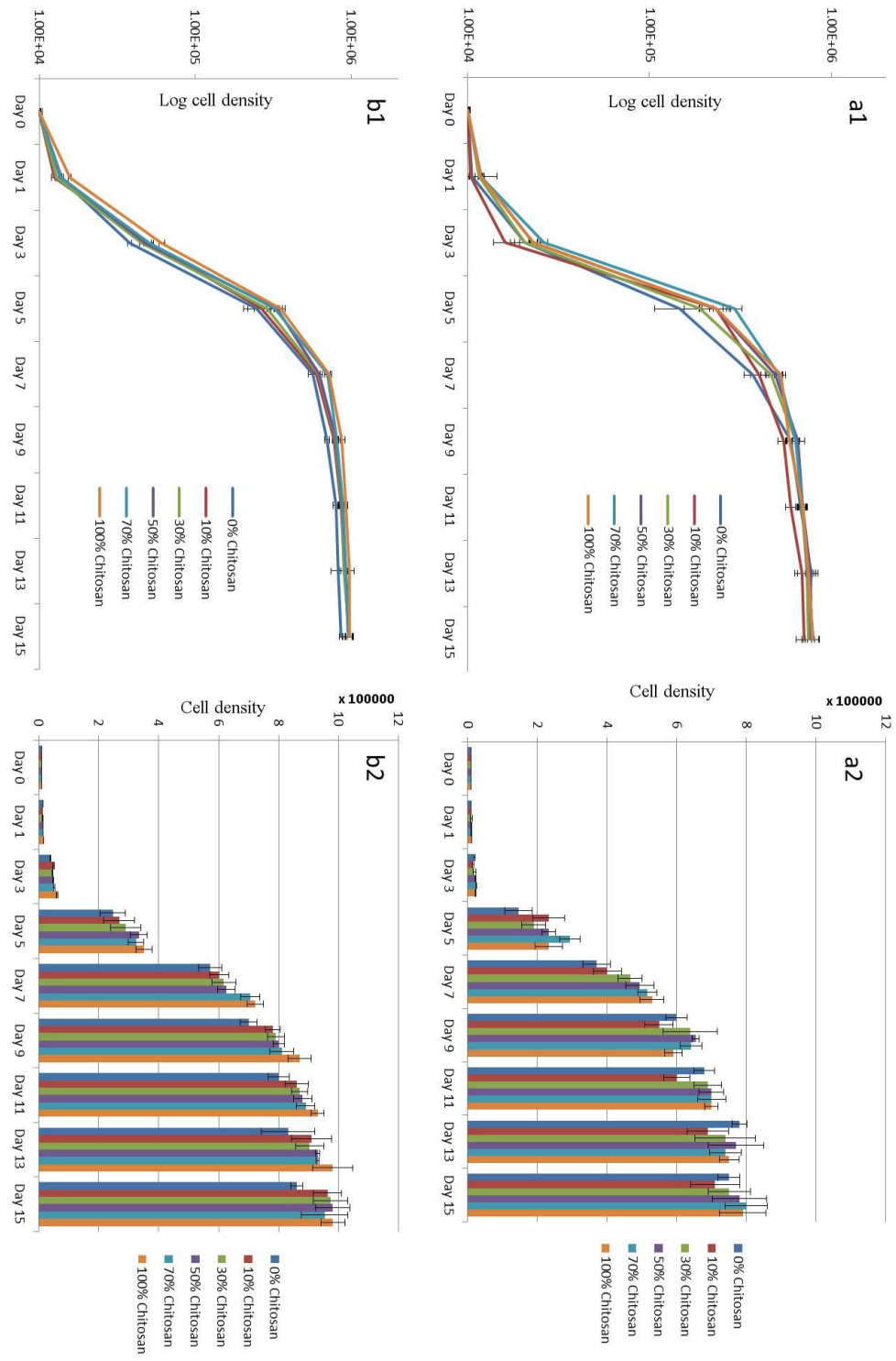

(Continued on next page)

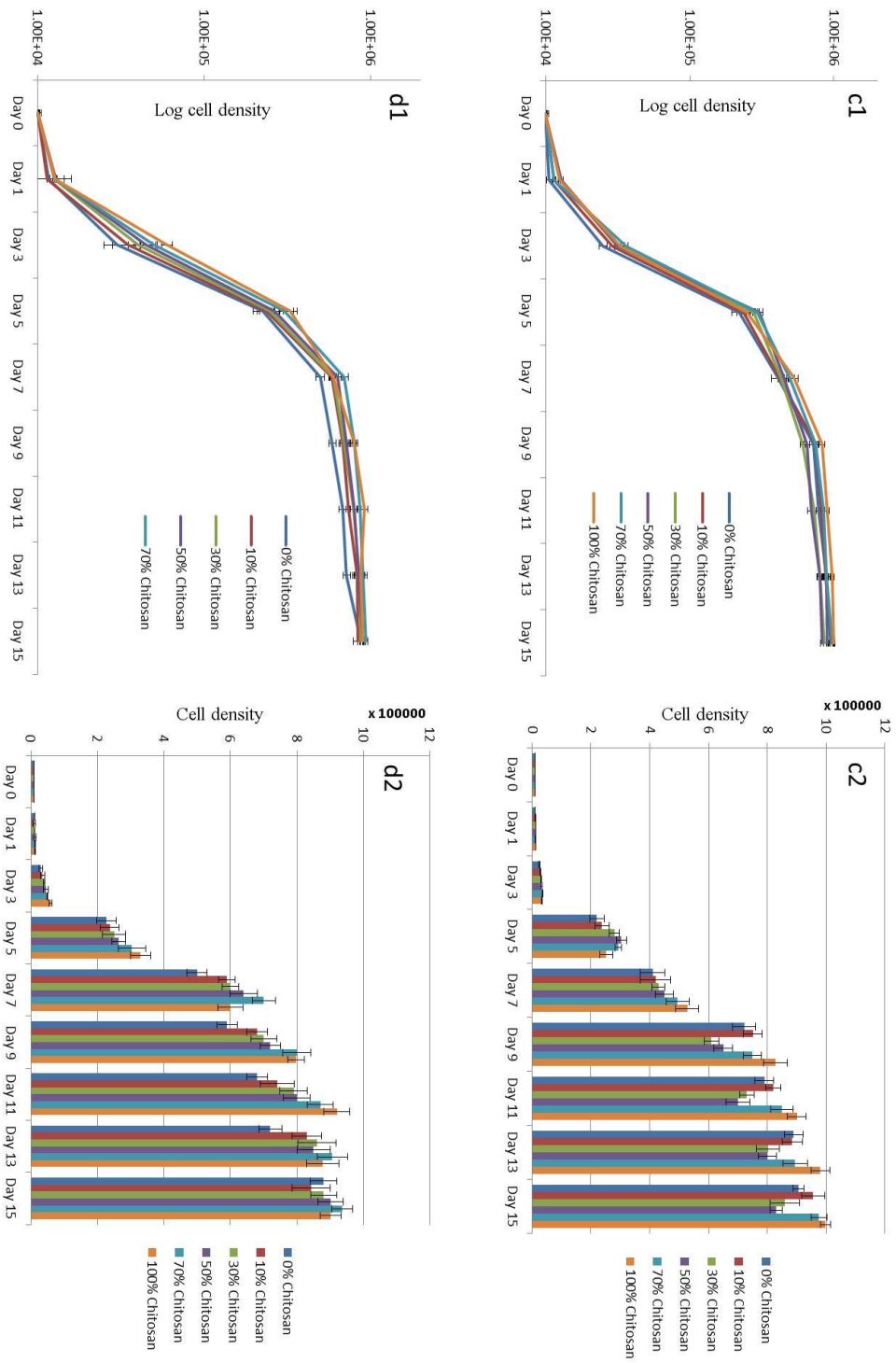

Figure 26: Logarithm of the number of hMSCs as correlated to alamarBlue reduction in scaffolds with (a) 0.4 wt.% polymer conc., PS; (b) 0.4 wt.% polymer conc., PDMS; (c) 0.5 wt.% polymer conc., PS; and (d) 0.5 wt.% polymer conc., PDMS. The data is plotted as the mean [n=3] ± SD

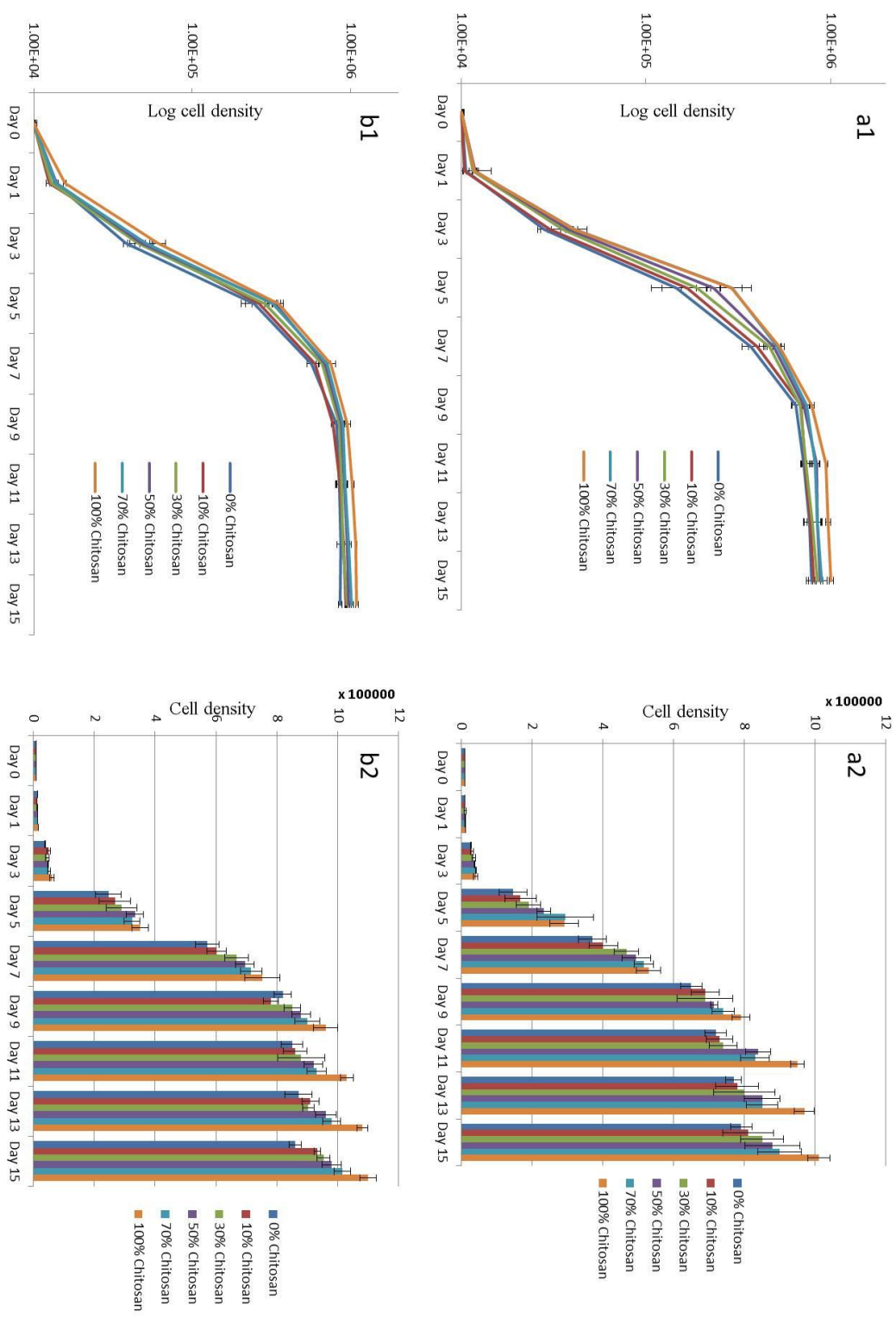

(Continued on next page)

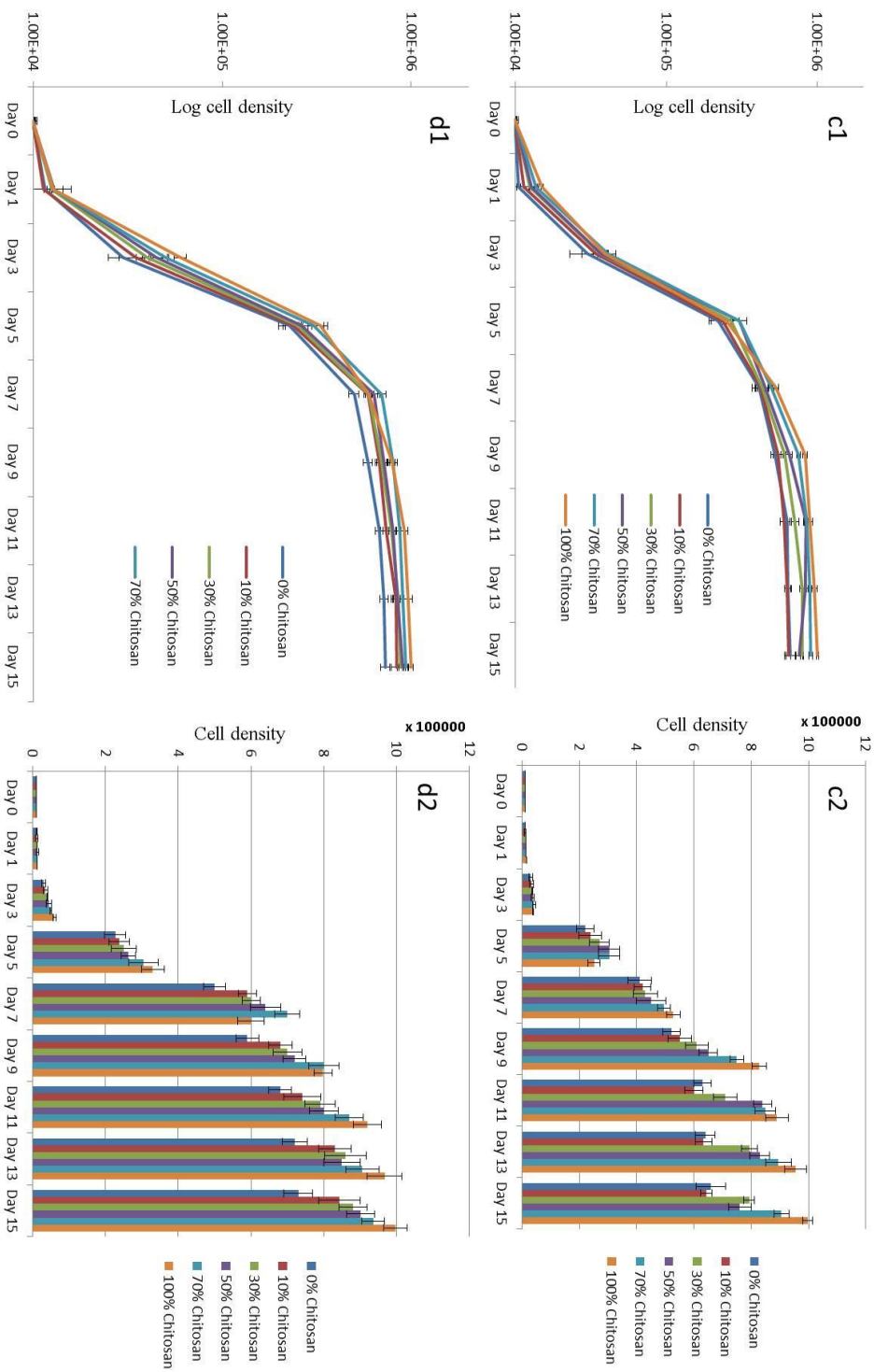

Figure 27: Logarithm of the number of fibroblasts as correlated to alamarBlue reduction in scaffolds with (a) 0.4 wt.% polymer conc., PS; (b) 0.4 wt.% polymer conc., PDMS; (c) 0.5 wt.% polymer conc., PS; and (d) 0.5 wt.% polymer conc., PDMS. The data is plotted as the mean [n=3] ± SD

4.7.1 Effect of composition

In figure 25, DLD-1 cells generally favoured pure collagen scaffolds. Take, for instance, the bar chart as presented in figure 25(a2). The yields for DLD-1 cells inside pure collagen scaffolds (0% chitosan) were markedly higher throughout the entire 15-day culture period. This phenomenon was obvious in all concentration and substrate groups.

Although pure collagen scaffolds generated higher yields of DLD-1 cells than pure chitosan scaffolds, this relationship did not seem to follow a linear path in between the two extremes. Therefore the correlation of higher DLD-1 cell number with lower chitosan content could not be established from this experiment.

In general, hMSCs displayed greater affinity towards scaffolds with higher chitosan content, though exceptions do exist such as the bars for cell yields in scaffolds with 30% and 50% chitosan in figure 26(c2). Likewise, a clear trend could not be established from this experiment alone.

For fibroblasts in figure 27, as the cell yields showed a clear trend with increased chitosan content across both substrate and concentration groups, a correlation could be established that the yield of fibroblasts increase with increased chitosan content. Further statistically-sound investigation needs to be conducted to ascertain the relationship between cell yield and chitosan content in fibroblasts.

4.7.2 Effect of overall polymer concentration

An observation can be made, by comparing figure 25(a2) with (c2), and (b2) with (d2), that DLD-1 cell yields were higher in scaffolds made from solution with higher overall polymer concentration, as all the bars in figure25(c2) and (d2) were higher than those in (a2) and (b2) respectively. However, to establish the correlation between cell yield and overall polymer concentration, a thorough study is needed in future.

The trend was less than clear, and to some extent reversed, in hMSCs and fibroblasts.

4.7.3 Effect of substrate

In figure 25, DLD-1 cell yields were higher in (b2) and (d2) than those in (a2) and (c2) respectively. In addition, by comparing (a1) with (b1), (c1) with (d1), DLD-1 cells cultured in PDMS wells reached their saturation faster than those in PS wells and at higher yields. Therefore, DLD-1 cells favoured PDMS 96-well plates.

However, in figure 26 and 27, hMSCs and fibroblasts showed no such clear trend.

4.7.4 Summary

To wrap up, three observations could be made from the figures as follows:

- DLD-1 cells favoured scaffolds with higher overall polymer concentration.
- DLD-1 cells favoured PDMS 96-well plate
- Fibroblasts favoured scaffolds with higher chitosan content.

As discussed in chapter 4.3, higher chitosan content and/or lower overall polymer concentration correspond to larger pores, and vice versa.

For DLD-1 cells, although there was a markedly increase of cell yield in scaffolds with higher overall polymer concentration, it is inconclusive to state that DLD-1 cells favoured smaller pores. Because, on the other hand, DLD-1 cell yields did not show a clear trend that they increased with decreasing chitosan content, which correspond to smaller pores.

For hMSCs, no conclusive correlation was observed from the data collected. This may be because of the difficulty in culturing hMSCs.

For fibroblasts, it can be established that the cells favoured scaffolds with higher chitosan content. However, another observation that fibroblasts cell yields did not increase in scaffolds with lower overall polymer concentration, led to another inconclusive relationship between fibroblast yield and pore size.

Overall speaking, all three cell types proliferated in all of the collagen/chitosan scaffolds and in both PS and PDMS wells. Unfortunately, during the course of this study, the relationship of cells with regard to pore size could not be established.

5. Conclusion and Future Works

In this study, the author aimed to develop and optimise freeze-dried collagen/chitosan scaffolds for 3D culture. The purpose of this study was to address the problem of using small-format culture wells for the fabrication of freeze-dried collagen-based scaffolds for studies of cell growth in 3D culture in static and microfluidic perfusion bioreactors. The research consists of three stages:

- Stage 1: Development of freeze-dried collagen/chitosan scaffolds based on concentration and compositional factors of the polymer;
- Stage 2: Optimisation of the developed scaffolds (substrate-specific) in terms of surface properties and thickness;
- Stage 3: Characterisations and *in vitro* cell studies using DLD-1 cells, hMSCs and fibroblasts to assess the suitability of the developed scaffolds for 3D culture

5.1 Conclusion

In stage 1, experiments were carried out according to the experimental matrix (Table 1) and freeze drying protocols (Table 2 and 3), and it was concluded that collagen/chitosan solution concentration of 0.4 wt.% and 0.5 wt.% (overall polymer concentration) were suitable candidates for freeze-drying fabrication process. Average pore size was 150 μm, and pore size increased with increasing chitosan content. In addition, scaffolds with lower overall polymer concentration

registered larger pore size generally. There was no difference between scaffolds made in PS wells and those in PDMS wells.

However, scaffolds developed in 96-wells had either bowl-shaped top surface in PS wells or dome-shaped top surface in PDMS wells. These were unfavourable as unevenness causes unreliable cell in-growth data and surface morphology without any control was itself not scientifically-sound.

Therefore, in stage 2, novel surface treatment methods were developed to fabricate collagen/chitosan scaffolds with flat top surfaces in both PS and PDMS 96-well plates. To summarise the processes, scaffolds in PS wells were topped up with a thin layer of water film before freeze-drying; while scaffolds in PDMS wells went through pre-cooling and the freeze-drying protocol was tailored to ensure the contents stayed sub-zero during the whole process.

Finally, in stage 3, scaffolds were observed under MPM and their pore size in relation to chitosan content was again confirmed. In DSC, it was established that heat capacity increases with increased chitosan content in the polymer. In FTIR, characteristic peaks of the polymer were confirmed. Moreover, scaffolds with lower overall polymer concentration, and scaffolds in PDMS 96-well plate disintegrated faster in water.

Three cell types were tested on those novel scaffolds and revealed that DLD-1 cells favoured scaffolds with higher overall polymer concentration and/or in PDMS wells; whilst fibroblasts favoured scaffolds with higher chitosan content. No conclusive observation could be made from hMSC culture. All three cell

types proliferated in collagen/chitosan scaffolds in both PS and PDMS 96-well plates.

Based on the experimental procedure and data analysed, the following conclusions can be devised:

- Collagen and chitosan can be fabricated by freeze-drying technique in both PS and PDMS 96-well plate;
- The most suitable overall concentrations of collagen/chitosan were 0.4 wt.% and 0.5wt.%, and the preferred composition depends on specific requirement and application;
- The average pore size in collagen/chitosan 3D scaffolds increases with increased chitosan content and/or lower overall polymer concentration. There was no difference between scaffolds made in PS wells and those in PDMS wells;
- For scaffolds in PS 96-well, water film surface treatment was found to yield reproducible and desirable features in collagen/chitosan scaffolds; whereas for scaffolds in PDMS 96-well, a change in the freeze-drying regime can produce defect-free scaffolds without meniscus shape on the surface;
- The profile of freeze-dried collagen/chitosan 3D scaffolds in both polystyrene and PDMS 96-wells after optimisation was thin (1 mm in thickness) and flat;

- Cells (DLD-1 cells, hMSCs and fibroblasts) can proliferate in collagen/chitosan 3D scaffolds in both polystyrene and PDMS wells.

5.2 Future works

The following areas merit further research.

- Sterialisation technique: while in this study the author only used UV radiation, it could be worthwhile to investigate further as UV has been reported to cause polymer chain scission;
- Imaging capturing and analysis using MPM is indeed an intriguing task yet full of potential. With better visualisation of the inner cross-sectional structure of the scaffolds in future research, alterations could be made to tailor to specific needs of the particular tissue engineering application;
- The use of PDMS well plate in the current study is to shed light on the surface property and its effect on natural polymer scaffolds, with the ultimate aim to perform 3D culture in microfluidic perfusion bioreactors. Therefore, further studies are needed before full rollout of perfusion culture in PDMS bioreactors;
- Other fabrication technique, namely, electrospinning, may be useful to fabricate scaffolds in a controlled manner and merit further research;
- A thorough cell study to be performed to evaluate and compare across different scaffold/substrate combinations and concentrations.

References

[1] Langer, R. and Vacanti, J. P. (1993). Tissue engineering. *Science,* 260, 920-926.

[2] Nair, L. (2007). Biodegradable polymer as biomaterials. *Progress in Polymer Science,* 32(8-9), 762-798.

[3] Parikh, S. N. (2002). Bone graft substitutes: past, present, future. *Journal of Postgraduate Medicine,* 48(2), 142-148.

[4] O'Shaughnessy, T. J.; Lin, H. J. and Ma, W. (2003). Functional synapse formation among rat cortial neurons grown on three-dimensional collagen gels. *Neuroscience Letters,* 340, 169-172.

[5] Cho, S. (2005). Fabrication and characterization of porous alginate/polyvinyl alcohol hybrid scaffolds for 3D cell culture. *Journal of Biomaterial Science Polymer Edition,* 16(8), 933-947.

[6] Domard, A. and Taravel, M. N. (1995). Collagen and its interaction with chitosan: II. Influence of the physicochemical characteristics of collagen. *Biomaterials,* 16(11), 865–71.

[7] Gingras, M.; Beaulieu, M.M.; Gagnon, V.; Durham, H. D. and Berhod, F. (2008). In vitro study of axonal migration and myelination of motor neurons in a three-dimensional tissue engineering model. *Glia,* 56, 354-364.

[8] Tangsadthakun, C.; Kanokpanont, S.; Sanchavanakit, N.; Pichyangkura, R.; Banaprasert, T.; Tabata, Y. and Damrongsakkul, S. (2007). The influence of molecular weight of chitosan on the physical and biological properties of collagen/chitosan scaffolds. *J. Biomaterials Science Polymer Edition,* 18(2), 147-163.

[9] Tangsadthakun, C.; Kanokpanont, S.; Sanchavanakit, N.; Banaprasert, T. and Damrongsakkul, S. (2006). Properties of collagen/chitosan scaffolds for skin tissue engineering. *Journal of Metals, Materials and Minerals*, 16(1), 37.

[10] Che, Z. M.; Jung, T. H.; Choi, J. H.; Yoon-do, J.; Jeong, H. J.; Lee, E. J. and Kim, J. (2006). Collagen-based coculture for invasive study on cancer cells-fibroblasts interaction. *Biochem. Biophys. Res. Commun*., 346, 268–275.

[11] Sabeh, F.; Shimizu-Hirota, R. and Weiss, S. J. (2009). Protease-dependent versus independent cancer cell invasion programs: Three-dimensional amoeboid movement revisited. *J. Cell Biol*., 185, 11–19.

[12] Inoue, T.; Toda, S.; Narisawa, Y. and Sugihara, H. (2001). Subcutaneous adipocytes promote the differentiation of squamous cell carcinoma cell line (DJM-1) in collagen gel matrix culture. *J. Invest. Dermatol*., 117, 244–250.

[13] Shanmugasundaram, N.; Ravichandran, P.; Reddy, P. N.; Ramamurty, N.; Pal, S. and Rao, K. P. (2001). Collagen-chitosan polymeric scaffolds for the *in vitro* culture of human epidermoid carcinoma cells. *Biomaterials*, 22, 1943–1951.

[14] Matthew, B. M. and Antonios, G. M. (2007). Polymer scaffold fabrication. In: *Principles of Tissue Engineering*, third edition. New York: Elsevier, pp. 309-322.

[15] Joseph, V. and Charles, A. V. (2007). The history and scope of tissue engineering. In: *Principles of Tissue Engineering*, third edition. New York: Elsevier, pp. 3-6.

[16] Langer, R. and Lavik, E. (2004). Tissue engineering: current state and perspective. *Applied Microbiology and Biotechnology*, 65(1), 1-8.

[17] Will, J. (2008). Porous ceramic bone scaffolds for vascuarized bone tissue regeneration. *Journal of Material Science: Material Medicine*, 19, 2781-2790.

[18] Zmora, S. (2002). Tailoring the pore architecture in 3-D alginate scaffolds by controlling the freezing regime during fabrication. *Biomaterials*, 23, 4087-4094.

[19] Anders, M.; Hansen, R.; Ding, R. X.; Rauen, K. A.; Bissell, M. J. and Korn, W. M. (2003). Disruption of 3D tissue integrity facilitates adenovirus infection by deregulating the coxsackievirus and adenovirus receptor. *Proceedings of the National Academy of Science*, 100(4), 1943-1948.

[20] Chang, J. C.; Hsu, S. H. and Su, H. L. (2009). The regulation of the gap junction of human mesenchymal stem cells through the internalization of quantum dots. *Biomaterials*, 30(10), 1937-1946.

[21] Cukierman, E.; Pankov, R.; Stevens, D. R. and Yamada, K. M. (2001). Taking cell-matrix adhesions to the third dimension. *Science*, 294, 1708-1712.

[22] Jacks, T. and Weinberg, R. A. (2002). Taking the study of cancer cell survival to a new dimension. *Cell*, 111(7), 923-925.

[23] Duggal, S.; Frønsdal, K. B.; Szöke, K.; Shahdadfar, A.; Melvik, J. E. and Brinchmann, J. E. (2009). Phenotype and gene expression of human mesenchymal stem cells in alginate scaffolds. *Tissue Engineering Part A*, 15(7), 1763-1773.

[24] Potapova, I. A.; Brink, P. R.; Cohen, I. S. and Doronin, S. V. (2008). Culturing of human mesenchymal stem cells as 3Daggregates induces functional expression of CXCR4 that regulates adhesion to endothelial cells. *Journal of Biological Chemistry*, 283(19), 13100-13107.

[25] Rodriguez, A. M. and Vacanti, C. A. (1998) Tissue engineering of cartilage. *Frontiers in Tissue Engineering*, 400-411.

[26] Sahai, E. and Marshall, C. J. (2003). Differing modes of tumour cell invasion have distinct requirements for Rho/ROCK signalling and extracellular proteolysis. *Nature Cell Biology*, 8, 690-692.

[27] Weaver, V. M.; Petersen, O. W.; Wang, F.; Larabell, C. A.; Briand, P.; Damsky, C. and Bissell, M. J. (1997). Reversion of the malignant phenotype of human breast cells in three-dimensional culture and in vivo by integrin blocking antibodies. *Journal of Cell Biology*, 137, 231-245.

[28] Wolf, K.; Mazo, I.; Leung, H.; Engelke, K.; von Andrian, U. H.; Deryugina, E. I.; Strongin, A. Y.; Bröcker, E. B. and Friedl, P. (2003). Compensation mechanism in tumor cell migration: mesenchymal–amoeboid transition after blocking of pericellular proteolysis. *Journal of Cell Biology*, 160, 267-277.

[29] Dado, D. and Levenberg, S. (2009). Cell–scaffold mechanical interplay within engineered tissue. *Seminars in Cell & Developmental Biology*, 20(6), 656-664.

[30] Levenberg, S.; Huang, N. F.; Lavik, E.; Rogers, A. B.; Itskovitz-Eldor, J. and Langer, R. (2003). Differentiation of human embryonic stem cells on three-dimensional polymer scaffolds. *Proceedings National Academy of Science*, 100, 12741-12746.

[31] Chan, B. P. and Leong, K. W. (2008). Scaffolding in tissue engineering: general approaches and tissue-specific considerations. *European Spine Journal*, 17(4), 467-479.

[32] Globus, R. K.; Doty, S. B.; Lull, J. C.; Holmuhamedov, E.; Humphries, M. J. and Damsky, C. H. (1998). Fibronectin is a survival factor for differentiated osteoblasts. *Journal of Cell Science*, 111, 1385-1393

[33] Horton, M. A. (1997). The alpha v beta 3 integrin vitro receptor. International. *Journal Biochemistry and Cell Biology*, 29, 721-725.

[34] Grayson, W. L.; Ma, T. and Bunnell, B. (2004). Human mesenchymal stem cell tissue development in 3D PET matrices. *Biotechnology Progress*, 20, 905-912.

[35] Garcia, Y. (2007). Assessment of cell viability in a three-dimensional enzymatically crosslinked collagen scaffold. *Journal of Material Science, 18*, 1991-2001.

[36] Balasundaram, G. and Webster, T. J. (2007). Increased osteoblast adhesion on nanograined Ti modified with KRSR. *J Biomedical Materials Research A*, 80(3), 602-611.

[37] Ishida, K. and Yamaguchi, I. (2004). Role of albumin in osteoblastic cells: enhancement of cell proliferation and suppression of alkaline phosphatase activity. *International Journal of Molecular Medicine, 14*(6), 1077-1081.

[38] Shachar, M. and Cohen, S. (2003). Cardiac tissue engineering, ex-vivo: design principles in biomaterials and bioreactors. *Heart Failure Reviews*, 8, 271-276.

[39] Li, Y. M.; Schilling, T.; Benisch, P.; Zeck, S.; Meissner-Weigl, J.; Schneider, D.; Limbert, C.; Seufert, J.; Kassem, M.; Schütze, N.; Jakob, F. and Ebert, R. (2007). Effects of high glucose on mesenchymal stem cell proliferation and differentiation. *Biochemical and Biophysical Research Communications*, 363(1), 209-215.

[40] Weil, B. R.; Abarbanell, A. M.; Herrmann, J. L.; Wang, Y. and Meldrum, D. R. (2009). High glucose concentration in cell culture medium does not acutely affect human mesenchymal stem cell growth factor production or proliferation. *American Journal of Physiology*, 296, 1735-1743.

[41] Zhao, F.; Pathi, P.; Grayson, W.; Xing, Q.; Locke, B. R. and Ma, T. (2008). Effects of oxygen transport on 3-D human mesenchymal stem cell metabolic

activity in perfusion and static cultures: experiments and mathematical model. *Biotechnology Progress,* 21(4), 1269-1280.

[42] Leon, C. A. (1998). New Perspectives in mercury porosimetry. *Adv. Colloid Interface Sci.,* 76-77, 341-372.

[43] Kuboki, Y.; Takita, H.; Kobayashi, D.; Tsuruga, E.; Inoue, M. and Murata M. (1998). BMP-induced osteogenesis on the surface of hydroxyapatite with geometrically feasible and nonfeasible structures: topology of osteogenesis. *Journal of Biomedical Materials Research,* 39(2), 190-199.

[44] Hulbert, S. F.; Young, F. A.; Mathews, R. S.; Klawritter, J. J.; Talbert, C. D. and Stelling, F. H. (1970). Potential of ceramic materials as permanently implantable skeletal prostheses. *Journal of Biomedical Materials Research,* 4(3), 433-456.

[45] Cheung, H. Y.; Lau, K. T.; Lu, T. P. and Hui, D. (2006). A critical review on polymer-based bio-engineered materials for scaffold development. *Composites: Part B,* 38, 291-300.

[46] Murphy, C. M.; Haugh, M. G. and O'Brien, F. J. (2010). The effect of mean pore size on cell attachment, proliferation and migration in collagen-glycosaminoglycan scaffolds for bone tissue engineering. *Biomaterials,* 31, 461–466.

[47] Kirkpatrick, C. J. and Dekker, A. (1992). Quantitative evaluation of cell interaction with biomaterials in vitro. *Advanced Biomater*ials, 17, 93-102.

[48] Gurav, N. (1997). *Biocompatibility Testing of Resorbable Materials Using Improved In-vitro Techniques*. University of London.

[49] Hunter, A.; Archer, C. W.; Walker, P. S. and Blunn, G. W. (1995). Attachment and proliferation of osteoblasts and fibroblasts on biomaterials for orthopaedic use. *Biomaterials,* 16, 287–295.

[50] Mayer, U.; Szulczewski, D. H.; Moeller, K.; Heide, H. and Jones, D. B. (1993). Attachment kinetics and differentiation of osteoblasts on different biomaterial surfaces. *Cells and Materials*, 3, 129–140.

[51] Howlett, C. R.; Evans, M. D. M.; Walsh, W. R.; Johnson, G. and Steele, J. G. (1994). Mechanism of initial attachment of cells derived from human bone to commonly used prosthetic materials during cell culture. *Biomaterials*, 3, 213–222.

[52] Malik, M. A.; Puleo, D. A.; Bizios, R. and Doremus, R. H. (1992). Osteoblasts on hydroxyapatite, alumina and bone surfaces *in vitro* morphology during the first 2h of attachment. *Biomaterials*, 13, 123–128.

[53] Mayer, U.; Szulczewski, D. H.; Moeller, K.; Heide, H. and Jones, D. B. (1993). Attachment kinetics and differentiation of osteoblasts on different biomaterial surfaces. *Cells and Mater*ials, 3, 129-140.

[54] Chung, T. W.; Yang, J.; Akaike, T.; Cho, K. Y.; Nah, J. W.; Kim, S. I. and Cho, C. S. (2002). Preparation of alginate/galactosylated chitosan scaffold for hepatocyte attachment. *Biomaterials*, 23, 2827- 2834.

[55] Karbasi, S.; Mirzahed, H.; Orang, F. and Urban, J. P. G. (2005). A comparison between cell viability of chondrocytes on a biodegradable polyester urethane scaffold and alginate beads in different oxygen tension and pH. *Iranian Polymer Journal*, 14(9), 823-830.

[56] Nuttelman, C. R.; Tripodi, M. C. and Anseth, K. S. (2005). Synthetic hydrogel niches that promote hMSC viability. *Matrix Biology*, 24(3), 208-218.

[57] Nuttelman, C. R.; Benoit, D. S.; Tripodi, M. C.; Anseth, K. S. (2006). The effect of ethylene glycol methacrylate phosphate in PEG hydrogels on mineralization and viability of encapsulated hMSCs. *Biomaterials*, 27(8), 1377-1386.

[58] Zhao, F.; Grayson, W. L.; Ma, T.; Brunnell, B. and Lu, W. W. (2006). Effects of hydroxyapatite in 3-D chitosan-gelatin polymer networks on human mesenchymal stem cell construct development. *Biomaterials*, 27(9), 1859-1867.

[59] Choong, C.; Hutmacher, D. W. and Triffitt, J. T. (2006). Co-culture of bone marrow fibroblasts and endothelial cells on modified polycaprolactone substrates for enhanced potentials in bone tissue engineering. *Tissue Engineering*, 12(9), 2521-2531.

[60] Li, W. J.; Tuli, R.; Huang, X.; Laquerriere, P. and Tuan, R. S. (2005). Multilineage differentiation of human mesenchymal stem cells in a three-dimensional nanofibrous scaffold. *Biomaterials*, 26 (25), 5158-5166.

[61] Li, W. J.; Laurencin, C. T.; Caterson, E. J.; Tuan, R. S. and Ko, F. K. (2002). Electrospun nanofibrous structure: a novel scaffold for tissue engineering. *Journal Biomedical Material Research*, 60, 613-621.

[62] Yang, X. B.; Roach, H. I.; Clarke, N. M.; Howdle, S. M.; Quirk, R. and Shakesheff, K. M. (2001). Human osteoprogenitor growth and differentiation on synthetic biodegradable structures after surface modification. *Bone*, 29(6), 523-531.

[63] Ma, T.; Li, Y.; Yang, S. T. and Kniss, D. A. (2000). Effects of pore size in 3-D fibrous matrix on human trophoblast tissue development. *Biotechnology and Bioengineering*, 70, 606-618.

[64] Nuttelman, C. R.; Tripodi, M. C. and Anseth, K. S. (2004). In vitro osteogenic differentiation of human mesenchymal stem cells photoencapsulated in PEG hydrogels. *Journal Biomedical Materials Research Part A*, 68(4), 773-782.

[65] Buschmann, M. D.; Gluzband, Y. A.; Grodzinsky, A. J. and Hunziker, E. B. (1995). Mechanical compression modulates matrix biosynthesis in chondrocyte/agarose culture. *Journal Cell Science*, 108, 1497-1508.

[66] Buschmann, M. D.; Gluzband, Y. A.; Grodzinsky, A. J.; Kimura, J. H. and Hunziker, E. B. (1992). Chondrocytes in agarose culture synthesize a mechanically functional extracellular matrix. *Journal Orthopedic Research*, 10, 745-758.

[67] Lee, D. A.; Noguchi, T.; Knight, M. M.; O'Donnell, L.; Bentley, G. and Bader, D. L. (1998). Response of chondrocyte subpopulations cultured within unloaded and loaded agarose. *Journal Orthopedic Research*, 16, 726-733.

[68] Mauck, R. L.; Soltz, M. A.; Wang, C. C.; Wong, D. D.; Chao, P. H.; Valhmu, W. B.; Hung, C. T. and Ateshian, G. A. (2000). Functional tissue engineering of articular cartilage through dynamic loading of chondrocyte-seeded agarose gels. *Journal of Biomechanical Engineering*, 122, 252-260.

[69] Mauck, R. L.; Yuan, X. and Tuan, R. (2006). Chondrogenic differentiation and functional maturation of bovine mesenchymal stem cells in long-term agarose culture. *Osteoarthritis and Cartilage*, 14(2), 179

[70] Raghunath, J.; Salacinski, H. J.; Sales, K. M.; Butler, P. E. and Seifalian, A. M. (2005). Advancing cartilage tissue engineering: the application of stem cell technology. *Current Opinion in Biotechnology*, 16, 503-509.

[71] Diduch, D. R.; Jordan, L. C.; Mierisch, C. M. and Balian, G. (2000). Marrow stromal cells embedded in alginate for repair of osteochondral defects. *Arthroscopy*, 16, 571-577.

[72] Batorsky, A.; Liao, J.; Lund, A. W.; Plopper, G. E. and Stegemann, J. P. (2005). Encapsulation of adult human mesenchymal stem cells within

collagen-agarose microenvironments. *Biotechnology and Bioengineering*, 92(4), 492-500.

[73] Drury, J. and Mooney, D. (2003). Hydrogels for tissue engineering: scaffold design variables and applications. *Biomaterials*, 24(24), 4337-4351.

[74] Woolverton, C. J.; Fulton, J. A.; Lopina, S. T. and Landis, W. J. (2002). Mimicking the natural tissue environment. In: *Tissue Engineering and Biodegradable Equivalents*, CRC Press, pp. 43-76.

[75] Chang, S. C.; Rowley, J. A.; Tobias, G.; Genes, N. G.; Roy, A. K.; Mooney, D. J.; Vacanti, C. A. and Bonassar, L. J. (2001). Injection molding of chondrocyte/alginate constructs in the shape of facial implants. *Journal Biomedical Material Research*, 55, 503-511.

[76] Chubinskaya, S.; Huch, K.; Schulze, M.; Otten, L.; Aydelotte, M. B. and Cole, A. A. (2001). Gene expression by human articular chondrocytes cultured in alginate beads. *Journal of Histochemistry and Cytochemistry*, 49, 1211-1220.

[77] Fragonas, E.; Valente, M.; Pozzi-Mucelli, M.; Toffanin, R.; Rizzo, R.; Silvestri, F. and Vittur, F. (2000). Articular cartilage repair in rabbits by using suspensions of allogenic chondrocytes in alginate. *Biomaterials*, 21, 795-801.

[78] Paige, K. T.; Cima, L. G.; Yaremchuk, M. J.; Schloo, B. L.; Vacanti, J. P. and Vacanti, C. A. (1996). De novo cartilage generation using calcium alginate-chondrocyte constructs. *Plastic Reconstructive Surgery*, 97, 168-180.

[79] Rowley, J. A.; Madlambayan, G. and Mooney, D. J. (1999). Alginate hydrogels as synthetic extracellular matrix materials. *Biomaterials*, 20, 45-53.

[80] Paige, K.; Cima, L. G.; Yaremchuk, M. J.; Vacanti, J. P. and Vacanti, C. A. (1995). Injectable cartilage. *Plastic Reconstructive Surgery*, 96, 1390-1400.

[81] Erickson, G. R.; Gimble, J. M.; Franklin, D. M.; Rice, H. E.; Awad, H. and Guilak, F. (2002). Chondrogenic potential of adipose tissue-derived stromal cells in vitro and in vivo. *Biochemical and Biophysical Research Communications*, 290, 763-769.

[82] Rowley, J. A.; Madlambayan, G. and Mooney, D. J. (1999). Alginate hydrogels as synthetic extracellular matrix materials. *Biomaterials*, 20, 45–53.

[83] Lawson, M. A.; Barralet, J. E.; Wang, L.; Shelton, R. M. and Triffitt, J. T. (2004). Adhesion and growth of bone marrow stromal cells on modified alginate hydrogels. *Tissue Engineering*, 10(9-10), 1480-1491.

[84] Van Susante, J. L.; Buma, P.; van Osch, G. J.; Versleyen, D.; van der Kraan, P. M.; van der Berg, W. B. and Homminga, G. N. (1995). Culture of chondrocytes in alginate and collagen carrier gels. *Acta Orthopaedica Scandinavica*, 66, 549-556.

[85] Zhang, W. J.; Laue, C. H.; Hyder, A. and Schrezenmeir, J. (2001). Purity of alginate affects the viability and fibrotic overgrowth of encapsulated porcine islet xenografts. *Transplant Proceedings*, 33, 3517–3519.

[86] Ogura, N.; Kawada, M.; Chang, W. J.; Zhang, Q.; Lee, S. Y.; Kondoh, T. and Abiko, Y. (2004). Differentiation of the human mesenchymal stem cells derived from bone marrow and enhancement of cell attachment by fibronectin. *Journal Oral Science*, 46(4), 207-213.

[87] Martino, M. M.; Mochizuki, M.; Rothenfluh, D. A.; Rempel, S. A.; Hubbell, J. A. and Barker, T. H. (2009). Controlling integrin specificity and stem cell differentiation in 2D and 3D environments through regulation of fibronectin domain stability. *Biomaterials*, 30(6), 1089-1097.

[88] Lodish, H.; Berk, A.; Matsudaira, P.; Kaiser, C. A.; Krieger, M.; Scott, M. P.; Zipursky, S. L. and Darnell, J. (2000). Integrating cells into tissues. *Molecular Cell Biology*, 197–234.

[89] Aigner, J.; Tegeler, J.; Hutzler, P.; Campoccia, D.; Pavesio, A.; Hammer, C.; Kastenbauer, E. and Naumann, A. (1998). Cartilage tissue engineering with novel nonwoven structured biomaterial based on hyaluronic acid benzyl ester. *Journal Biomedical Material Research*, 42(2), 172-81.

[90] Lisignoli, G.; Cristino, S.; Piacentini, A.; Cavallo, C.; Caplan, A. I.; Facchini, A. (2005). Hyaluronan-based polymer scaffold modulates the expression of inflammatory and degradative factors in mesenchymal stem cells: Involvement of Cd44 and Cd54. *Journal of Cellular Physiology*, 207(2), 364-373.

[91] Radice, M.; Brun, P.; Cortivo, R.; Scapinelli, R.; Battaliard, C. and Abatangelo G. (2000). Hyaluronan-based biopolymers as delivery vehicles for bone-marrow-derived mesenchymal progenitors. *Journal of Biomedical Material Research*, 50(2), 101-109.

[92] Chung, C. and Burdick, J. A. (2009). Influence of three-dimensional hyaluronic acid microenvironments on mesenchymal stem cell chondrogenesis. *Tissue Engineering Part A*, 15(2), 243-254.

[93] Schmitt, B.; Ringe, J.; Haupl, T.; Notter, M.; Manz, R.; Burmester, G. R.; Sittinger, M. and Kaps, C. (2003). BMP2 initiates chondrogenic lineage development of adult human mesenchymal stem cells in high-density culture. *Differentiation*, 71(9-10), 567-577.

[94] Tigli, R. S.; Ghosh, S.; Laha, M. M.; Shevde, N. K.; Daheron, L.; Gimble, J.; Gümüsderelioglu, M. and Kaplan, D. L. (2009). Comparative chondrogenesis of human cell sources in 3D scaffolds. *Journal of Tissue Engineering and Regenerative Medicine*, 3(5), 348-360.

[95] Kleinman, H. K.; McGarvey, M. L.; Hassell, J. R.; Star, V. L.; Cannon, F. B.; Laurie, G. W. and Martin, G. R. (1986). Basement membrane complexes with biological activity. *Biochemistry*, 25, 312-318.

[96] Kleinman, H. K.; McGarvey, M. L.; Liotta, L. A.; Gehron, R. P.; Tryggvason, K. and Martin, G. R. (1982). Isolation and characterization of type IV procollagen, laminin, and heparan sulfate proteoglycan from the EHS sarcoma. *Biochemistry*, 21, 6188-6193.

[97] Soofi, S. S.; Last, J. A.; Liliensiek, S. J.; Nealey, P. F. and Murphy, C. J. (2009). The elastic modulus of MatrigelTM as determined by atomic force microscopy. *Journal of Structural Biology*, 167(3), 216-219.

[98] Word, A. G. and Courts, A. (1978). The Science and Technology of Gelatin. *Molecular Nutrition*, 22(4), 444-445.

[99] Kenchington, A. W. (1958). Chemical modification of the side chains of gelatin. *Biochemical Journal*, 68, 458-468.

[100] Shin, Y. M.; Kim, K. S.; Lim, Y. M.; Nho, Y. C. and Shin, H. (2008). Modulation of spreading, proliferation, and differentiation of human mesenchymal stem cells on gelatin-immobilized poly(l-lactide-*co*-ecaprolactone) substrates. *Biomacromolecules*, 9(7), 1772-1781.

[101] Huang, Y.; Onyeri, S.; Siewe, M.; Moshfeghian, A. and Madihally, S. V. (2005). In vitro characterization of chitosangelatin scaffolds for tissue engineering. *Biomaterials*, 26(36), 7616-7627.

[102] Madihally, S. V. and Matthew, H. W. (1999). Porous chitosan scaffolds for tissue engineering. *Biomaterials*, 20(12), 1133-1142.

[103] Chandy, T. and Sharma, C. P. (1990). Chitosan as a biomaterial. *Biomaterials, Artificial Organs and Tissue Engineering*, 18, 1-24.

[104] Suh, J. K. F. and Matthew, H. W. T. (2000). Application of chitosan-based polysaccharide biomaterials in cartilage tissue engineering: A review. *Biomaterials*, 21(24), 2589-2598.

[105] Ben-Ari, A.; Rivkin, R.; Frishman, M.; Gaberman, E.; Levdansky, L. and Gorodetsky, R. (2009). Isolation and implantation of bone marrow–derived mesenchymal stem cells with fibrin micro beads to repair a critical-size bone defect in mice. *Tissue Engineering Part A*, 15(9), 2537-2546.

[106] Bensaïd, W.; Triffitt, J. T.; Blanchat, C.; Oudina, K.; Sedel, L. and Petite, H. (2003). A biodegradable fibrin scaffold for mesenchymal stem cell transplantation. *Biomaterials*, 24(14), 2497-2502.

[107] Ho, W.; Tawil, B.; Dunn, J. C. Y. and Wu, B. M. (2006). The behaviour of human mesenchymal stem cells in 3D fibrin clots: dependence on fibrinogen concentration and clot structure. *Tissue Engineering*, 12(6), 1587-1595.

[108] Neuss, S.; Schneider, R. K.; Tietze, L.; Knüchel, R. and Jahnen-Dechent, W. (2009). Secretion of fibrinolytic enzymes facilitates human mesenchymal stem cell invasion into fibrin clots. *Cells Tissues Organs*, 191(1), 36-46.

[109] Alberts, B.; Johnson, A.; Lewis, J.; Raff, M.; Roberts, K. and Walter P. (2007). In: *Molecular Biology of the Cell*, fifth edition. London: Garland Science, pp. 146-147.

[110] Brinckmann, J. (2006). Collagens at a glance. In: *Collagen: Primer in Structure, Processing and Assembly*. New York: Springer, pp. 1-7.

[111] Schegg, B.; Hülsmeier, A. J.; Rutschmann, C.; Maag, C. and Hennet, T. (2009). Core glycosylation of collagen is initiated by two β(1-*O*)galactosyltransferases. *Molecular and Cellular Biology*, 29(4), 943-952.

[112] Csaki, C.; Matis, U.; Mobasheri, A. and Shakibaei, M. (2008). Co-culture of canine mesenchymal stem cells with primary bone-derived osteoblasts promotes osteogenic differentiation. *Histochemistry and Cell Biology*, 131(2) 251-266.

[113] Ito, T.; Sawada, R.; Fujiwara, Y. and Tsuchiya, T. (2008). FGF-2 increases osteogenic and chondrogenic differentiation potentials of human mesenchymal stem cells by inactivation of TGF-β signalling. *Cytotechnology*, 56(1), 1-7.

[114] Shakibaei, M.; De Souza, P. and Merker, H. J. (1997). Integrin expression and collagen type II implicated in maintenance of chondrocyte shape in monolayer culture: an immunomorphological study. *Cell Biology International*, 21(2), 115-125.

[115] Fratzl, P. (2008). Collagen: Structure and Mechanics, an Introduction. In: *Collagen: Structure and Mechanics*. New York: Springer, pp. 1-12.

[116] Au-yeung, K. L.; Sze, K. Y.; Sham, M. H. and Chan, B. P. (2009). Development of a micromanipulator-based loading device for mechanoregulation study of human mesenchymal stem cells in three-dimensional collagen constructs. *Tissue Engineering Part C Methods*, 16(1), 93-107.

[117] Han, B.; Huang, L. L. H.; Cheung, D.; Cordoba, F. and Nimni, M. (1999). Polypeptide growth factors with a collagen binding domain: Their potential for tissue repair and organ regeneration. In: *Tissue Engineering of Vascular Prosthetic Grafts*. London: RG Landes, pp. 287-299.

[118] Hui, T. Y.; Cheung, K. M.; Cheung, W. L.; Chan, D. and Chan, B. P. (2008). In vitro chondrogenic differentiation of human mesenchymal stem cells in collagen microspheres: influence of cell seeding density and collagen concentration. *Biomaterials*, 29(22), 3201-3212.

[119] Neuss, S.; Stainforth, R.; Salber, J.; Schenck, P.; Bovi, M.; Knüchel, R. and Perez-Bouza, A. (2008). Long-term survival and bipotent terminal differentiation of human mesenchymal stem cells (hMSC) in combination

with a commercially available three-dimensional collagen scaffold. *Cell Transplantation,* 17(8), 977-986.

[120] Yoneno, K.; Ohno, S.; Tanimoto, K.; Honda, K.; Tanaka, N.; Doi, T.; Kawata, T.; Tanaka, E.; Kapila, S. and Tanne, K. (2005). Multidifferentiation potential of mesenchymal stem cells in three-dimensional collagen gel cultures. *Journal of Biomedical Material Research Part A,* 75(3), 733-741.

[121] O'Brien, F. J.; Harley, B. A.; Yannas, I. V. and Gibson, L. (2004). Influence of freezing rate on pore structure in freeze-dried collagen-GAG scaffolds. *Biomaterials,* 25, 1077-1086.

[122] O'Brien, F. J.; Harley, B. A.; Yannas, I. V. and Gibson, L. (2005). The effect of pore size on cell adhesion in collagen-GAG scaffolds. *Biomaterials*, 26, 433-441.

[123] Muzzarelli, R. (1994). In: *Polymeric Biomaterials*. New York: Marcel Dekker, pp. 179-196.

[124] Jackson, R. I.; Busch, S. J. and Cardin, A. D. (1991). Glycosaminoglycans: molecular properties, protein interactions, and role in physiological processes *Physiol. Rev*., 71(2), 481-539.

[125] Xu, T.; Molnar, P.; Gregory, C.; Das, M.; Boland, T and Hickman, J. J. (2009). Electrophysiological characterisation of embryonic hippocampal neurons cultured in a 3D collagen hydrogel. *Biomaterials*, 30, 4377-4383.

[126] Ma, W.; Fitzgerald, W.; Liu, Q. Y.; O'Shaughnessy, T. J.; Maric, D.; Lin, H. J.; Alkon, D. L. and Barker, J. L. (2004). CNS stem and progenitor cell differentiation into functional neuronal circuits in three-dimensional collagen gels. *Exp. Neurol*., 190, 276-288.

[127] Harris, L. D.; Kim, B. S. and Mooney, D. J. (1998). Open pore biodegradable matrices formed with gas forming. *Biomedical Materials Research, 42(3),* 396-402.

[128] El-Ayoubi, R. (2008). Design and fabrication of 3D porous scaffolds to facilitate cell-based gene therapy. *Tissue Engineering, 14*(6), 1037-1048.

[129] Liao, C. J.; Chen, C. F.; Chen, J. H.; Chiang, S. F.; Lin, Y. J. and Chang, K. Y. (2002). Fabrication of porous biodegradable polymer scaffolds using a solvent merging/particulate leaching method. *Journal of Biomedical Materials Research*, 59(4), 676–81.

[130] Lee, S. B.; Kim, Y. H.; et al. (2004). Study of gelatin-containing artificial skin V: fabrication of gelatin scaffolds using a salt-leaching method. *Biomaterials*, 26, 1961-1968.

[131] Subia, B.; Kundu, J. and Kundu, S. C. (2010). Biomaterial scaffold fabrication techniques for potential tissue engineering applications. In: *Tissue Engineering*. Mumbai: Indian Institute of Technology, pp. 141-159.

[132] Czernuszka, J. T. (2003). Making tissue engineering scaffolds work. *European Cells and Materials*, 5, 29-40.

[133] Huang, Y. C. and Mooney, D. J. (2005). Gas forming to fabricate polymer scaffolds in tissue engineering. In: *Scaffoldings in tissue engineering*. London: Taylor and Francis group CRC press, pp. 61-72.

[134] Matthews, J. A.; Wnek, G. E.; Simpson, D. G. and Bowlin, G. L. (2002). Electrospinning of collagen nanofibers. *Biomacromolecules*, 3(2), 232-238.

[135] Barnes, C. P.; Smith, M. J.; Bowlin, G. L.; et al. (2006). Feasibility of electrospinning the globular proteins hemogloblin and myogloblin. *Journal of Engineered Fibers and Fabrics*, 1(2), 16-28.

[136] MaManus, M.; Boland, E.; et al. (2007). Electrospun nanofiber fibrinogen for urinary tract tissue reconstruction. *Biomedical Materials*, 2(4), 257-262.

[137] Boland, E. D.; Coleman, B. D.; et al. (2005). Electrospinning polydioxanone for biomedical applications. *Acta Biomaterialia*, 1(1), 115-123.

[138] Jha, B. S.; et al. (2011) Two pole air gap electrospinning. *Acta Biomaterialia*, 7(1), 203-215.

[139] Telemeco, T. A.; Ayres, C.; Bowlin, G. L.; et al. (2005). Regulation of cellular infiltration into tissue engineering scaffolds composed of sublimed diameter fibrils produced by electrospinning. *Acta Biomaterialia*, 1(4), 377-385.

[140] Sell, S. A.; et al. (2006). Electrospun polydioxanone-elastin blends. *Biomedical Materials*, 1(2), 72-80.

[141] McClures, M. J.; et al. (2009). Electrospun polydioxane-polycaprolactone-silk fibroin-blended scaffolds. *Biomedical Materials*, 4(5), 90-98.

[142] Jha, B. S.; Ayres, C. E.; et al. (2011). Electrospun collagen a tissue engineering scaffold with unique functional properties in a wide variety of applications. *Journal of Nanomaterials*, 2011, 1-15.

[143] Abdelaal, O. A. and Darwish, S. M. (2011). Fabrication of tissue engineering scaffolds using rapid prototyping techniques. *World Academy of Science, Engineering and Technology*, 5, 1325-1333.

[144] Kumar, S. and Kruth, J. P. (2010). Composites by rapid prototyping technology. *Materials and Design*, 31(2), 850-856.

[145] Naing, M. W.; Chua, C. K. and Leong, K. F. (2008). Computer Aided Tissue Engineering Scaffold Fabrication. In: *Virtual Prototyping & Bio Manufacturing in Medical Applications*. New York: Springer, pp. 67-85.

[146] Shanjani, Y.; De Croos, J. N. A.; Pilliar, R. M.; Kandel, R. A. and Toyserkani, E. (2010). Solid freeform fabrication and characterization of porous calcium polyphosphate structures for tissue engineering purposes. J *Biomedical Materials Research Part B: Applied Biomaterials*, 93B(2), 510-519.

[147] Hua, F. J.; Nam, J. D. and Lee, D. S. (2001). Preparation of a macroporous poly(L-lactide) scaffold by liquid-liquid phase separation of a PLLA/1,4-dioxane/water ternary system in the presence of NaCl. *Macromol. Rapid Comm*., 22(13), 1053-1057.

[148] Aubert, J. H. and Clough RL. (1985). Low density, microcellular polystyrene foams. *Polymer*, 26(13), 2047-2054.

[149] Sylwester, A. P. and Renschler, C. L. (1989). Refractory films from spin-cast carbon. *Synthetic Materials*, 29(2-3), 253-258.

[150] Aubert, J. H. (1988). Isotactic polystyrene phase diagrams and physical gelation *Macromolecules*, 21, 3468-3473.

[151] Nam, Y. S. and Park, T. G. (1999). Biodegradable polymeric microcellular foams by modified thermally induced phase separation method. *Biomaterials*, 20(19), 1783-1790.

[152] Gao, C. Y.; Li, A.; Feng, L. X.; Yi, X. S. and Shen, J. C. (2001). Factors controlling the preparation of porous polyurethane membranes via thermally induced phase separation. *Acta Polymeica. Sinica*, 19, 351-356.

[153] Gao, C. Y.; Li, A.; Feng, L. X.; Yi, X. S. and Shen, J. C. (2000). Factors controlling surface morphology of porous polystyrene membranes prepared by thermally induced phase separation. *Polymer Interernational,* 49, 323-328.

[154] Zhu, Y. B.; Gao, C. Y.; Guan, J. J. and Shen, J. C. (2003). Engineering porous polyurethane scaffolds by photografting polymerization of methacrylic acid for improved endothelial cell compatibility. *Journal of Biomedical Materials Research,* 67A, 1367-1373.

[155] Adams, G. (2007). The principles of freeze-drying. In: second edition, *Cryopreservation and Freeze-Drying Protocols*. New Jersey: Humana Press, pp. 15-38.

[156] Abdelwahed, W.; Degobert, G. and Fessi, H. (2006). Freeze-drying of nanocapsules: Impact of annealing on the drying process. *International Journal of Pharmaceutics*, 324(1), 74-82.

[157] Elaine, M. (2007). Array Tape for Miniaturised Genotyping. *Genetic Engineering and Biotechnology,* 22.

[158] Ray, M. (1999). In: *Microplate History*, second ed. Online: Microplate Org..

[159] Kricka, L. J.; Master, S. R. (2009). Quality Control and Protein Microarray. *Clinical Chem*istry, 55, 1053-55.

[160] Isett, K.; George, H.; Herber, Wayne. and Amanullah, A. (2007). Twenty-four-well plate miniature bioreactor high-throughput system. *Biotechnology and Bioengineering*, 98(5), 1017-28.

[161] Monks, T. (2000). *Multi-well plate*. US Patent USD420743 S.

[162] Mathus, G. (1999). *Multi-well plate*. US Patent US5972694 A.

[163] Koshy, P. T. K.; Rowan, A. D.; Life, P. F. and Cawston, T. E. (1999). 96-Well Plate Assays for Measuring Collagenase Activity Using 3H-Acetylated Collagen. *Analytical Biochemistry*, 275(2), 202-207.

[164] Mata, A.; Fleischman, A. J. and Roy, S. (2005). Characterisation of polydimethylsiloxane (PDMS) properties for biomedical micro/nanosystems. *Biomed Microdevices,* 7(4), 281-293.

[165] McDonald, J. C. and Whitesides, G. M. (2002). Poly(dimethylsiloxane) as a material for fabricating microfluidic devices. *Accounts of Chemical Research, 35(7),* 491-499.

[166] Ng, J. M. K.; Gitlin, I.; Strook, A. D. and Whitesides, G. M. (2002). Components for integrated poly(dimethylsiloxane) microfluidic systems. *Electrophoresis, 23(13),* 3461-3473.

[167] Xia, Y. and Whitesides, G. M. (1998). Soft lithography. *Angewandte Chemie International Edition, 37(5),* 550-575.

[168] Jo, B. H.; van Lerberghe, L. H.; Motsegood, K. M. and Beebe, D. J. (2000). Plasma-Based Surface Modification of Polydimethylsiloxane for PDMS-PDMS Molding. *Journal of Microelectromechanical Systems, 9(1),* 76-81.

[169] Mata, A.; Boehm, C.; Fleischman, A. J.; Muschler, G. and Roy, G (2002). Characterization of polydimethylsiloxane (PDMS) properties for biomedical micro/nanosystems. *Journal of Biomedical Materials Research, 62(4),* 499-506.

[170] Visser, S.A.; Hergenrother, R. W. and Cooper. S. L. (1996). Nanofibers and their applications in tissue engineering. In: *Polymers and Biomaterials Science*. London: Academic Press, pp. 50-60.

[171] Chou, H. P.; Thorsen, T.; Scherer, A. and Quake, S. R. (2000). Programmable Microfluidics Using Soft Lithography. *Science*, 288, 113-116.

[172] Regehr, K. J.; Domenech, M.; Koepsel, J. T.; Carver, K. C.; Ellison-Zelski, S. J.; Murphy, W. L.; Schuler, L. A.; Alarid, E. T. and Beede, D. J. (2009). Biological implications of polydimethylsiloxane-based microfluidic cell culture. *The Royal Society of Chemistry*, 2009(9), 2132-2139.

[173] Kane, R.; Takayama, S.; Ostuni, E.; Ingber, D. and Whitesides, G. (1999). Combining microscience and neurobiology. *Biomaterials*, 20, 2363-2376.

[174] Jo, B.; van Lerberghe, L.; Motsegood, K. and Beebe, D. (2000). Biological implications of polydimethylsiloxane-based microfluidic cell culture. *Microelectomechical Systems*, 9, 76-81.

[175] Leclerc, E.; Sakai, Y. and Fujii, T. (2003). Cell Culture in 3-Dimensional Microfluidic Structure of PDMS (polydimethylsiloxane). *Biomedical Microdevices*, 5, 109-114.

[176] Boxshall, K.; Wu, M. H.; Cui, Z. F.; Watts, J. F. and Baker, M. A. (2006). Simple surface treatments to modify protein adsorption and cell attachment properties within a Poly(dimethylsiloxane) microbioreactor. *Surface and Interface Analysis*, 38, 198-201.

[177] Mygind, T.; Stiehler, M.; Baatrup, A.; Li, H.; Zou, X.; Flyvbjerg, A.; Kassem, M. and Bunger, C. (2006). Mesenchymal stem cell ingrowth and differentiation on coralline hydroxyapatite scaffolds. *Biomaterials*, 28, 1036-1047-1057.

[178] Zou, X.; Li, H.; Baatrup, A.; Lind, M. and Bunger, C. (2003). Engineering of bone tissue with porcine bone mattow stem cells in three-dimensional trabecular metal: *in vitro* and *in vivo* studies. *APMIS*, 109, 127-132.

[179] Ishaug-Riley, S. L.; Crane-Kruger, G. M.; Yaszemski, M. J.and Mikos, A. G. (1998). Three-dimensional culture of rat calvarial osteoblasts inporous biodegradable polymers. *Biomaterials*, 19(15), 1405-1412.

[180] Weinand, C.; Pomerantseva, I.; Neville, C. M. Gupta, R. and Weiberg, E. (2005). Hydrogel-beta-TCP scaffolds and stem cells for tissue engineering bone. *Bone*, 38(4), 555-563.

[181] Rucci, N.; Migliaccio, S.; Zani, B. M.; Taranta, A. and Teti, A. (2002). Characterisation of the osteoblast-like cell phenotype under microgravity conditions in the NASA-approved Rotating Wall Vessel bioreactor (RWV). *J. Cell Biochemistry*, 85(1), 167-179.

[182] Sikavitsas, V. I.; Bancroft, G. N. and Mikos, A. G. (2002). Formation of three-dimensional cell/polymer constructs for bone tissue engineering in a spinner flask and a rotating wall vessel bioreactor. *J. Biomedical Materials Research*, 62(1), 136-148.

[183] Goldstein, A. S.; Juarez, T. M.; Helmke, C. D.; Gustin, M. C. and Mikos, A. G. (2001). Effect of convection on osteoblastic cell growth and function in biodegradable polymer foam scaffolds. *Biomaterials*, 22(11), 1279-1288.

[184] Holtorf, H. L.; Jansen, J. A. and Mikos, A. G. (2005). Flow perfusion culture induces the osteoblastic differentiation of marrow stroma cell-

scaffold constructs in the absence of dexamethasone. *J. Biomedical Materials Research A*, 72(3), 326-334.

[185] Williams, J. L.; Iannotti, J. P.; Ham, A.; Bleuit, J. and Chen, J. H. (1994). Effects of fluid shear stress on bone cells. *Biotechnology*, 31(2), 163-170.

[186] Figallo, E.; Cannizzaro, C.; Gerecht, S.; Burdick, J. A.; Langer, R.; Elvassore, N. and Vunjak-Novakovic, G. (2007). Micro-bioreactor array for controlling cellular microenvironments. *Lab on a Chip*, 7, 710-719.

[187] Sim, W. Y.; Park, S. W.; Park, S. H.; Min, B. H.; Park, S. R. and Yang, S. S. (2007). A pneumatic micro cell chip for the differentiation of human mesenchymal stem cells under mechanical stimulation. *Lab on a Chip*, 7, 1775-1782.

[188] Wu, M. H.; Huang, S. B.; Cui, Z. F. and Lee, G. B. (2008). A high throughput perfusion-based microbioreactor platform integrated with pneumatic micropumps for three-dimensional cell culture. *Biomedical Microdevices*, 10(2), 309-319.

[189] Kimura, H.; Yamamoto, T.; Sakai, H.; Sakai, Y. and Fuji, T. (2008). An integrated microfluidic system for long-term perfusion culture and on-line monitoring of intestinal tissue models. *Lab on a Chip*, 8, 741-746.

[190] Khademhosseini, A.; Du, Y.; Rajalingam, B.; Vacanti, J. P. and Langer, R. S. (2008). Microscale technologies for tissue engineering. In: *Advances in Tissue Engineering*. London: Imperial College Press, pp. 349-369.

[191] Leclerc, E.; Sakai, Y. and Fuji, T. (2004). Microfluidic PDMS (polydimethylsiloxane) bioreactor for large-scale culture of hepatocytes. *Biotechnology Progress*, 20, 750-755.

[192] Huang, C. W.; Huang, S. B. and Lee, G. B. (2006). Pneumatic micropumps with serially connected actuation chambers. *Journal of Micromechanics and Microengineering*, 16, 2265-2272.

[193] Wu, M. H.; Cai, H.; Xu, X.; Urban, J. P. G. and Cui, Z. F. (2005). A SU-8/PDMS hybrid microfluidic device with integrated optical fibers for online monitoring of lactate. *Biomedical Microdevices*, 7(4), 323- 329.

[194] Rogers, J. A. and Nuzzo, R. G. (2005). Recent progress in soft lithography. *Materials Today*, 8(2), 50-56.

[195] Yoshii, Y.; Waki, A.; Yoshida, K.; Kakezuka, A.; Kobayashi, M.; Namiki, H.; Kuroda, Y.; Koyono, Y.; Yoshii, H.; Furukawa, T.; Asai, T.; Okazawa, H.; Gelovani, J. G. and Fujibayashi, Y. (2011). The use of nanoimprinted scaffolds as 3D culture models to facilitate spontaneous tumor cell migration and well-regulated spheroid formation. *Biometerials*, 32, 6052-6058.

[196] Cikierman, E.; Pankox, R.; Steven, D. R. and Yamada, K. M. (2001). Taking cell-matrix adhesions to the third dimension. *Science*, 294(5547), 1708-1712.

[197] Mizushima, H.; Wang, X.; Miyatomo, S.and Mekada, E. (2009). Intefrin signal masks growth-promotion activity of HB-EGF in monolayer cell cultures. *J. Cell Science*, 122(23), 4277-4286.

[198] Yamada, K. M.; Cikierman, E. (2007). Modeling tissue morphogenesis and cancer in 3D. *Cell*, 130(4), 601-610.

[199] Stachowiak, A. N. and Irvine, D. J. (2008). Inverse opal hydrogel-collagen composite scaffolds as a supportive microenvironment for immune cell migration. *J. Biomedical Materials Research A*, 85, 815–828.

[200] Wolf, K.; Muller, R.; Borgmann, S.; Brocker, E. B. and Friedl, P. (2003). Amoeboid shape change and contact guidance: T-lymphocyte crawling

through fibrillar collagen is independent of matrix remodeling by MMPs and other proteases. *Blood*, 102, 3262–3269.

[201] Spencer, N. J.; Cotanche, D. A. and Klapperich, C. M. (2008). Peptide- and collagen-based hydrogel substrates for in vitro culture of chick cochleae. *Biomaterials*, 29, 1028–1042.

[202] Cortial, D.; Gouttenoire, J.; Rousseau, C. F.; Ronziere, M. C.; Piccardi, N.; Msika, P.; Herbage, D.; Mallein-Gerin, F. and Freyria, A. M. (2006). Activation by IL-1 of bovine articular chondrocytes in culture within a 3D collagen-based scaffold: an in vitro model to address the effect of compounds with therapeutic potential in osteoarthritis. *Osteoarthritis Cartilage*, 14, 631–640.

[203] Kim, J. B. (2005). Review: three-dimensional tissue culture models in cancer biology. *Seminars in Cancer Biology*, 15, 365-377.

[204] Smith, S. H.; Wolman, S. R.; Hackett, A. J. (1984). The biology of breast cancer at the cellular level. *Biochemical and Biophysical Acta*, 783, 103-123.

[205] Petersen, O. W.; Ronnov-Jessen, L.; Howlett, A. R. and Bissell. M. J. (1992). Interaction with basement membrane serves to rapidly distinguish growth and differentiation pattern of normal and malignant human breast epithelial cells. *Proceedings from National Acadacemy of Science USA*, 89, 9064-9068.

[206] Bergstraesser, L. M. and Weitzman, S. A. (1993). Culture of normal and malignant primary epithelial cells in a physiological manner simulates in vivo patterns and allows discrimination of cell type. *Cancer Research*, 53, 2644-2654.

[207] KunzoSchughart, L. A.; Heyder, P.; Schroeder, J. and Knuechel, R. (2001). A heterologous 3D co-culture model of breast tumour cells and fibroblasts to

study tumour-associated fibroblast differentiation. *Experimental Cell Research*, 266, 74-86.

[208] Caplan, A. I. (1991). Mesenchymal stem cells. *J. Orthop. Research*, 9, 641-650.

[209] Caplan, A. I. and Bruder, S. P. (2001). Mesenchymal stem cells: building blocks for molecular medicine in the 21st century. *Trends in Molecular Medicine*, 7, 259-264.

[210] Li, W. J.; Tuli, R.; Okafor, C.; Derfoul, A.; Danielson, K. G.; Hall, D. J. and Tuan, R. S. (2005). A three-dimensional nanofibrous scaffold for cartilage tissue engineering using human mesenchymal stem cells. *Biomaterials*, 26, 599-609.

[211] Tuan, R. S.; Boland, G. and Tuli, R. (2002). Adult mesenchymal stem cells and cell-based tissue engineering. *Arthritis Research and Therapy*, 5(1), 32-38.

[212] Hing, K. A. (2004). Bone repair in the twenty-first century: biology, chemistry or engineering. *Philosophical Transactions. Series A, Mathematical, Physical, and Engineering Sciences, 362(1825)*, 2821-2850.

[213] Bruder, S. P.; Jaiswal, N. and Haynesworth, S. E. (1997). Growth kinetics self-renewal and the osteogenic potential of purified human mesenchymal stem cells during extensive subcultivation and following cryopreservation. *J. Cell Biochemistry*, 64, 278-294.

[214] Tuli, R.; Seghatoleslami, M. R.; Tuli, S.; Wang, M. L.; Hozack, W. J.; Manner, P. A.; Denielson, K. G. and Tuan, R. S. (2002). A simple high-yield method for obtaining multipotential mesenchymal progenitor cells from trabecular bone. *Molecule Biotechnology*. 23(1), 37-49.

[215] Karageorgiou, V. and Kaplan, D. (2005). Porosity of 3D biomaterial scaffolds and osteogenesis. *Biomaterials*, 26(27), 5474-5491.

[216] Bruder, S. P.; Fink, D. J. and Caplan, A. I. (1994). Mesenchymal stem cells in bone development, bone repair, and skeletal regeneration therapy. *J. Cell Biochem.*, 56, 283–294.

[217] Caplan, A. I. and Bruder, S. P. (2001). Mesenchymal stem cells:bBuilding blocks for molecular medicine in the 21st century. *Trends in Molecular Medicine*, 7, 259–264.

[218] Jaiswal, N.; Haynesworth, S. E.; Caplan, A. I. and Bruder, S. P. (1997). Osteogenic differentiation of purified, culture-expanded human mesenchymal stem cells in vitro. *J. Cell Biochem* ., 64, 295–312.

[219] Halvorsen, Y. D.; Franklin, D.; Bond, A. L.; Hitt, D. C.; Auchter, C.; Boskey, A. L.; Paschalis, E. P.; Wilkison, W. O. and Gimble, J. M. (2001). Extracellular matrix mineralization and osteoblast gene expression by human adipose tissue-derived stromal cells. *Tissue Engineering*, 7, 729–741.

[220] Yoshimoto, H.; Shin, Y. M.; Terai, H. and Vacanti, J. P. (2003). A biodegradable nanofiber scaffold by electrospinning and its potential for bone tissue engineering. *Biomaterials*, 24, 2077–2082.

[221] Grayson, W. L.; Ma, T. and Bunnell, B. (2004). Human mesenchymal stem cells tissue development in 3D PET matrices. *Biotechnology Progress*, 20, 905–912.

[222] Meinel, L.; Karageorgiou, V.; Hofmann, S.; Fajardo, R.; Snyder, B.; Li, C.; Zichner, L.; Langer, R.; Vunjak-Novakovic, G. and Kaplan, D. L. (2004). Engineering bone-like tissue *in vitro* using human bone marrow stem cells and silk scaffolds. *Journal of Biomedical Materials Research A*, 71, 25–34.

[223] Takahashi, Y. and Tabata, Y. (2004). Effect of the fiber diameter and porosity of non-woven PET fabrics on the osteogenic differentiation of mesenchymal stem cells. *J. Biomaterials Science Polymer Edition*, 15, 41–57.

[224] Lee, C. H.; Singla, A. and Lee, Y. (2001). Biomedical applications of collagen. *International J. Pharm.,* 221, 1–22.

[225] Li, W. J.; Tuli, R.; Huang, X.; Laquerriere, P. and Tuan, R. S. (2005). Multilineage differentiation of human mesenchymal stem cells in a threedimensional nanofibrous scaffold. *Biomaterials,* 26, 5158–5166.

[226] Donzelli, E.; Salvade, A.; Mimo, P.; Vigano, M.; Morrone, M.; Papagna, R.; Carini, F.; Zaopo, A.; Miloso, M.; Baldoni, M. and Tredici, G. (2006). Mesenchymal stem cells cultured on a collagen scaffolds: *in vitro* osteogenic differentiation. *Oral biology,* 52, 64-73.

[227] Fibbe, W. E. (2002). Mesenchymal stem cells: a potential source for skeletal repair. *Annals of the Rheumatic Diseases,* 61(II), ii29–31.

[228] Kawaguchi, H.; Hirachi, A.; Hasegawa, N.; Iwata, T.; Hamaguchi, H.; Shiba, H.; et al. (2004). Enhancement of periodontal tissue regeneration by transplantation of bone marrow mesenchymal stem cells. *J. Periodontol,* 75, 1281–7.

[229] Grinnell, F. (2003). Fibroblast biology in three-dimensional collagen matrices. *Trends in Cell Biology,* 13(5), 264-269.

[230] Grinnell, F. (1994). Fibroblasts, myofibroblasts, and wound contraction. *J. Cell Biol.,* 124, 401–404.

[231] Wakatsuki, T.; et al. (2000). Cell mechanics studied by a reconstituted model tissue. *Biophysical Journal,* 79, 2353–2368.

[232] Silver, F. H.; et al. (2003). Mechanobiology of force transduction in dermal tissue. *Skin Research and Technology*, 9, 3–23.

[233] Venugopal, J. R.; Zhang, Y. Z.; Ramakrishna, S. (2006). In vitro culture of human dermal fibroblasts on electrospun polycaprolactone collagen nanofibrous membrane. *Artificial Organs,* 30(6), 440-446.

[234] Al-Nasiry, S.; Geusens, N.; Hanssens, M.; Luyten, C. and Pijnenborg, R. (2007). The use of alamar blue assay for quantitative analysis of viability, migration and invasion of choriocarcinoma cells. *Human Reproduction*, 22(5), 1304-1309.

[235] Fields, R. D. and Lancaster, M. V. (1993). Dual-attribute continuous monitoring of cell proliferation/cytotoxicity. *American Biotechnology Laboratory*, 11, 48–50.

[236] Ahmed, S. A; Gogal, R. M. and Walsh, J. E. (1994). A new rapid and simple non-radioactive assay to monitor and determine the proliferation of lymphocytes: an alternative to [3H]thymidine incorporation assay. *J. Immunol. Methodology*, 170, 211–224.

[237] Mosmann, T. (1983). Rapid colorimetric assay for cellular growth and survival: application to proliferation and cytotoxicity assays. *J. Immunol. Methodology,* 65, 55–63.

[238] O'Brien, J.; Wilson, I.; Orton, T. and Pognan, F. (2000). Investigation of the AB (resazurin) fluorescent dye for the assessment of mammalian cell cytotoxicity. *European Journal of Biochemistry,* 267, 5421–5426.

[239] Goegan, P.; Johnson, G. and Vincent, R. (1995). Effects of serum protein and colloid on AB assay in cell cultures. *Toxiology In Vitro*, 9, 257–266.

[240] Nociari, M. M.; Shalev, A.; Benias P. and Russo, C. (1998). A novel one-step, highly sensitive fluorometric assay to evaluate cell-mediated cytotoxicity. *J. Immunol. Methodology*, 213, 157–167.

[241] Jones, R. G. (1995). Silicon-containing polymers. *Polymer International*, 42(2), 235.

[242] Zeigler, J. M. and Fearson, F. W. G. (1990). *Silicon-based Polymer Science*. New York: The American Chemical Society, pp. 190-191.